



FINAL REPORT

Contract NAS8-38481

PHASE II  
RAIN RATE INSTRUMENT  
FOR DEPLOYMENT AT SEA

March 30, 1992

FWG ASSOCIATES, INC.  
*"Continuity with the Future"*

Submitted by:

FWG Associates, Inc.  
217 Lakewood Drive  
Tullahoma, TN 37388

Submitted to:

NASA Marshall Space Flight Center  
Code AP29-G/Monica Heidelberg  
Marshall Space Flight Center, AL 35812

**FINAL REPORT**

**Contract NAS8-38481**

PHASE II  
RAIN RATE INSTRUMENT  
FOR DEPLOYMENT AT SEA

March 30, 1992

## TABLE OF CONTENTS

<u>Section</u>		<u>Page</u>
1.0	INTRODUCTION	1
1.1	Objectives	1
2.0	INSTRUMENT DESCRIPTION	4
2.1	Design Principle	4
2.2	Optical Imaging System	6
2.3	Signal Processing Electronics	13
2.4	Data Acquisition and Reduction	23
3.0	DATA PROCESSING	26
3.1	Sources of Errors in the Measurement	26
3.2	Quantification Effects	27
3.3	Correction Factors	28
4.0	CALIBRATION AND FIELD TESTING	34
4.1	Calibration	34
4.2	Field Testing	34
5.0	DATA ANALYSIS AND RESULTS	37
5.1	Data Analysis Software	37
5.2	Data Analysis Procedures and Results	37
6.0	MARKET ANALYSIS	46
6.1	Patent Search	46
6.2	Joint Ventures	46
6.3	Capitalization	46
6.4	Potential Markets	51
6.5	Outline of Development and Production Plan	52

## TABLE OF CONTENTS (Continued)

<u>Section</u>	<u>Page</u>
7.0 REFERENCES	58
APPENDIX A - MECHANICAL DRAWINGS	A-1
APPENDIX B - DETAILS OF OPTICAL COMPONENTS	B-1
APPENDIX C - ANALYSIS	C-1
APPENDIX D - CIRCUIT BOARD SCHEMATICS	D-1
APPENDIX E - OPERATIONS MANUAL	E-1
APPENDIX F - BASIC PROGRAM	F-1

## LIST OF FIGURES

<u>Figure</u>	<u>Page</u>
1.1 Rainfall rate and droplet size distribution system.	2
1.2 Rainfall rate and droplet size distribution system and accessory components.	2
2.1 Internal structure of optical sensing head.	5
2.2 Basic mount forms; rod mounts (above) and component mounts (below).	7
2.3 Laser light source and single-mode fiber coupler.	8
2.4 Optical beam transforming component configuration.	9
2.5 Light path through the RRS optical sensing head.	11
2.6 Two lens imaging system.	12
2.7 Operational amplifier circuit.	16
2.8 Component layout of the detector board.	17
2.9 Processor board.	17
2.10 Assembly of the processor board, the four detector boards, and an output card in the wired cardcage.	19
2.11 The electronics housing cabinet.	19
3.1 Rejection of particles triggering end fibers.	29
3.2 A droplet may trigger more or less fibers than its actual size depending upon the location of its center and the percentage of fiber area which will trigger the electronic system.	32
4.1 Configuration of the RRS field tests.	35
5.1 Evolution of raindrop size distribution with time (February 14, 1992 field test).	41
5.2 Measured, temporal, and average rain rate.	43

## LIST OF FIGURES (Continued)

<u>Figure</u>	<u>Page</u>
5.3 Radar reflectivity computed from $\sum n(D) D^6$ variation with time.	44
6.1 Letter seeking joint working relationship.	47
6.2 Marketing letter to accompany brochure.	53
6.3 Questionnaire designed for a marketing study.	53
6.4 Mini-brochure on RRS.	54
E.1 Rain rate sensor FWG Model RP101A.	E-5
E.2 Rail lens system.	E-5
E.3 Laser-coupler arrangement: (a) (First View); (b) (Second View).	E-9
E.4 Beam transforming components (Internal View).	E-13
E.5 32 Fiber array head.	E-15

## LIST OF TABLES

<u>Table</u>	<u>Page</u>
3.1 Correction Factors	31
4.1 Recorded Field Tests	36
5.1 Raw Data Files From the February 14, 1992 Field Test (RR21492.ARC)	38
5.2 Sample of Data From File RAIN.D14 Measured February 25, 1992	39
6.1 Companies Solicited for Potential Joint Ventures	48
6.2 Customers From the Government and Private Sectors	55
A.1 "Off-The-Shelf" Parts List	A-2
A.2 "Custom-Machined" and Fabricated Parts List	A-3
B.1 Optical Components Required for the RRS	B-2

## 1.0 INTRODUCTION

### 1.1 Objectives

A rain rate sensor, RRS, for measuring rainfall rate and droplet size distribution has been designed, constructed, and field tested under NASA Contract NAS8-38481, SBIR Phase II study. Figure 1.1 is a photograph of the system which consists of the optical sensing head and an electronics data acquisition and processing unit, DAPU. The unique feature of the RRS is that the sensor head may be remotely deployed relative to the power source and DAPU as illustrated photographically in Figure 1.2. Power is supplied to the sensor head with a 632.8 nm wavelength laser through a single-mode fiber. Data is transferred from the sensor head to the DAPU through a 32 optical fiber bundle. Data reduction is carried out by a 386 or 486 based PC. The system is illustrated with a lap top computer. The capability to isolate the sensor head from the electronic equipment and power source makes the RRS a unique instrument for measuring rain rates in hard to access regions; for example, over oceans from aboard ships.

The principle of the optical array probe is based on technology developed for meteorological applications at the National Center for Atmospheric Research (NCAR)<sup>[1-3]</sup>. Although several modifications have been made to the application of the principle during this development, many studies of the basic approach performed by several investigators<sup>[4-8]</sup> have provided a solid foundation for the design.

The optical array probe system is an imaging device that uses an expanded laser beam as a light source and an optical system to focus the beam into a specified probe volume of the droplet flow field. Illumination from the beam casts an image of the droplet passing through the probe volume onto an array of optical fibers. This image is, in turn, transmitted through optic fibers to a series of detectors located in the data



Figure 1.1 Rainfall rate and droplet size distribution system.

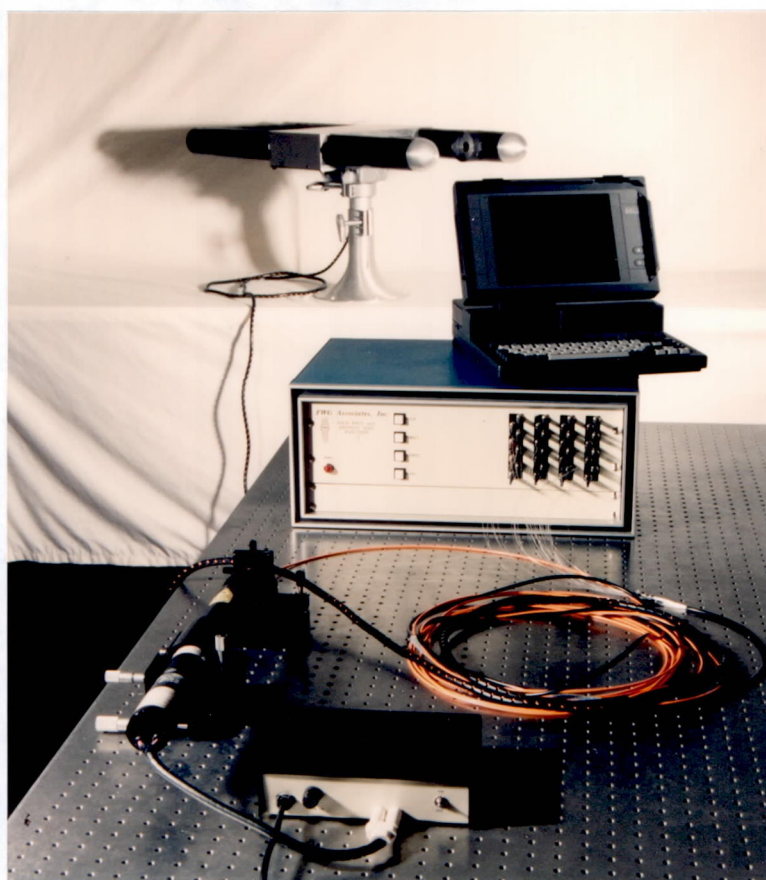


Figure 1.2 Rainfall rate and droplet size distribution system and accessory components.

acquisition and processor unit. The instrument currently has the capability of transmitting data over a distance of approximately 40 feet.

Most presently available instruments include the light source, the detector, and some of the signal processing electronics as a integral part of the optical sensing head. Incorporating these components with the sensor head increases the weight of the instrument and additionally, since they are exposed with the sensor to the rain environment, make the system susceptible to electrical damage from lightning. The FWG RRS system avoids potential difficulty with lightning since the Phase II designed optical array probe offers excellent electrical isolation of all components except the sensor head. As noted, the system described in this report transmits data over a fiber optic cable which reduces the electrical coupling between the RRS and the remotely located power source and data handling electronics.

A detailed description of the RRS and system design is given in Section 2.0. Section 3.0 describes the RRS data output and data reduction procedures. A description of the field tests carried out with the RRS is presented in Section 4.0 and of the data analysis and results of these tests is presented in Sections 5.0. Additional details of the design criteria and philosophy employed in the Phase II development are provided in the Phase I Final Report, NASA Contract NAS8-38040 dated July 27, 1989. Finally, Section 6.0 describes production and marketing plans for transition to Phase III, commercialization.

## 2.0 INSTRUMENT DESCRIPTION

In this section, the design principles of the hardware, the light beam source and optical path, the image technique, and the data acquisition and processor electronics are described.

### 2.1 Design Principle

The prototype rain rate sensor is constructed on a three-rail design principle (see Figure 2.1) with the optical components on sliding plates which can be moved along the rails until the desired adjustment of the optical beam is achieved. The plates are then locked in place with lock screws. Adjustment of the lenses, prisms, and other components of the sensor, as well as adjustment of the width of the sampling plane is thus possible with this arrangement. This design philosophy was used in the prototype to allow flexibility in positioning of the optical components of the sensor relative to the sampling plane thus allowing a number of optical configurations to be tested during field studies. During the testing and calibration phases of the RRS, the effect of adjustment to the optical configuration for rain droplet diameter spectra variability, rainfall rate variability, and the uncertainty in the application of the sensor was investigated. Although variability of the prototype optical configuration is desirable, it is anticipated that the production model of the sensor will be of simpler construction and of a relatively fixed geometry.

The housing of the RRS was designed to place the sampling plane in a space of undisturbed rainfall for accurate measurement of droplet flux. The original Phase I design, which called for the two parallel cylindrical probes to extend from a symmetric airfoil, has been abandoned. This original concept was intended for deployment from a kite in tow mode behind a ship, but later direction from NASA, indicating bad experiences with

kites on ships, redirected deployment of the sensor to that from a mast or from a pedestal. The revised design has eliminated the airfoil body and supported the parallel optical beam housings with a centrally located plate mounted on a pedestal. With the newer design, longer optical path lengths required to provide good focus of droplets in the sampling plan was achieved by folding the beam as described later.

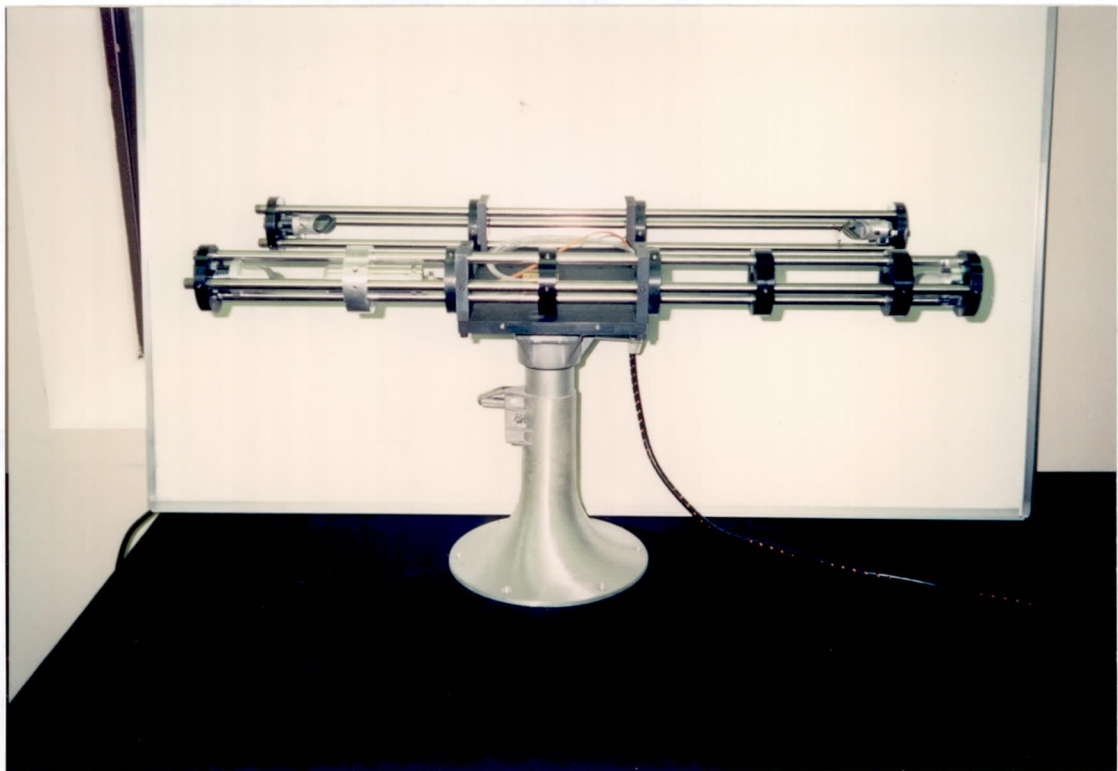


**Figure 2.1 Internal structure of optical sensing head.**

The internal structure of the prototype sensor (Figure 2.1) consists of two sets of three Thompson steel rods which are supported, roughly in center span, by aluminum rod mounts secured to an aluminum base plate (Drawing FWG-RR-005, Appendix A). The optical components of the sensor are mounted in aluminum disks made to slide along the rods, allowing variation of the lengths between components (Drawings FWG-RR-008,

012, 015, 017, 027 - Appendix A). Provision is made to allow the rod mounts to be moved in order to vary the separation between the parallel optical beam housing probes. The optical beam housings are aluminum tubes which protect the optical components and shroud the laser light (Drawing FWG-RR-023, 023A, 006 - Appendix A). These tubes slide over the rods and are held in place with screws in the rod mounts.

The critical design parameter in the housing was the stiffness of the tri-rod system relative to vertical deflection at the ends of the rods. It was determined that a deflection of four arc-minutes or less at the end of the probes was required to keep a ribbon beam of 1/4 in. thickness positioned on the fiber optic receiver array. Based on this criteria, separation of the rods and the rod diameter were determined to be 2 in. and 1/2 in., respectively. A greater separation between the rods would have allowed the use of a smaller diameter rod, but the final diameter of the probe would have become cumbersome. It is anticipated that the production design will use the protective tube to provide additional structural support, allowing a probe outside diameter of 2 in. instead of the 3 in. as required for the prototype. The basic forms of the rod mount and the optical component holders are shown schematically in Figure 2.2. A hole through the center of the holders allow for free passage of laser light or the mounting of an optical component, such as a lens. Mechanical drawings for all major components are included in Appendix A.

## **2.2 Optical Imaging System**

Currently the system employs a 10 milliwatt helium-neon laser light source (see Figure 2.3). The light is transported to the optical head of the sensor through a single-mode optical fiber. The single-mode fiber is intended to act as a "low-pass" optical filter allowing only the DC component of the light signal to pass. This approach "filters" out

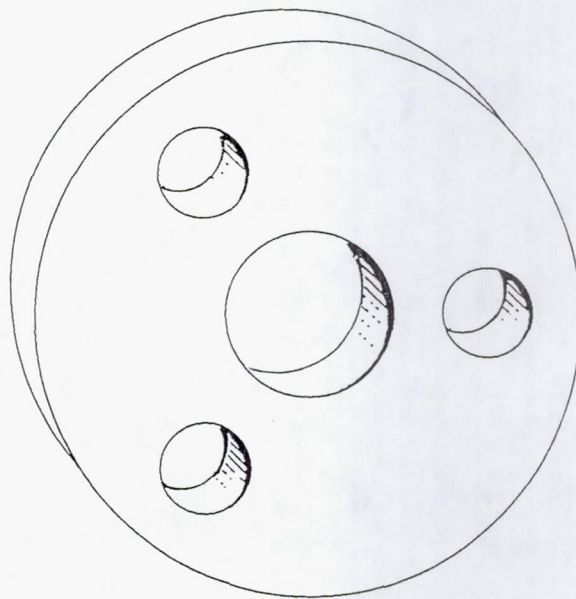
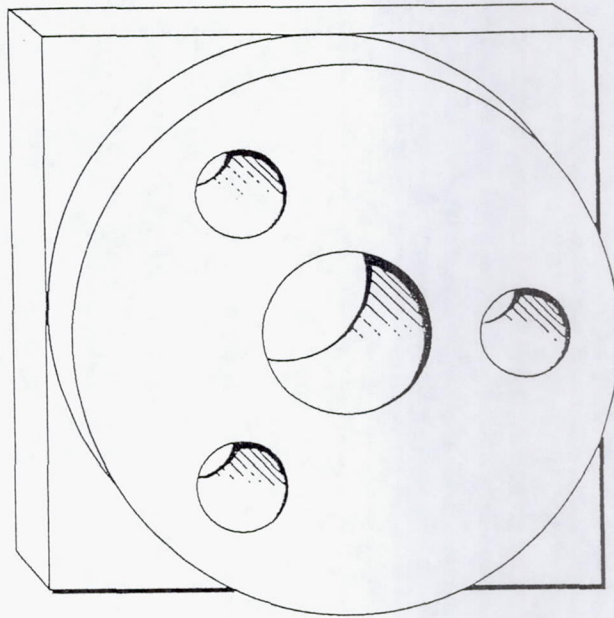
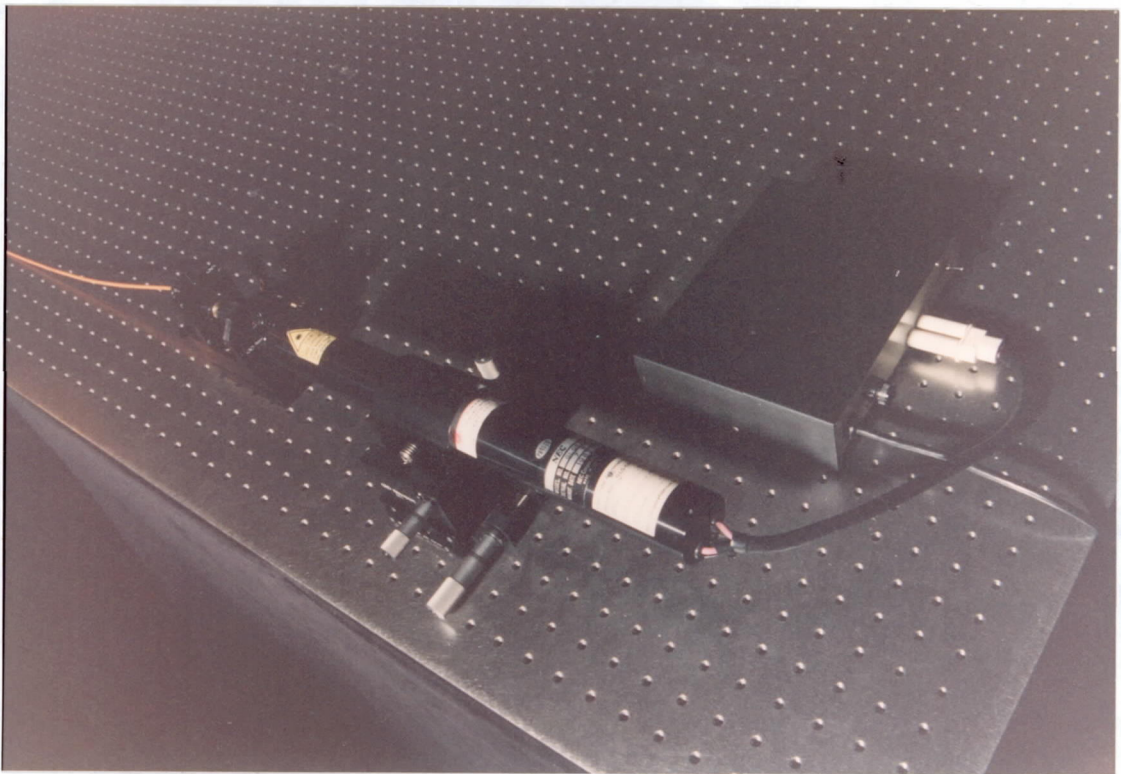


Figure 2.2 Basic mount forms; rod mounts (above) and component mounts (below).

most of the higher frequency noise. The single-mode fiber provides an efficient optical path between the laser on the ground to the sensor which can be positioned some distance away. In the prototype, the light source and optical head can be separated by as much as 40 feet. It is anticipated that this length is greater than that required for general applications of the RRS in typical Tropical Rainfall Measuring Mission (TRMM) field studies. However, greater distance can easily be achieved with a longer fiber bundle.



**Figure 2.3 Laser light source and single-mode fiber coupler.**

The output end of the single-mode fiber is placed in contact with a 2 mm OD graded index (GRIN) lens. This arrangement is shown schematically in Figure 2.4. Details of the optical components such as the GRIN lens is given in Appendix B. The  $6\ \mu$  diameter light beam, emanating from the end of the single-mode fiber, is expanded

6

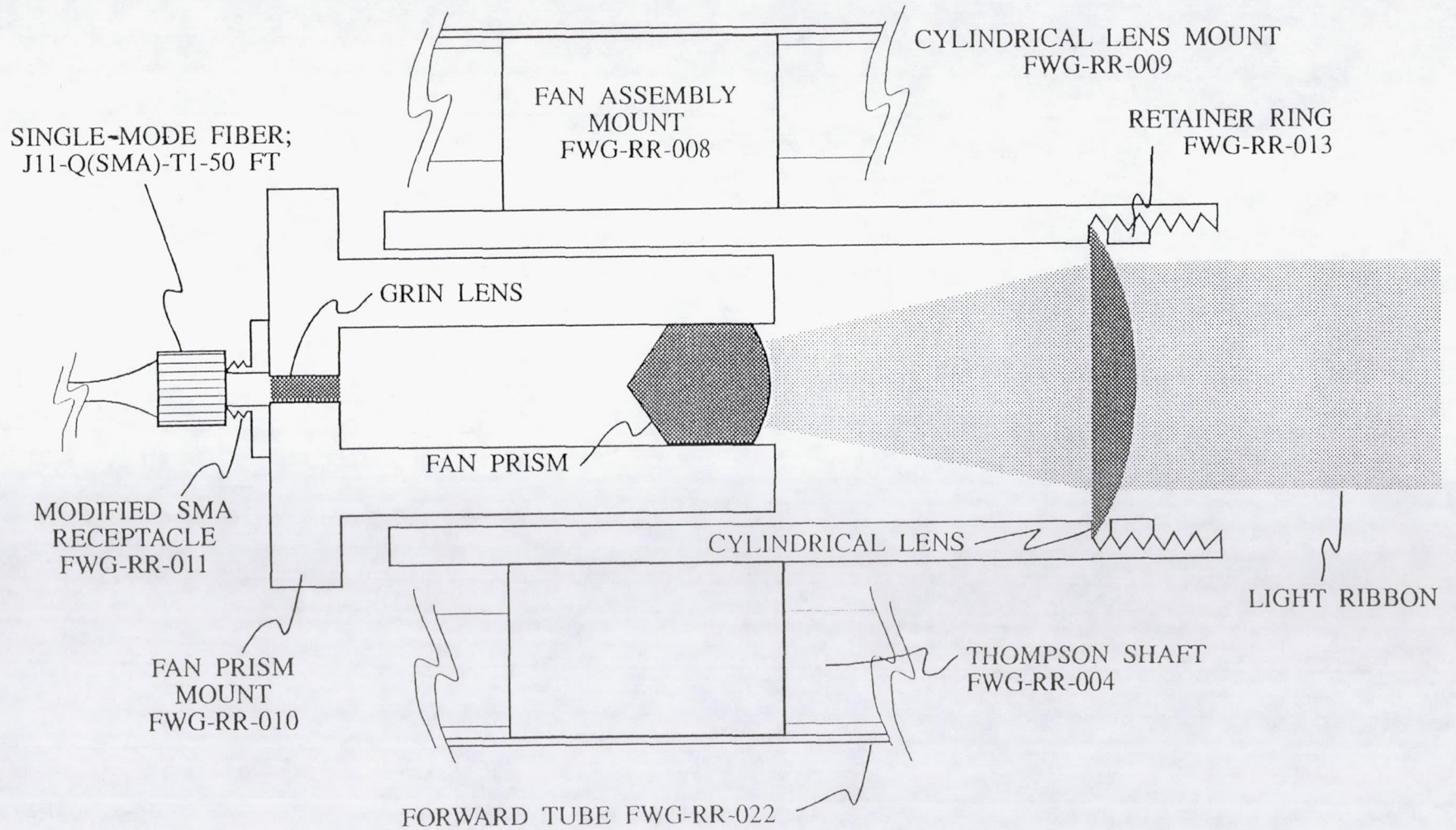
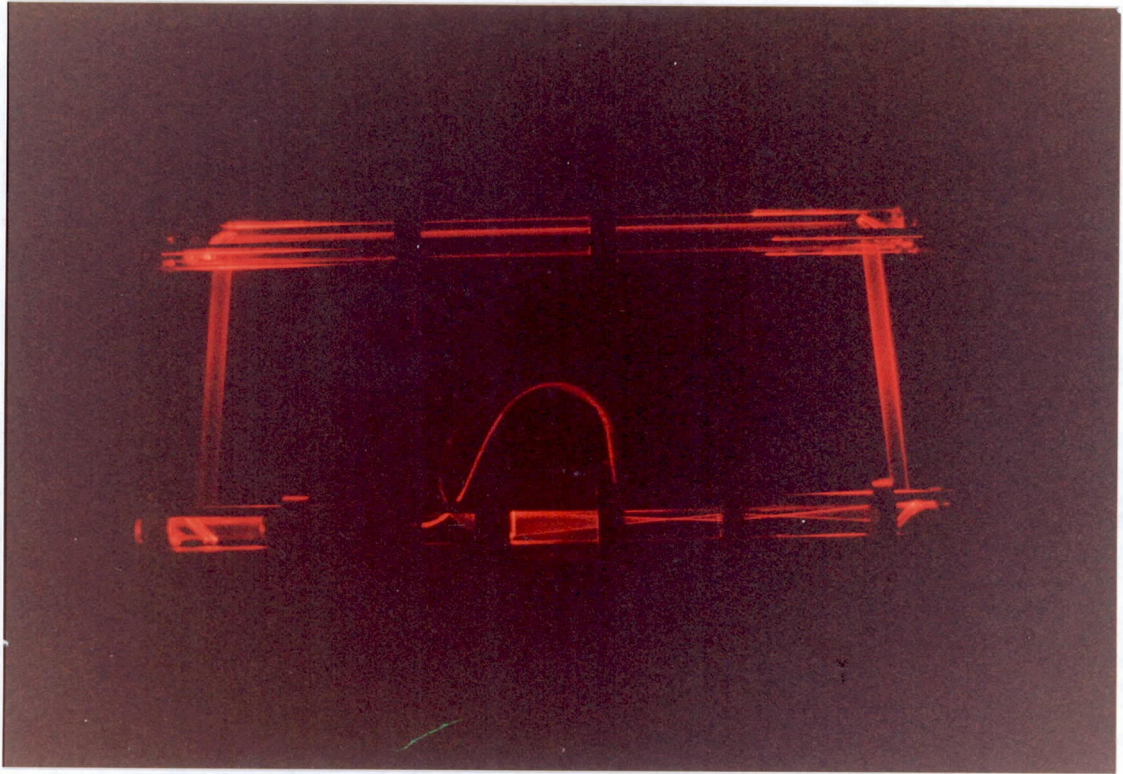


Figure 2.4 Optical beam transforming component configuration.

to a 2 mm circular beam by the GRIN lens. This circular beam travels a short distance and then passes through a 30° line generator or diverging fan prism. The diverging fan of light is collimated into a ribbon of light having a rectangular cross-section approximately 20 mm wide and 2 mm thick.

The ribbon of light exits the cylindrical lens and encounters a 45° elliptical flat mirror which turns the beam to pass through the sampling volume or probe volume (see Figure 2.5). The probe volume is thus approximately 20 mm by 2 mm in cross-section and approximately 14 cm in length (i.e., the region in which droplets are in focus). The beam crosses the probe area and is turned by a second 45° mirror. This mirror directs the ribbon beam to the rear portion of the instrument (see Figure 2.5). Another pair of mirrors, similarly placed at the rear of the instrument, turn the signal beam through a U-turn such that the beam is now passing through the housing on the same side of the instrument from which it entered via the single-mode fiber. The path of the light beam is illustrated aesthetically in Figure 2.5. Folding of the beam is utilized to enhance depth of field. The longer the distance from the image to the focal plane, the greater the depth of field in the sample volume. The beam now encounters a two lens imaging system shown schematically in Figure 2.6.



**Figure 2.5** Light path through the RRS optical sensing head.

The purpose of the two lens imaging system is to provide the capability of the RRS to resolve a wider range of particle sizes, from a few microns to several millimeters in diameter. With the imaging system, the image of the droplet on the fiber array is magnified enabling the resolution of the RRS to be adjusted. Currently the system is configured to measure raindrop diameters in the size range of approximately 0.3 mm to 5 mm. However, as noted, this range can be controlled by repositioning the imaging lens with respect to one another and to the fiber bundle head. The analyses used to determine the magnification factor is given in Appendix C.

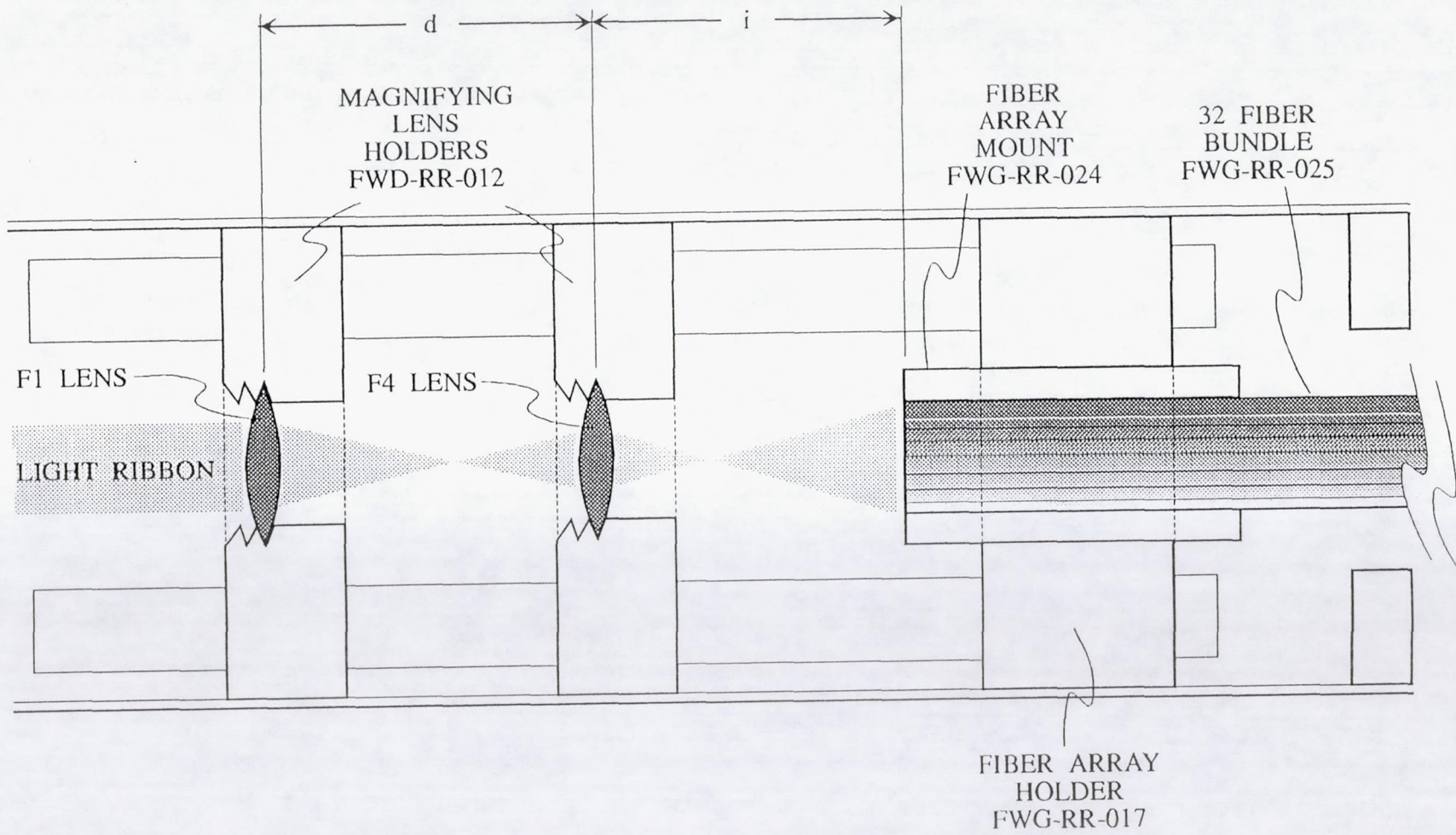


Figure 2.6 Two lens imaging system.

As depicted in Figure 2.6 the 32 fiber array is located in the image plane of the two lens imaging system. The 32 fiber bundle (part number FWG-RR-025) is secured to the fiber array mount (part number FWG-RR-024) which is secured to the three rail support structure with the fiber array holder (part number FWG-RR-017). When bolted together, the two sections of the fiber array mount (see detailed drawing in Appendix A) "sandwich" the 32 fibers between them. Once the fibers are secured in the fiber array mount, the fiber ends are terminated and carefully polished to maximize their light capturing capability.

The prototype sensor is equipped with a fiber bundle that is approximately 40 feet in length. The fiber array mount is secured to one end of the bundle and is designed to allow for "in-the-field" replacement and repair of individual fibers. However, production models of the RRS will feature "quick-connect" type connections for the fiber bundle thus allowing replacement of a damaged fiber bundle or control of the distance of the sensor head from the electronics through use of different length fiber bundles.

### **2.3 Signal Processing Electronics**

The electronics system of the RRS converts the droplet image on the fiber array to an electronic signal which represents a count of the number of fibers occluded. The electronics system is comprised of an optical-to-electronic signal converter, an analog-to-digital signal converter, and a 32-bit to 8-bit data processor board. The output from the signal processor goes to a data logging computer. (A variety of PC computers including a 386 lap top and a 486 Tri-Star have been used). The output from the computer is stored on hard disk and also displayed on the computer CRT. Each file stored on hard disk files and shown on the CRT display consists of (1) the maximum number of fibers occluded during the raindrops passage through the sample volume, (2) the number of

"time slices" or times the droplet is sampled (sampled at 83 KHz) while passing through the sample volume, (3) the time measured relative to the reference time of 00:00:00 Greenwich Mean Time (GMT) January 1, 1970 (value from the C program software) that the particle exits the sample volume, (4) an on/off error signal if two or more non-neighboring fibers are triggered (i.e., two or more droplets passing through the array simultaneously), and (5) an on/off error signal if either or both of the end fibers are triggered.

To extract the desired information the electronics system is designed for the following tasks:

1. Conversion of the optical signal to an electronic signal.
2. Detection of the raindrop shadow upon the optical fiber array.
3. Counting of the optical fibers shadowed by the raindrop.
4. Sensing whether or not an end fiber is shadow.
5. Sensing whether or not non-adjacent fibers are shadowed simultaneously (i.e., multiple raindrops).
6. Determination of the raindrop dwell time in the probe volume.
7. Storage of data for post-analysis to raindrop size distribution and rain rate.

A bank of photodetectors which sense the optical output from each individual fiber is the sensing arrangement employed. Presently, the data output is stored on hard disk files and post-analyzed. The final production version of the system will, however, incorporate the data analysis software for real time display.

For detection of the optical signals, the system requires that 32 individual signals be analyzed to produce an aggregate signal, independent of which signals are present and

indicative of raindrop size. The analog photocurrent produced by the device is a scaled measure of the number of fibers blocked and hence the size of the raindrop. The system also requires the detection of non-adjacent fiber signals (as in the presence of two raindrops in the probe volume). Additionally, individual fiber information is needed for determination of end fiber shadowing which indicates a raindrop may be partially outside of the probe volume. For these reasons, a bank of photodetectors which sense the optical output from each individual fiber is the sensing arrangement employed.

Each optical fiber is connected to an individual photodetector. Integrated circuit amplifiers are used to boost the detector signals to a usable level. The validity of individual electronic signals are then confirmed by comparison of the signals with an adjustable threshold signal. The result is 32 TTL-level signals corresponding to the light falling on the optical probe fiber array referenced to a threshold. Figure 2.7 illustrates the basic operational amplifier circuit utilized by the RRS. The 32-channel detecting system consists of four 4.5 in. by 6.5 in. printed wire-wrap circuit boards. Each of the four boards is identical and one spare detector board has been fabricated. The component layout of the detector boards is illustrated in Figure 2.8. A circuit board schematic is given in Appendix D.

Counting and discrimination tasks are accomplished by a dedicated signal processor. The speed at which data acquisition is required for accurate measurements necessitates that some type of pre-processing occur prior to data retrieval by the computer. The signal processor reduces the 32 binary signals to five binary data signals and two error signals and generates a computer synchronization signal. Figure 2.9 illustrates the processor board layout. The processor board schematic is given in Appendix D.

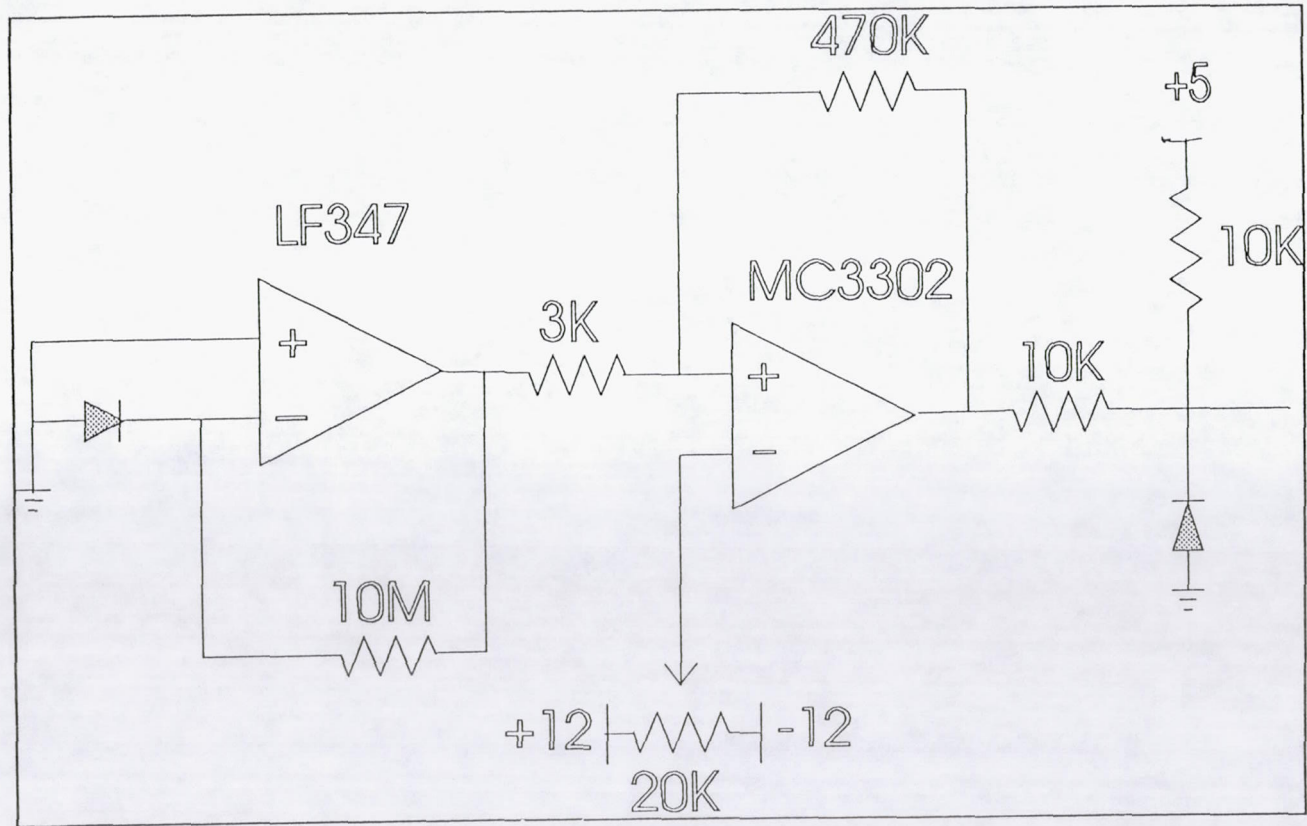


Figure 2.7 Operational amplifier circuit.

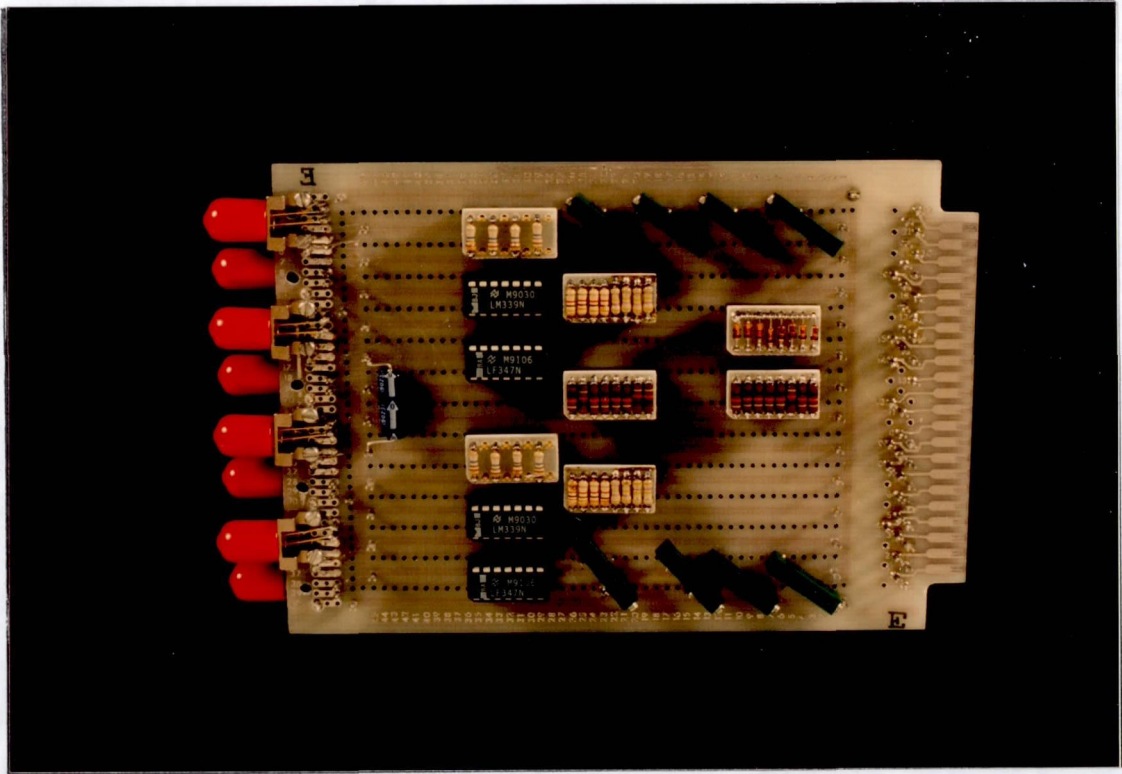


Figure 2.8 Component layout of the detector board.

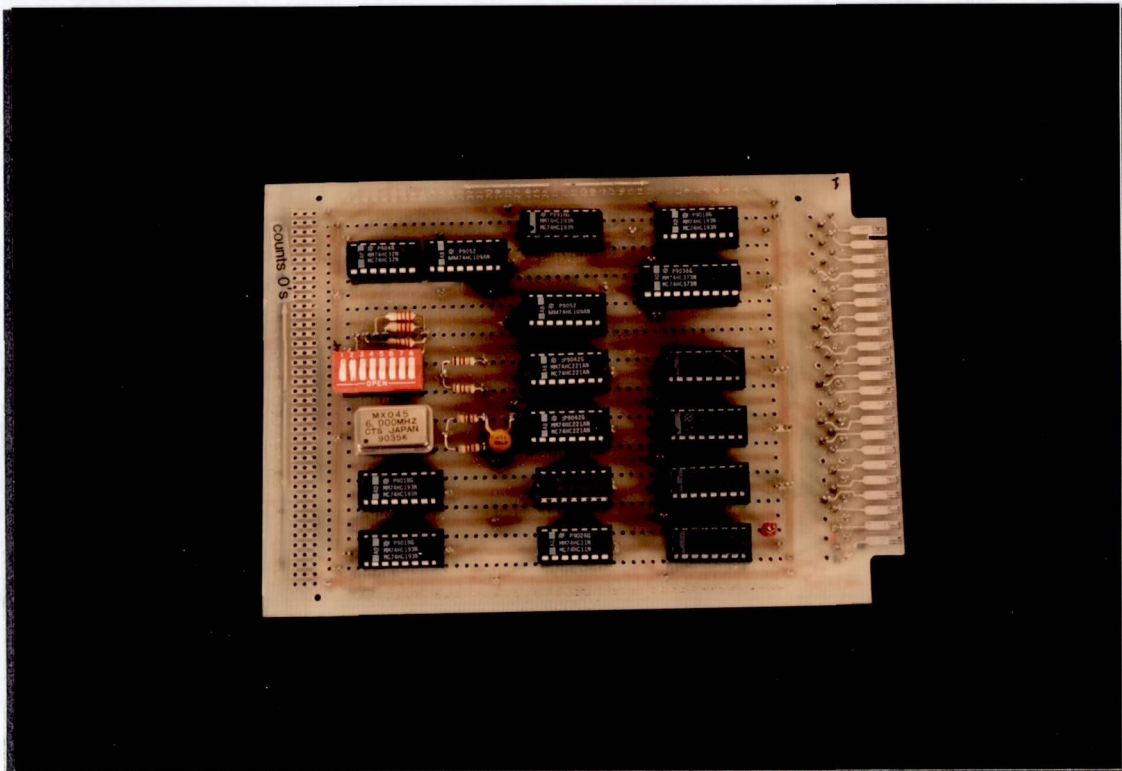


Figure 2.9 Processor board.

The data output of the signal processor board is classified by the computer. Segmentation of all data into groups corresponding to individual raindrops is performed, then identification of the largest number in the group and summation of the number of data samples in the group is accomplished to yield the maximum diameter of the raindrop under analysis and the "time slices" or number of times sampled. These data are stored on hard disk and almost simultaneously displayed on the CRT.

Figure 2.10 illustrates how the processor board along with the four detector boards and an output card are assembled in a 19-inch by 5.25-inch wired cardcage containing a triple output power supply. The cardcage assembly is housed in a 21×15×9 in. cabinet with various front-panel enunciators. The cabinet is pictured in Figure 2.11.

Characteristics of the optical signal influenced the type of photodetectors used in the electronic system. Optical power of approximately one microwatt, which is produced by a 10 milliwatt HeNe laser, reaches each of the detectors with an approximate minimum reduction of 20 percent of the steady-state signal when shadowed. The maximum frequency to be sensed was determined to be around 16 KHz. The Centronics OSD3-5T photodetector meets the desired criteria and is also within a desirable price range. The OSD3-5T is a small active area device with good responsivity. It is housed in a 4.88 mm diameter TO18 case.

The OSD3-5T detectors are mounted onto the circuit boards with AMP 501184 active device mounts and the 500 micron optical fiber is terminated with AMP 501074 fiber optic connectors. These two AMP parts are designed to work in conjunction with each other and the combination provides a very efficient and low signal loss means of coupling the fibers to the photodetectors.

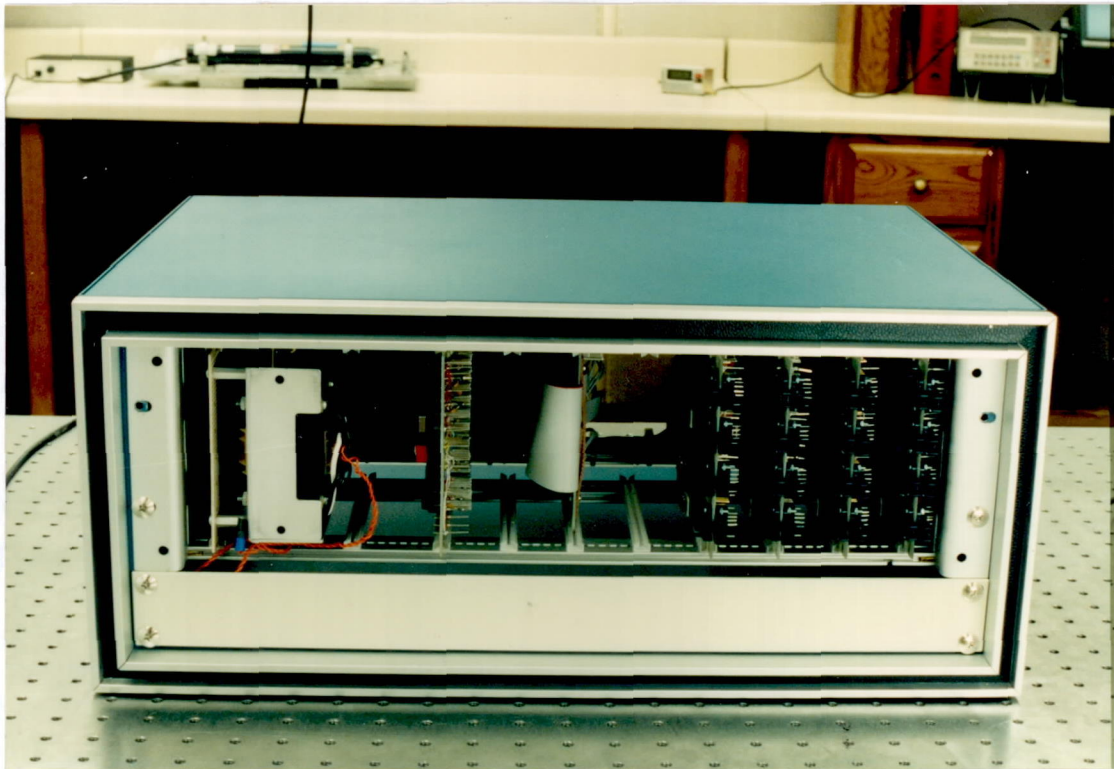


Figure 2.10 Assembly of the processor board, the four detector boards, and an output card in the wired cardcage.



Figure 2.11 The electronics housing cabinet.

The detector signal, resulting from photonic excitation, must be conditioned in order for the optical information to be used accurately. The photodiode has a non-linear voltage response due to its sensitivity variation with voltage. Therefore, the diode must be installed to operate with a constant voltage. For this reason, the photodiodes current output is used to monitor the incident light energy since the two quantities are linearly related. Constant voltage, namely zero volts, is ensured with the zero input impedance resulting from the virtual ground of an operational amplifier. Additionally, photodiode current is converted to voltage by the amplifier's high gain. This configuration known as a trans-impedance amplifier, produces an output by the relationship  $V_{out} = I_{in} \times R_{fb}$ . For the RRS electronics system, this basic circuit was duplicated for each photodetector channel to produce a bank of electronic signals ranging from zero to twelve volts.

Many factors affect the choice of amplifiers. Of highest priority is the requirement of low input offset current. Since the trans-impedance amplifier utilizes electrical current to produce an output, offset current will be amplified by the same amount as the photodiode current thus causing output errors which could be in the hundreds of millivolts for high feedback resistor values. Operational amplifiers containing FET input stages have an offset current that is several orders of magnitude less than bipolar-input amplifiers, therefore an FET input was required. Flexibility was also required of this component. The ability for the amplifier to function with a power source common to other electronic components and to consume low power has facilitated the implementation in the portable instrument. Bandwidth and temperature stability were also considered in the selection of the amplifier.

A Motorola Semiconductor LF347 quad JFET amplifier was selected to perform the trans-impedance function. This amplifier meets all the above requirements and

additionally is packaged four per chip, thus reducing parts count, wiring board space, and cost. The FET input offers the low offset current sought but does not require delicate handling to prevent damage from electrostatic discharge.

The final requirement of the particle detection circuit is a conversion of the amplifier output signal to a binary signal which indicates either the presence or absence of a particle in the probe volume. This function, performed by a comparator, is effectively a one-bit analog-to-digital conversion executed by an operational amplifier in an open-loop configuration (see Figure 2.7). High speed is not required from this component as the response time is limited by hysteresis resistors. These resistors, in addition to 0.01  $\mu$ F capacitors are used to eliminate oscillations that may be incited by slowly varying input signals. The only other requirement of the voltage comparator (besides standard error specifications) is an output that is compatible with the data processor board. The National Semiconductor MC3302 possesses an open-collector output that can be used with a pull-up resistor and a separate power supply. Also, it is packaged four per chip as the LF347 amplifier is, so four channels of detector signals may be amplified and digitized with two integrated circuits.

The signal conditioning subsystem produces 32 channels of discrete-level, or digital, data. These data change state whenever any of the fibers in the array receives less light than the threshold signal level, which can occur at any time. However, the nature of the data processing system requires that the signals be polled in discrete time intervals. This periodic sampling of the data allows measurements to be taken, processed, and stored by a digital computer.

Precautions must be taken due to sampling the continuous-time data that would not be required with un-sampled signals. Most importantly, the sampling frequency must

be no less than twice the bandwidth of the desired signal to prevent aliasing, or false interpretation of signal frequency content. Since the upper frequency limit for the photodetector signals is 16 KHz and the lower limit is zero, the minimum acceptable sampling frequency is 32 KHz. However, other sampling considerations must be made due to the nature of the data.

The timing of the data-reading operation relative to the position of the raindrop under measurement in the probe volume can produce errors that would seriously skew the statistics of reduced population data. For a given raindrop with velocity  $V$  and radius  $R$  sampled  $N$  times per second, error in the diameter measurement will result due to sampling the photodetector data at an instant when the horizontal center line of the raindrop is not exactly in line with the fiber optic array. This error cannot be eliminated, but it can be minimized to a level that does not dominate over the other error sources in the entire system. A worst case scenario was analyzed and the results show that for the particle which would be sampled the least number of times (namely, 10 samples), a 0.4 percent error of diameter measurement will be suffered if the raindrop center line does not coincide with the fiber optic array center line exactly between samples. Any other sampling instance will reduce the error. To sample this worst-case raindrop ten times, the sample rate must be equal to 83.3 KHz. This error is much lower than other end-to-end errors in the system.

The 32-bit data is to be sampled at the above rate. However, the signal processor board requires a higher clock speed due to the nature of its operation. The signal processor electronics first loads the 32 binary signals into a battery of input buffers. Next, it performs a parallel-to-serial conversion and shifts the 32 signals through a counting circuit at a rate of 64 times the sample rate, or approximately 5 MHz. The

results of the counting operation are the number of fibers blocked and the results of error bit tests. This information is temporarily stored as eight bits in an output buffer. Upon receiving a signal from timing logic in the signal processor, the byte is loaded onto an output bus for use by external devices. The byte remains on the bus until new data is loaded. A "data ready" signal changes state during the reloading period signalling that data read during that interval is not valid. Wiring schematics for all of the electronic components are included in Appendix D.

#### **2.4 Data Acquisition and Reduction**

The Rain Rate and Droplet Size Analyzer Electronic Signal Processing System gathers and processes data at a rate of approximately 83 KHz. A Data Translation DT2817 digital I/O board was chosen to provide the path for the RRS rain rate data to the host processor. The DT2817 32-line digital I/O subsystem is a standard half-size PCB and plugs right into an IBM PC or compatible back-plane through an edge connector. The RRS interface is made through a single, 50-pin, 3M-type connector. The DT2817 architecture consists of one control register and four data registers.

Each data register is associated with a corresponding I/O port and occupies a unique location in the I/O address space of the host processor. The base address is occupied by the control register and can be located anywhere between address 200 (hex) and 3F8 (hex). The four I/O port registers occupy locations consecutive to the base address. Even though all registers provide read/write access the RRS interface requires only one port in read access mode. FWG has field tested the RRS configured with two different types of personal computers and the factory selected base address of 228 (hex) has worked well in both cases. The computer accepts data from the RRS via data register Port 0 at address 229 (hex).

The data acquisition and reduction algorithm developed for the RRS is written in the C programming language and sets up the I/O port by writing a control byte into the control register located at 228 (hex). Even though the control byte consists of eight bits, only four are used. Each bit is used to control the direction of data flow through each of the four I/O ports. When a bit is clear, its I/O port is selected for input and data can be transmitted from the RRS to the host processor. Bit 0 controls the direction of data flow on I/O Port 0 so the first step of the data acquisition algorithm is to write a 0 into bit 0 of the control register. Once this is accomplished, data register Port 0 is ready to be read from.

As mentioned earlier in this section, the RRS collects and processes one byte of data at a rate of about 83 KHz. In order for the data reduction algorithm to process every piece of data, the host computer must be capable of reading the I/O port and executing a few simple instructions during one clock cycle. This is achieved very rapidly with a 486 based microcomputer having a clock speed of 33 MHz. However, through field testing and analysis FWG has determined that adequate rain rate data can be acquired and reduced with an 386SX based microprocessor operating at a clock speed of 20 MHz. This makes the prototype RRS package even more portable since notebook and lap top computers are readily available that operate in this range. Note, the computer is not considered part of the RRS system; hence, the flexibility of computer compatibility is an asset to the RRS system.

After sending the proper byte to the control register, the data acquisition algorithm begins to read data register Port 0. The data byte consists of five data bits, two error bits, and one synchronization, or data ready, bit. The five data bits comprise an integer between 0 and 31 corresponding to the number of fibers blocked, which corresponds to

the size of the particle on that particular sample. Each raindrop will have several samples associated with it, with the exact number of samples per particle depending on the acquisition speed of the host computer and the raindrop fall velocity.

The data reduction algorithm compares each sample with the one before it and saves the one that had the most fibers blocked. Also saved along with the drop size is the time of day and the number of times, if any, that the error bits were triggered. Currently the data acquisition/reduction algorithm stores the raindrop data in an ASCII data file. However, if disk space or drive access time dictates, a binary format which is more efficient in access time and disk space can readily be established.

### 3.0 DATA PROCESSING

#### 3.1 Sources of Errors in the Measurement

The accuracy of the RRS measurement can be influenced by a number of factors. Mechanical, optical or electrical malfunctions can produce errors in the measurement due to:

- a) vibrations,
- b) optical misalignment,
- c) electrical noise pickup, and
- d) dirty windows (rain or dirt).

These errors are believed to be minimized by the physical construction of the sensor head and by proper maintenance and operation procedures.

Also, deviations of design input parameters from the actual physical characteristics of the rain being sensed can create errors. These include:

- a) non-opaque droplets (estimated to be small),
- b) diffraction effects (estimated to be small;  $\lambda/D$  small),
- c) cladding thickness (included in correction factors but actual thickness difficult to determine accurately),
- d) non-spherical droplets (estimated to be small),
- e) depth-of-field effects (estimated to be small because folding of the light beam has effectively placed the image at infinity), and
- f) presence of two or more particles passing through sampling volume simultaneously (corrected for in post-analysis).

Finally, features inherent in the sensing technique employed with the RRS can create errors if not corrected for during processing of the data. These features can be classified as quantification effects.

### 3.2 Quantification Effects

The rain rate detection system has a linear array of 32 optic fibers of 0.5 mm diameter (including cladding) forming a total length of 16 mm. The particle size is determined from the number of fibers shadowed as each particle passes through the sample volume; hence, the size distribution measurement depends on the optical system arrangement. When the light falling on a fiber end is reduced such that the voltage output of the photodetector to which it is connected is reduced by more than roughly 50 percent (called the trigger threshold voltage), a flip-flop memory element is switched from 0 to 1. The fiber is then recorded as occluded.

Without magnification a droplet of a size which triggers one fiber is 0.5 mm. A droplet which shadows all 32 fibers, in principle, would be recorded as 16 mm in diameter. There are two factors for which the above arguments are not exactly correct. One is that the sensor is designed such that when any particle triggers either of the fibers on the end of the array, an error is recorded and the droplet is rejected in the post-analysis. The reason is that an unknown portion of the particle is out of view and, therefore, its size cannot be correctly determined. So, within the 32 fiber elements, only particles small enough to shadow sufficient area of one fiber element to trigger it and large enough to shadow as many as 30 elements, can be differentiated. The second factor is that the RRS is optically designed to magnify the droplet image (see Section 2.2); with the present magnification being approximately 1.28. Thus, a 0.39 mm particle shadows a single element and the range of measured particle sizes is from 0.39 mm to 11.7 mm. The sensor thus resolves droplet diameter sizes in quantized increments of 0.39 mm.

The above described end fiber rejection and quantization effects are accounted for with correction factors.

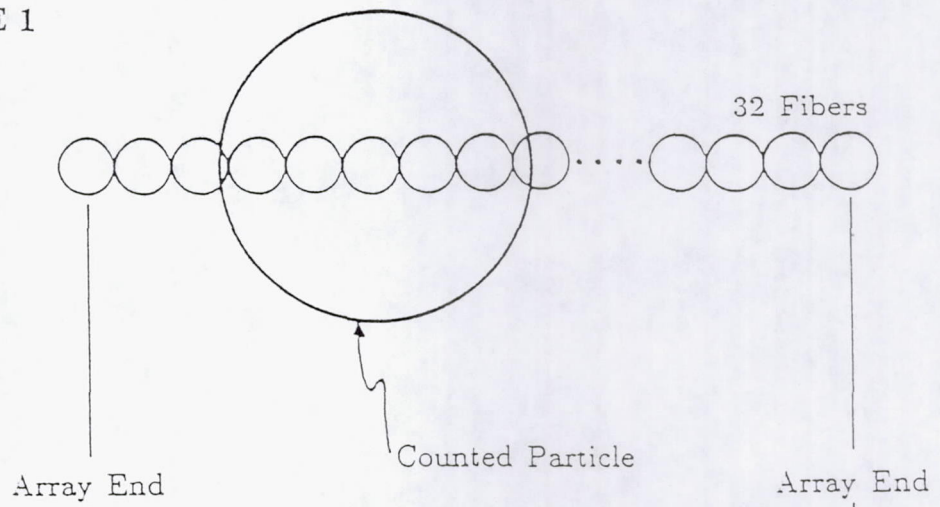
### 3.3 Correction Factors

For the rejection system, the electronic logic circuits are incorporated into the device which allow the rejection of images crossing the ends of the fibers to prevent fractional images from being counted (see Figure 3.1). A computer program was developed to determine correction factors for raindrops which are not counted by the system due to triggering the end fibers of the array. The program generates a computer array of 32 fibers. Bands used to determine which fibers are occluded when a droplet is passed through the sensor are setup relative to one end of the array. The distance to each band is based on the cladding thickness of the fibers and the threshold necessary to trigger a fiber. It is assumed that the necessary fraction of area of the fiber end shadowed to trigger that fiber is proportional to the threshold voltage set during calibration. For the present system this is roughly 50 percent.

The computer simulates the passage of droplets through the array. A random number generator is used to determine the center of each droplet measured relative to the left-hand side of the fiber array. In turn, the size of each droplet is selected with a random number generator. Both the center location and droplet size are selected from a uniform distribution. Passage of the droplet through the array is then simulated and the number of fibers triggered is determined. Based on the number of fibers triggered, the droplet is stored in a bin ranging in size from 0 to 30 fiber diameter (the first and last fiber are excluded). The bin size corresponds to the size of the droplet stored.

The computer simulation was run for 500,000 droplets having a uniform distribution in sizes from 0 to the maximum size of 16 mm (a particle which covers the entire 32 fiber array). The simulated number of droplets calculated for each size band were divided into the actual number of droplets in that size range generated randomly by

CASE 1



CASE 2

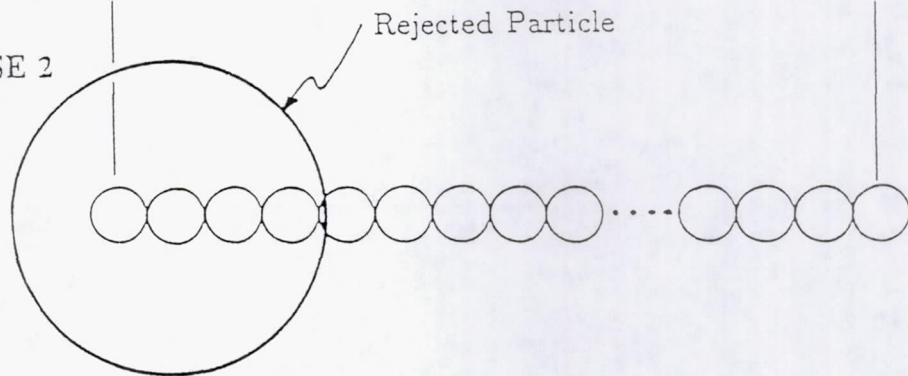


Figure 3.1 Rejection of particles triggering end fibers.

the computer program. This ratio represents a correction factor. The correction factor so determined is a function only of geometry and is therefore universally valid for the given fiber array geometry and calibrated triggering threshold.

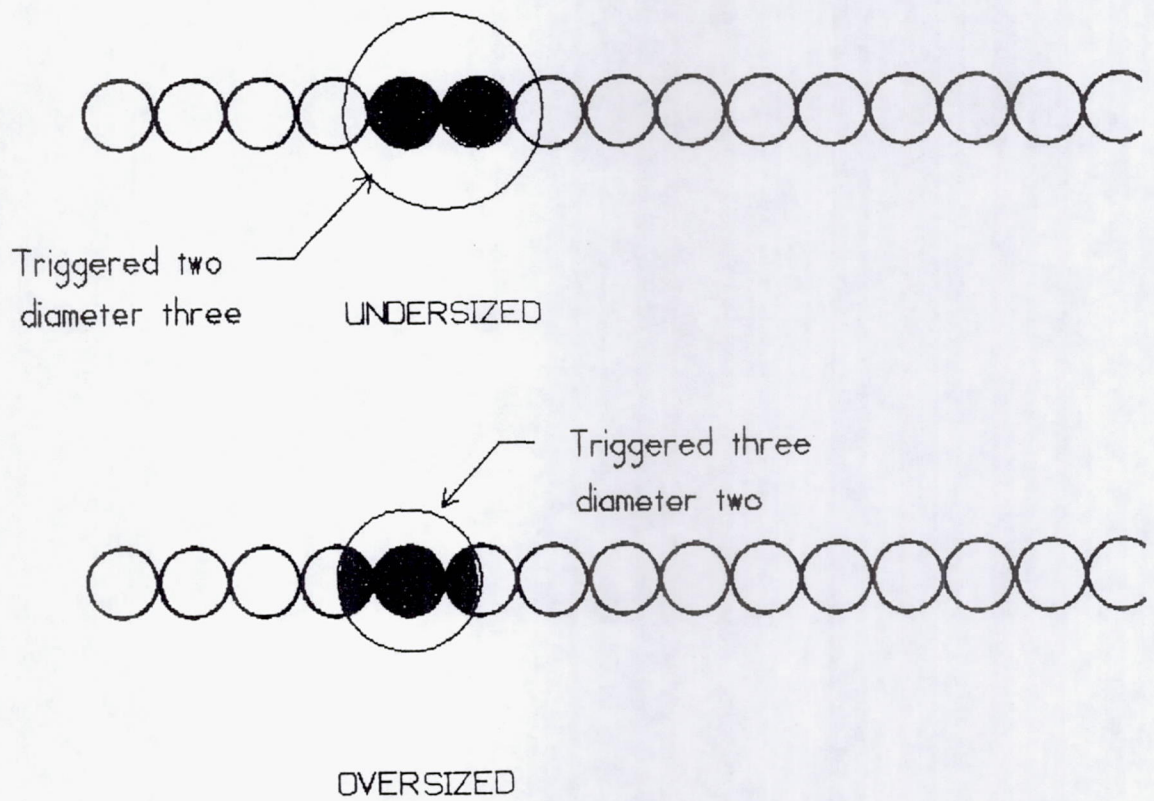
During post-processing of the data, the number of particles sensed by the RRS are multiplied by the correction factor. This adjustment corrects for those particles omitted by the electronics due to a particle of that size which triggered an end fiber. Table 3.1 shows the correction factors currently employed in the post-analysis software described in Section 5.0. FNUM is the correction factor for number of droplets. Since the number of droplets missed by the system are a function only of geometry and the correction factors are multiplicative, they can be applied across the board regardless of the actual rain rate distribution.

Correction factors for the volume of droplets in each bin size (FVOL Table 3.1) were similarly computed. To compute the volume of water associated with each droplet size bin, the sensed number of droplets times the volume of a spherical droplet of that bin size diameter is multiplied by the correction factor to produce the corrected volume of water contained in the actual droplets of all sizes which lie within the range of  $D_i$  and  $D_i + \Delta D$ .

A second correction is required to account for those raindrops which trigger  $i$  fibers when the droplet is actually of a size corresponding to  $i-1$  (over) or  $i+1$  (under) fibers. Figure 3.2 illustrates an  $i$  size droplet which belongs in an  $i-1$  size bin. Correction factors were also developed for the number of droplets which were over or undersized. These were determined by the same simulation with 500,000 randomly generated droplets. A number of particles that would be measured as being in bin  $i$  and which actually belong in either bin  $i+1$  (under) or in bin  $i-1$  (over), respectively, were computed with the

Table 3.1 Correction Factors

FNUM	FVOL	FOVER	FUNDER
0.00000	0.00000	0.03744	0.00000
1.08848	0.27205	0.67640	0.00000
1.08682	0.50971	0.55940	0.00000
1.11782	0.66413	0.52816	0.00000
1.16622	0.78679	0.51368	0.00000
1.21110	0.87941	0.50888	0.00000
1.24631	0.94735	0.50549	0.00000
1.31316	1.03070	0.50201	0.00000
1.36190	1.09409	0.50448	0.00000
1.40926	1.15151	0.49526	0.00000
1.49326	1.23463	0.49892	0.00000
1.55540	1.29969	0.49253	0.00000
1.64697	1.38426	0.49522	0.00000
1.71958	1.45783	0.48362	0.00000
1.81749	1.54659	0.48476	0.00000
1.94453	1.65642	0.48906	0.00000
2.06103	1.76372	0.49288	0.00014
2.21045	1.88801	0.49710	0.00000
2.38550	2.04370	0.49717	0.00000
2.58394	2.21511	0.48435	0.00000
2.85254	2.44304	0.49496	0.00000
2.99449	2.56551	0.47851	0.00000
3.35470	2.87029	0.48280	0.00000
3.79866	3.24633	0.47903	0.00000
4.19670	3.58673	0.47392	0.00000
4.93050	4.19454	0.49850	0.00000
5.67110	4.82753	0.47416	0.00000
7.18704	6.08903	0.47908	0.00051
8.97322	7.56433	0.45897	0.00000
13.32763	11.25330	0.47314	0.00103
21.89112	18.46042	0.46188	0.00000
75.82524	63.55808	0.00000	0.00000
0.00000	0.00000	0.00000	0.00000



\*Shaded area represents triggered area

**Figure 3.2** A droplet may trigger more or less fibers than its actual size depending upon the location of its center and the percentage of fiber area which will trigger the electronic system.

simulation program. The ratio of  $(i+1)/i$  and  $(i-1)/i$  were computed as correction factors. These are listed in Table 3.1 as FOVER and FUNDER, respectively. The FOVER and FUNDER correction factors are applied in the analysis program by multiplying the number of droplets in the  $i$ th bin by the  $i$ th correction factor then adding (over) or subtracting (under) the computed value to the  $i+1$ th bin number. The FOVER and FUNDER correction factors along with the FNUM and FVOL correction factors are stored directly in the post-analysis software for analyzing the raw measured rain droplet counts from the system (see Section 5.0).

## 4.0 CALIBRATION AND FIELD TESTING

### 4.1 Calibration

Detailed calibration procedures are provided in the operations and calibration manual which accompanies the RRS. This manual is provided in Appendix E. Primarily, calibration consists of individually adjusting the threshold voltage of each of the 32 fiber optic channels. The threshold voltage is compared with the detector voltage as displayed on an oscilloscope CRT. The detector voltage is the output value from the respective light detector channel exposed to unimpeded light from the optical system. The channel trim-pot (variable resistor) is adjusted until the threshold voltage is approximately 52 percent of the detector output voltage.

It is assumed that the voltage output of each fiber detector channel will be proportionate to the area of the fiber end obscured by a droplet. Computer optimization studies have shown that the optimum droplet classification as to bin size is achieved when 48 percent of the area of the fiber end is occluded (see Figure 3.2).

### 4.2 Field Testing

Testing of the RRS was carried out at FWG Corporate Headquarters in Tullahoma, Tennessee during the winter period of December 1991 to March 1992. During the month of February and March several hours of rain rate data were recorded and analyzed. This section describes the tests carried out. Results of the tests are documented in Section 5.0.

Figure 4.1 illustrates the configuration of the RRS during field tests. G1 and G2 reference to rain gauges which independently and simultaneously monitored the amount of rainfall during the recording. However, during periods of light rainfall G1 and G2 do not collect sufficient water for resolution on the gauge scale. Subsequently, the rain gauges were backed-up with a large pan, 10 inches in diameter. Following a test, the



Table 4.1 Recorded Field Tests

DATE	G1 (mm)	G2 (mm)	10" PAN (ml)	RRS Number Droplets	FILENAME
02-12-92	1.0	1.0	N/A	10K	RR21292.ARC
02-14-92	0.8	0.8	N/A	9K	RR21492.ARC
02-17-92	5.0	5.0	250.8	11K	RR21792.ARC
02-23-92	1.0	1.0	49.6	3.5K **	RR22392.ARC
03-06-92	tr.	tr.	38.2	3.8K	RR30692A.ARC
03-06-92	3.1	2.8	163.3	4.3K	RR30692B.ARC
03-09-92	2.0	2.0	102.0	4K	RR30992.ARC
03-10-92	tr.	tr.	25.4	13K	RR31092.ARC
03-19-92	1.3	1.3	65.1	5K	RR31992.ARC

\*\* Due to an optical path obstruction only about 1500 drops have unusable data.

## 5.0 DATA ANALYSIS AND RESULTS

### 5.1 Data Analysis Software

The present RRS system utilizes post-data analysis. The data analysis software is written in Microsoft QUICK BASIC. The analysis program is given in Appendix F. The program converts the rain data from storage files into corrected raindrop size distribution and temporal and average rain rates.

### 5.2 Data Analysis Procedures and Results

An example of the data analysis procedure and results is given in this section. Analysis of the data collected during the experiment on February 14, 1992 is used for the example. The data were gathered over a period of approximately three hours (193.8 mins). Individual data files for consecutive 1,000 raindrops were stored during the field test. These files are listed as RAIN.D01 to RAIN.D18 (Table 5.1). A portion of a typical data file is shown in Table 5.2. The file consists of five columns:

- Column 1 is the maximum number of fibers occluded during passage of the raindrop through the sample volume.
- Column 2 is the number of time slices, or times the particle was sampled, at a rate of 83 Hz, during its passage through the sample volume.
- Column 3 is the time in seconds measured from 00:00:00, January 1, 1970, Greenwich Mean Time (GMT) at which the raindrop exited the sampling volume.
- Column 4 is a number indicating whether a two particle error was sensed (if 0 no error, if greater than 0, then an error).
- Column 5 is a number indicating whether an end fiber error occurred (if 0 no error, if greater than 0, then an error).

Table 5.1 Raw Data Files From the February 14, 1992 Field Test  
(RR21492.ARC)

RAIN.D08	20038	02-14-92	9:35a
RAIN.D09	20043	02-14-92	9:43a
RAIN.D10	20037	02-14-92	9:53a
RAIN.D11	20034	02-14-92	10:05a
RAIN.D12	20052	02-14-92	10:16a
RAIN.D13	20091	02-14-92	10:25a
RAIN.D14	20105	02-14-92	10:35a
RAIN.D15	20114	02-14-92	10:44a
RAIN.D16	20114	02-14-92	10:59a
RAIN.D17	20079	02-14-92	11:14a
RAIN.D18	20033	02-14-92	11:32a

Table 5.2 Sample of Data From File RAIN.D14 Measured February 25, 1992

COLUMN 1	COLUMN 2	COLUMN 3	COLUMN 4	COLUMN 5
2	4	699042340	0	0
3	5	699042341	0	0
1	2	699042343	0	0
4	5	699042344	0	0
3	4	699042345	0	0
1	3	699042346	0	0
1	5	699042346	0	0
2	7	699042346	0	0
1	2	699042347	0	0
4	5	699042348	0	0
2	4	699042348	0	0
4	4	699042348	0	4
4	5	699042349	1	0
1	2	699042349	0	0
1	3	699042350	0	0
2	4	699042350	0	0
1	3	699042351	0	0
3	4	699042352	0	0
2	9	699042352	0	0
2	4	699042352	0	0

These data were input to the rain rate and drop size distribution, data analysis program (see Appendix F). The analysis program is currently used in a post-experiment mode; however, the final production model will have this analysis built directly into the computer software for real time display of rain rate and raindrop size distributions. The analysis program reads in the correction factors, applies these to the raindrop size and volume distributions and computes the rain rate.

The RRS system software is currently setup to store increments of 1,000 raindrops per data file. However, the number of raindrops stored on a per data file basis, in any given experiment, is an input parameter and the number can easily be adjusted.

The results of the analysis are described in the following paragraphs. Figure 5.1 shows the drop size distribution evolving with time from the beginning of rainfall and the corresponding temporal or "instantaneous" rain rates from RAIN.D02, RAIN.D05, RAIN.D08 and RAIN.D17 during the February 14, 1992 experiment. One observes that the initial drop distribution contains a larger number of small raindrops but, as time evolves, the number of larger droplets increases and the number of smaller droplets decreases. This adjustment in the size distribution is apparently not proportional to rain rate, however. In the early part of the rainstorm, contributions to higher rain rate appears to come from a growth in number of droplets in the 1.0 to 1.4 mm range but, as the storm decays, the number of droplets in the 1.4 to 2.8 mm ranges increases. However, the rain rate has decreased to 0.64 mm/hr due to a substantial reduction in the number of droplets in the 0.4 to 1.4 mm range.

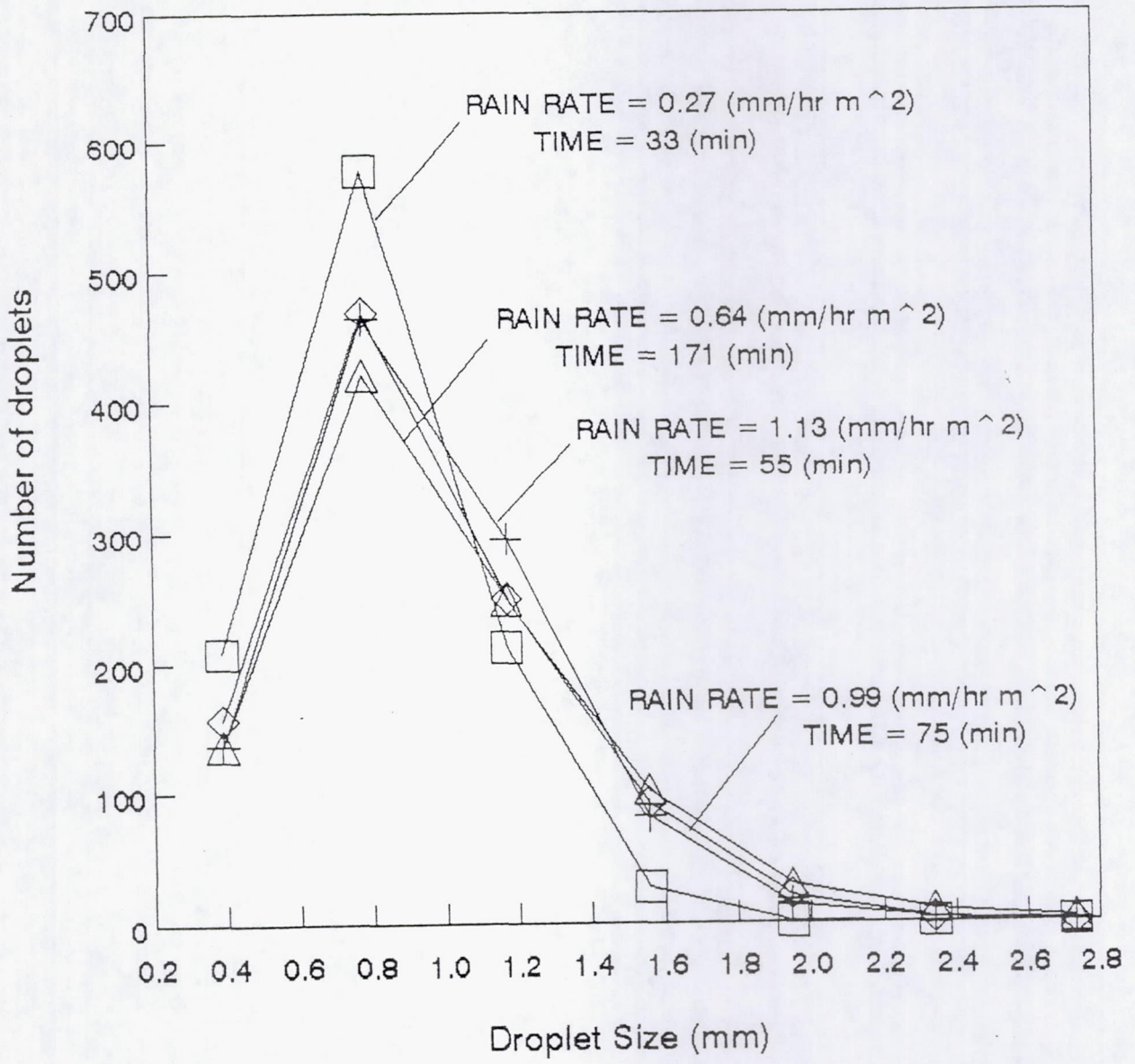


Figure 5.1 Evolution of raindrop size distribution with time (February 14, 1992 field test).

Figure 5.2 shows the rain rate as a function of time over the approximate three hour period of the field test. The average rain rate over the total period of the experiment, as determined from the instrument (0.67 mm/hr), and as determined by the rain gauges (0.79 mm/hr), is shown on the curve. The instruments value of average rain rate is approximately 15 percent lower than the gauge value. The rain gauges, utilized, however, cannot be read to an accuracy of more than 10 percent and, therefore, it is anticipated that the instrument rain rate measured is of equal accuracy if not more accurate.

A log normal curve fit of the raindrop distribution has been made and, in general, the data fit a curve well. Rain rates were calculated using the curve fit and integrating under the droplet distribution. These values, however, were lower than values determined by using the correction factor per droplet volume as discussed in Section 3.0.

Figure 5.3 shows the computed radar reflectivity determined from the relationship

$$Z = \sum_{D=0.5}^{D=7.9} n(D) D^6 \quad (1)$$

It was not possible to use the relationship

$$Z = AR^b \quad (2)$$

where  $A = 220$  and  $b = 1.6$  normally reported in the literature<sup>[9]</sup> because the data did not fit a Marshall Palmer distribution well.

The strong potential for this rain rate sensor for use in NASA's EOS program is obvious from Figure 5.3. With very minor computer software modifications, the sensor

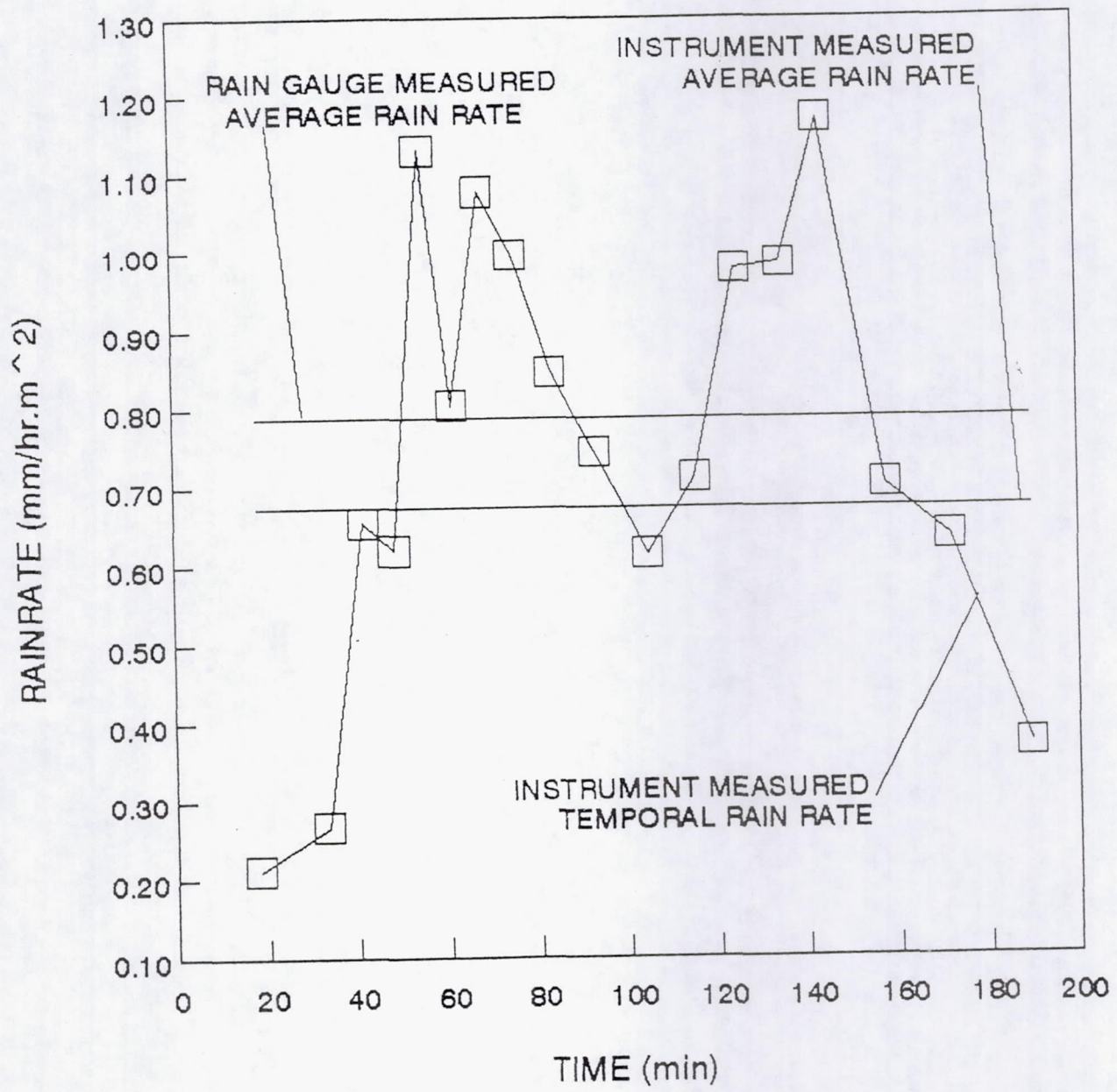


Figure 5.2 Measured, temporal, and average rain rate.

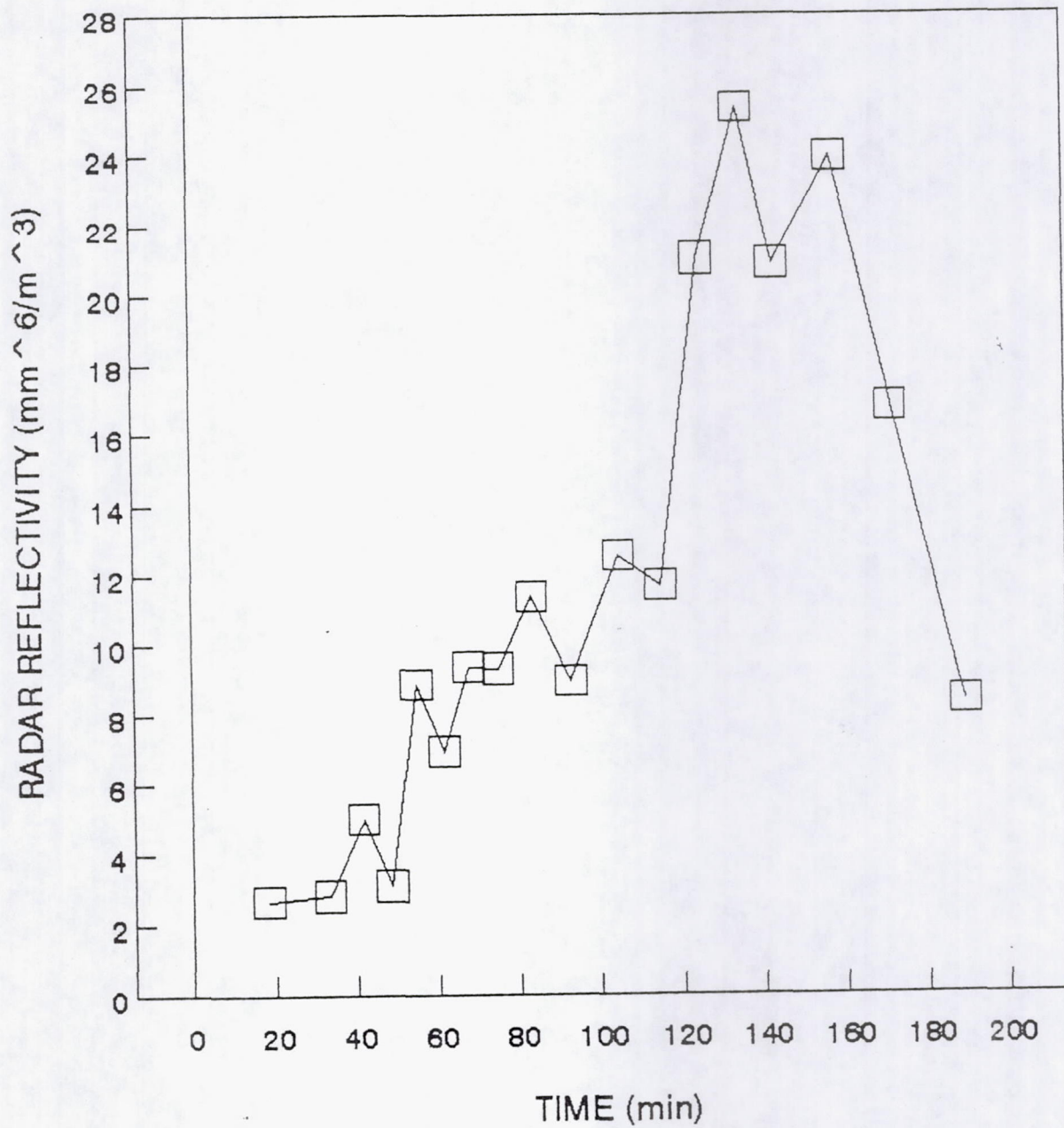


Figure 5.3 Radar reflectivity computed from  $\sum n(D) D^6$  variation with time.

can be programmed to display in virtually real time radar echos. This sensor mounted on an aircraft or on a buoy at sea and interrogated by a satellite could give an essential real time comparison with radar outputs monitored from space. This tool, when development is completed, will be an essential element to any of the TRMM's field projects or other rain monitoring field experiments. Considering that the cost of the unit is less than \$10,000.00, it should be a highly sellable item. With this in mind, a marketing program has been laid out as given in Section 6.0.

## **6.0 MARKET ANALYSIS**

### **6.1 Patent Search**

The initial step in determining the feasibility of marketing and producing the RRS was to conduct a patent search on the optical array probe, an instrument which was originally developed for meteorological applications at the National Center for Atmospheric Research (NCAR)<sup>[2]</sup>. This search was performed at the Patent and Trademark Depository Library (PTDL) located at Vanderbilt University in Nashville, Tennessee. Use of the optical array probe concept does not appear to be in violation of any patent rights. Consequently, a marketing strategy is being developed.

### **6.2 Joint Ventures**

Numerous companies within private industry, particularly those who currently develop electro-optical instrumentation, are prime candidates for a joint venture to produce the RRS developed by FWG under the SBIR Phase II contract with NASA. Therefore, FWG is actively polling these companies as to potential working relationships, which would be conducive to successful development and manufacturing of the RRS. Figure 6.1 illustrates a draft letter which is being circulated relative to initiating a Phase III joint activity. Table 6.1 is a list of private industry that produce instrumentation and advanced technological systems to which the letter is being circulated.

### **6.3 Capitalization**

FWG is also seeking capital to develop in-house production and marketing capabilities. Consideration is being given to using FWG's own capital but, at the same time, FWG will also investigate other sources of venture capital to fund this innovated project. The degree to which FWG can successfully provide in-house capital is dependent upon retention of the prototype RRS system and of the equipment used in its construction

Dear Sir:

FWG Associates, Inc. has developed under a SBIR Phase II contract a prototype instrument for measuring rain rate and droplet size distribution "distrometer". This instrument will be very useful to the NASA Earth Observing Satellite Program, in particular, the TRMM's project. Additionally, the instrument will have applications in other areas of particle and droplet size and flux rate measurements.

Potential customers include: NASA, NOAA, Army, various other governmental agencies, and many private industries have expressed a need for particle flux sensors and particle size spectrometers. The RRS is suitable, or could easily be adapted to suit many applications, of interest to these agencies as listed below.

• Applications

- Measuring rainfall rate and broad range particle size distributions
- Support satellite missions to measure tropical rainfall
- Quantitative measurements of droplet cloud uniformity
- Measurements to support cloud physics and parameterization studies
- Measure water droplet size distribution in a variety of test cells
- Monitor spatial distribution of liquid water content (LWC) in icing tests
- Measurements for inlet contamination and exhaust particles for jet engines
- Spatial distribution of particles surrounding rocket engines
- Environmental measurements to monitor stack emissions for particulates of contaminants
- Particle size measurements to analyze nozzle erosion in arc facilities
- Future applications to sounding rockets
- Particle size measurements for determining optimum smokes and obscurants for defeating lidar for millimeter wave radar targeting systems

• Questionnaire

A brief questionnaire, along with a mini-brochure, which describes (and pictures) the RRS, and lists numerous applications, has been prepared. A copy of the questionnaire is included in Appendix A. This packet has been sent, or is being sent, to various private companies and government agencies which are listed in Appendix B.

The unique feature of the sensor is that the sensing head is separate from the power source and data acquisition system. All power and return signals are transmitted through a fiber optic bundle thus allowing the sensor to be remotely deployed by various techniques such as carried aloft with a parafoil, deployed on a buoy system in the ocean, or mounted on a mast. Factors which make this capability attractive, is that during rain sensing and thunderstorms, a remote sensor head deployed on a mast (or by other methods as described above) well above a region where swirling wind effects and spray from surrounding terrain features (i.e., droplets from trees or breaking waves) may contaminate the measurements, are avoided. The use of a glass fiber bundle to transmit the source power and signals situation reduces the hazards of lightning strikes associated with other instruments deployed in similar fashion. The optics fiber effectively insulate the instrument head from the electronics and power source.

The capability to probe a smokestack or cooling tower plume by hoisting the sensor aloft with a large kite or parafoil, as illustrated in the brochure, has many advantages in terms of measuring particle or droplet distribution profiles and average values average over longtime periods which are not achievable with aircraft mounted probes.

FWG believes that this sensor would be a highly marketable product but, being a small business, does not have the capital or marketing and production skills to take full advantage of the instrument's commercialization value. Thus, FWG is seeking a joint sponsor interested in providing venture capital, as well as marketing and production experience and facilities. FWG is aware of your firm's prestigious status in atmospheric instrumentation and wish to determining whether you may be interested in discussing a potential working relationship. The enclosed final report explains the system's general description and capabilities. Also attached is the estimated costs to produce the unit and a list of additional R&D efforts to establish full marketing capability and production status of the system.

FWG would welcome the opportunity to show you this instrument and establish dialogue relative to a possible working relation. Please contact me relative to a demonstration.

Sincerely,

Dr. Walter Frost, P.E.  
President

Figure 6.1 Letter seeking joint working relationship.

**Table 6.1 Companies Solicited for Potential Joint Ventures**

Alden Electronics, Inc. 40 Washington Street Westborough, MA 01581	IN USA, Inc. 23 Farwell Street Newtonville, MA 02160
Atmospheric Instrumentation Research, Inc. (AIR) 8401 Baseline Road Boulder, CO 80303	Lightning Location and Protection, Inc. 2705 E. Medina Road Suite 111 Tucson, AZ 85706
Atmospheric Research Systems, Inc. 2350 Commerce Park Drive, N.E. Suite 3 Palm Bay, FL 32905	Media Imaging Technologies Corp. 2340 East Trinity Mills Road Suite 300 Carrollton, TX 75006
Climatronics Corporation 140 Wilbur Place Bohemia, NY 11716	Orbital Sciences Corporation 12500 Fair Lakes Circle Suite 350 Fairfax, VA 22033
COMET P.O. Box 3000 Boulder, CO 80307-3000	Radian Corporation P.O. Box 201088 Austin, TX 78720
Control Data Corporation Meridian Environmental Technologies, Inc. 8100 34th Avenue South Mail Drop HQBO 2T Minneapolis, MN 55425-1640	REMTECH, Inc. 1044 Townley Circle Longmont, CO 80501
Computer Sciences Corporation Virginia Technology Center 3170 Fairview Park Drive Falls Church, VA 22042	The Republic Group 5801 Lee Highway Arlington, VA 22207
Dimensions 91194 - St. Aubin cedex R.C.S. Corbeil-Essonnes - B 348 368 457	R.M. Young Company 2801 Aero-Park Drive Traverse City, MI 49684
Enterprise Electronics Corporation 128 South Industrial Blvd. Enterprise, AL 36330	Scientific Technology, Inc. (ScTI) 2 Research Place Rockville, MD 20850
GTE Contel Federal Systems 15000 Conference Center Drive Chantilly, VA 22021-3808	Setra Systems, Inc. 45 Nagog Park Acton, MA 01720
General Sciences Corporation 6100 Chevey Chase Drive Suite 200 Laurel, MD 20707	Sutron Corporation 2190 Fox Mill Road Herndon, VA 22071
Handar, Inc. 1188 Bordeaux Avenue Sunnyvale, CA 94089	Unisys Defense Systems, Inc. Shipboard and Ground Systems Group Great Neck, NY 11020-1696
Harris Corporation Government Information Systems Division P.O. Box 98000 Melbourne, FL 32902	Vaisala, Inc. 100 Commerce Way Woburn, MA 01801
	Zephyr Weather Information Service 40 Washington Street Westborough, MA 01581

and testing. Cost and time to repurchase equipment and produce another prototype would prohibit this small company from achieving a marketable product unless the instrument and ancillary equipment acquired under the Phase II contract is retained.

Production of this system would establish a product line of instruments for FWG and allow it to pursue further commercial applications. These results most effectively achieve the goals of the SBIR program by increasing private sector commercialization of innovated research. To quote Harry W. Johnson, Director of the NASA SBIR program, "One major national objective for the SBIR program is broad commercial applications for the results of R&D sponsored by the Federal government and performed by small businesses"<sup>[10]</sup>.

FWG is prepared to make a quick transition to commercial applications of the Phase II results. The availability of the prototype instrument as a marketing tool will assist FWG to begin demonstration immediately. The ancillary equipment for initial construction of the instrument is adequate for further development and to build a few units for immediate sale. Obviously, the ability to demonstrate the innovation system's working capability will significantly enhance solicitation of Phase III funding from the commercial sector.

The prototype instrument is a field tested unit, however, it is still in a research and development status and requires modification to be commercialized. It can be utilized as a research tool, but it will require additional manpower to perfect the unit and develop the modifications necessary to extend its use to other marketable applications. These other applications would emphasize the portability and mobility of the sensor head. For instance, it can be carried aloft and used to remotely monitor particulates from smoke stacks, measure raindrops and rate from aboard ships, and other highly innovative and

unique applications. The features of the system which allow the sensor head to be miniaturized and operated at large distances from the processor and power supply through the use of fiber optic cables is the truly innovative aspect of the prototype. FWG believes this is a highly marketable feature.

Although FWG is in a position to begin commercialization with in-house funds, other sources of capital will be sought. The Tennessee Technology Foundation is a possible source to identify available venture capital. FWG has had contact with this group in the past. The Tennessee Technology Foundation (TTF) is a private, nonprofit corporation chartered in 1982 for the purpose of promoting and supporting technology-based economic growth. Its charter provides for a mission that is statewide in scope. Consequently, in recent years, a significant amount of its resources have been devoted to its statewide mandate.

The Foundation attempts to fulfill its mission in two fundamental ways: First, it provides very specialized support to economic development organizations in targeting and recruiting high-tech industrial prospects. Second, it supports technology transfer from private and public research institutions brought to the marketplace and converted to business opportunities. In this role, the focus is on entrepreneurship and technology-based small business start-ups or expansions.

Specific services provided by TTF include: Siting and location analysis assistance; brokering technological research facilities and talent; interagency coordination of joint efforts to site national and international research centers; assistance in facilitating a rapid but effective transition into the corridor's and state's technical and business communities; new product/process commercialization assistance, and technical assistance to entrepreneurs, including the brokering of venture capital and other financial resources.

FWG plans direct contact with the president of TTF.

Other sources of venture capital within Tennessee include:

Tennessee Venture Capital Network  
7 Cope Administration Building  
Middle Tennessee State University  
Murfreesboro, TN 37132  
(615) 898-2100 / 1-800-344-TVCN

State of Tennessee  
Department of Economic and Community Development  
Tenth Floor, Andrew Jackson State Office Building  
Nashville, TN 37219  
(615) 741-1888

Outside of Tennessee, a list of over one hundred potential sources of follow-on funding for Small Business Innovation Research (SBIR) participants has been obtained from SBA's Commercialization Matching System (CMS). All organizations on this list have expressed an interest in technologies or industries related to SBIR activities and in considering opportunities in FWG's geographical area.

CMS is designed to implement and speed a basic aim of the SBIR program; the conversion of research into commercial applications and products through the use of non-Federal sources of capital. FWG is reviewing and attempting to establish contact with appropriate sources of capital and to conduct negotiations based on mutual interest.

#### **6.4 Potential Markets**

Potential markets include both the government and private industry sectors. The RRS is suitable, or could easily be adapted to suit many applications, of interest to these agencies as listed below.

##### **• Applications**

- Measuring rainfall rate and broad range droplet size distributions
- Support satellite missions to measure tropical rainfall
- Quantitative measurements of droplet cloud uniformity
- Measurements to support cloud physics and parameterization studies
- Measure water droplet size distribution in a variety of test cells
- Monitor spatial distribution of liquid water content (LWC) in icing tests
- Measurements for inlet contamination and exhaust particles for jet engines
- Spatial distribution of particles surrounding rocket engines

- Environmental measurements to monitor stack emissions for particulates
- Particle size measurements to analyze nozzle erosion in arc facilities
- Future applications to sounding rockets
- Particle size measurements for determining optimum smokes and obscurants for defeating lidar for millimeter wave radar targeting systems

A marketing letter (Figure 6.2), a brief questionnaire (Figure 6.3), and a mini-brochure (Figure 6.4), which describes (and pictures) the RRS and lists numerous applications, have been prepared. This packet has been sent, or is being sent, to various private companies and government agencies, a partial list of which is given in Table 6.2.

### **6.5 Outline of Development and Production Plan**

- Step 1: The initial step has been taken by requesting NASA to allow FWG Associates, Inc. to retain the prototype system, as well as the equipment obtained by FWG with contract funding to produce a modified prototype and for initial production.
- Step 2: The steps to seek a joint venture relationship with companies are under way.
- Step 3: Carry out some redesign and modifications to the prototype (this is contingent on retaining title to the RRS and to equipment used to construct and test the initial prototype).
- Step 4: Send out brochures and contact possible users.
- Step 5: Demonstrate the system to prospective users and buyers (this is contingent upon retaining title to the prototype system).
- Step 6: Setup a production system and a marketing strategy.

The above is the ideal plan and would be adjusted accordingly to which steps are successful and which are not.

Dear Sir:

FWG Associates, Inc. is announcing the new Rain Rate and Droplet Size Spectrometer "Distrometer". The unique feature of this instrument is that the sensing heads can be remotely positioned from the power supply and the data processing equipment through optical fiber cables. This allows measurements of rain rate to be made out of the region where spray from trees, splashing from objects, swirling winds due to terrain features or ship structures, spray from breaking wakes, etc. could contaminate the measurement. Moreover, deploying the sensor head with a parafoil, kite, or balloon allows probing of smokestacks, or plumes behind cooling towers, etc. enabling spatial and temporal profiles of droplet and/or particle size distributions to be measured. Specifics of the instrument are provided on the attached data sheet.

This new instrument is available to solve your particle flux rate and particle size distribution measurement needs, both from a research and an operational mode. If you have any questions regarding the instrument, please call FWG Associates, Inc. at the above address.

Sincerely,

Dr. Walter Frost, P.E.  
President

Figure 6.2 Marketing letter to accompany brochure.

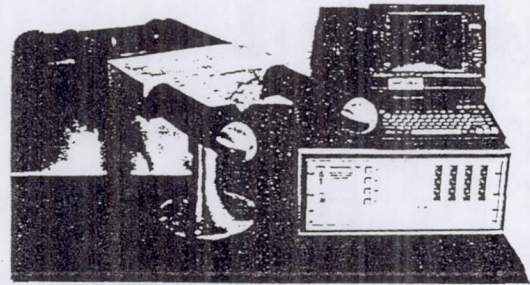
### QUESTIONNAIRE

- |    |  |     |    |
|----|--|-----|----|
| 1. | Do you think a sensor of this kind is needed?  | Yes | No |
| 2. | Would you be willing to market this sensor?  | Yes | No |
| 3. | Would you invest funds in producing this sensor?   | Yes | No |
| 4. | Do you need an instrument to measure rain rate in your work?                                 | Yes | No |
| 5. | Do you need an instrument for measuring droplet or particle size distribution "distrometer"? | Yes | No |
| 6. | Would you like to see more information on this system?                                       | Yes | No |
| 7. | Would you be willing to produce this system?   | Yes | No |
| 8. | Do you have any questions about this system?<br>(List them below.)                           | Yes | No |

Figure. 6.3 Questionnaire designed for a marketing study.

## GENERAL INFORMATION

FWG's Rain Rate and Droplet Size Spectrometer is an optical sensor capable of determining rain droplet size distributions and rainfall rates in near real time. The unique feature is that the optical head is remotely located from the power source and data processor system. All power and data transfer is carried out through an optical fiber bundle.



*Rain Rate and Droplet Size Sensor  
--- That Works*

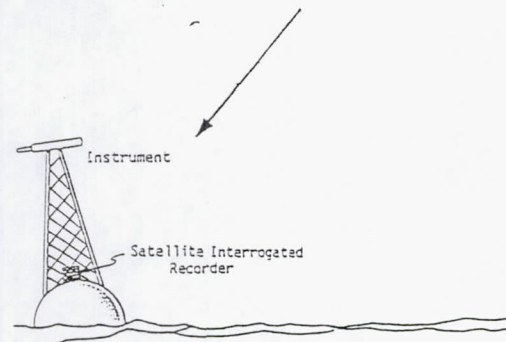
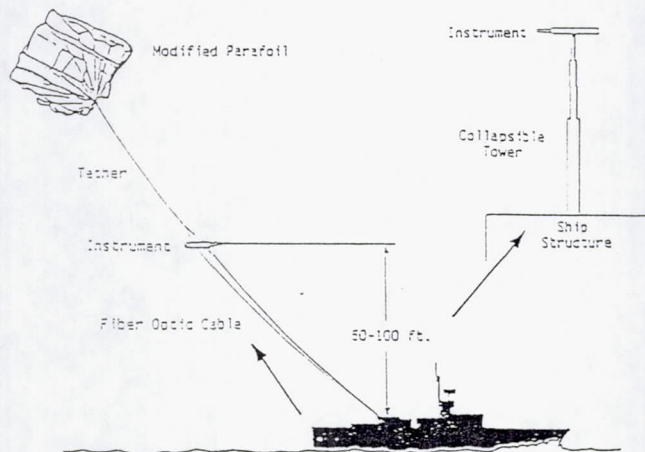
Sensor Instrumentation

## FEATURES

- Designed for use in Remote and Hostile Environments
- Precise and Reliable
- Rugged
- Real Time Droplet Size and Rate
- History of Precipitation Measurements
- Direct Read-Out
- PC Compatible Software

## APPLICATIONS

- Operational Monitoring
- Research Field Programs
  - Climate Studies
  - Wetland Analyses
  - Marine Environments
  - Oceans (from shipboard)
  - Flood Control



Potential Deployment Techniques for  
Rain Rate Measurements at Sea



FWG ASSOCIATES, INC.

217 Lakewood Drive  
Tullahoma, TN 37388  
Telephone (615) 455-1982  
FAX (615) 455-1805

Figure 6.4 Mini-brochure on RRS.

**Table 6.2 Customers From the Government and Private Sectors**

Mr. Donald R. Thornley  
 U.S. Army Test and Evaluation Command  
 TECOM White Sands Meteorological Team  
 AMSTE-TC-AM (WS)  
 White Sands Missile Range, NM 88002-5501

Mr. Robert Olsen  
 U.S. Army Atmospheric Sciences  
 Laboratory/SLCAS-AS-M  
 White Sands Missile Range, NM 88002-5501

Mr. Don Godwin  
 Kwajalein Missile Range/CSSD-KA-RI  
 P.O. Box 26  
 APO San Francisco 96555-2526

Mr. Kiyoji Tomita, Site Manager  
 Aeromet, Inc.  
 P.O. Box 67  
 APO San Francisco 96555

Mr. Dean S. Weingarten  
 U.S. Test and Evaluation Command  
 TECOM Yuma Meteorological Team  
 AMSTE-TC-AM (YU)  
 Yuma, AZ 85365-9102

Mr. Thomas O. McIntire  
 U.S. Army Yuma Proving Ground  
 STEYP-MT-I  
 Yuma, AZ 85365-9110

Mr. Steve W. Bieda, Jr.  
 U.S. Army Test and Evaluation Command  
 Director for Technology  
 TECOM Fort Huachuca Meteorological Team  
 /AMSTE-TC-AM (HU)  
 Fort Huachuca, AZ 85613-7110

Mr. Chris Biltoft  
 U.S. Army Dugway Proving Ground  
 STEDP-MT-M, Meteorological Division  
 Dugway, UT 84022-5000

Mr. Glen Boire  
 730 WS/CC  
 Vandenberg AFB, CA 93437-6021

Mr. Charles W. Fain  
 45 MS/MAD  
 Patrick AFB, FL 32925

Mr. Harold C. Herring  
 CSR 4600  
 Computer Sciences Raytheon  
 P.O. Box 4127  
 Patrick AFB, FL 32925-0127

Mr. Luis A. Padilla  
 45 MS/MAB  
 Patrick AFB, FL 32925

Col. John T. Madura, USAF  
 45 WS/CC  
 Patrick AFB, FL 32925

Mr. Billie F. Boyd  
 45 WS/WER  
 Patrick AFB, FL 32925

Lt. Col. Robert Hughes, USAF  
 AFFTC/WE  
 Edwards AFB, CA 93523-5000

Capt. Richard M. Harter, USAF  
 Det 6/17WS  
 Hill AFB, UT 84056-5000

Mr. Philip O. Harvey  
 AFFTC/WE  
 Edwards AFB, CA 93523-5000

Mr. Edward J. Keppel  
 AFDTTC/WE  
 Eglin AFB, FL 32542-5000

Capt. Robert M. Fogarty, USAF  
 6585 TESTG/WE  
 Holloman AFB, NM 88330-5000

Lt. Col. Joel D. Bonewitz, USAF  
 AFDTTC/WE  
 Eglin AFB, FL 32542-5000

Mr. Joseph Kerwin  
 AFDTTC/WE  
 Eglin AFB, FL 32542-5000

Capt. Arthur J. Nelson, USAF  
 HQ CSTC/WE  
 P.O. Box 3430  
 Onizuka AFB, CA 94088-3430

Capt. Eric W. Hatfield, USAF  
 HQ CSTC/WE  
 P.O. Box 3430  
 Onizuka AFB, CA 94088-3430

Capt. Tim Oram, USAF  
 Det 16, 25 WS  
 Nellis AFB, NV 89191-5000

Mr. Lloyd S. Corbett  
 Naval Weapons Center  
 Code 62542  
 China Lake, CA 93555-6001

Table 6.2 (Continued)

Mr. J.J. Genola ERAI 132 Gemstone Ridgecrest, CA 93555-9577	Lt. Col. M. Abel, USAF ESD/WE Hanscom AFB, MA 01731-5000
CPO Randall Landis, USN Naval Oceanography Det. Code 92 China Lake, CA 93555-6001	Lt. Col. Winston Crandall, USAF PL/WE Kirtland AFB, NM 87117
Mr. Darwin Tolzin PMTC - Code 3252 Point Mugu, CA 93042-5000	Maj. John Roadcap, USAF WL/DOW Wright-Patterson AFB, OH 45433
Mr. Leander F. Hall PMTC - Code 3254 Point Mugu, CA 93042-5000	Maj. J. Nuss, USAF USAFETAC/DO Scott AFB, IL 62225
Lt. Richard Kren, USN Officer-In-Charge Naval Oceanography Command Detachment Naval Air Station Patuxent River, MD 20670-5304	Maj. Thomas B. Dunmire, Jr. USAF BMO/WE Norton AFB, CA 92409-6468
Col. F. Hauth, USAF Office of Federal Coordinator for Meteorology Suite 900, 6010 Executive Blvd. Rockville, MD 20852	Lt. Ronald Comoglio, USAF ASD/WE Wright-Patterson AFB, OH 45433
CDR Robert Showalter, USN Office of Federal Coordinator for Meteorology Suite 900, 6010 Executive Blvd. Rockville, MD 20852	Mr. F.J. Schmidlin NASA/Goddard Space Flight Center Wallops Flight Facility Code 972 Wallops Island, VA 23337
Mr. James F. Morrissey GP/LYR Hanscom AFB, MA 01731	Mr. Kelly Hill NASA/Marshall Space Flight Center Mail Code ED-44 Atmospheric Effects Branch Huntsville, AL 35812
Mr. Gilbert K. Phelps HQ AFSC/WEO Andrews AFB, Washington, DC 20334-5000	Mr. Tim Wilfong NASA/Marshall Space Flight Center Mail Code ED-44 Huntsville, AL 35812
Lt. Col. Joseph Bassi, USAF SSD/WE P.O. Box 92960, LAAFB Los Angeles, CA 90009	Dr. Jack Ernst HQ, NASA/Weather Support Office Mail Code: MOW Washington, DC 20546
Maj. Jack Davidson, USAF SSD/WE P.O. Box 92960, LAAFB Los Angeles, CA 90009-2960	Col. John Upchurch, USAF HQ, NASA/Weather Support Office Mail Code: MOW Washington, DC 20546
Capt. Amy Chalfant, USAF ESD/WE Hanscom AFB, MA 01731-5000	Mr. Richard Cram Federal Building, E/CC11 Asheville, NC 28801
	Capt. Pat Hayes, USAF Det 9, HQ, AWS P.O. Box 12297 Las Vegas, NV 89112-0297

Table 6.2 (Continued)

HQ Air Weather Service  
AWS/DOZ  
Scott AFB, IL 62225-5001

Maj. Anita F. Dye, USAF  
4WW/Space Launch & Range Spt Sec  
Peterson AFB, CO 80914-5000

Capt. Carl Hoffman, USN  
PMW-141, SPAWARS  
Environmental Systems Office  
Washington, DC 20363

Mr. Mark Fair  
NOAA Weather Serv Nuclear Spt Ofc  
P.O. Box 94227  
Las Vegas, NV 89193

Mr. H.W. Church  
Sandia National Laboratories  
P.O. Box 5800, Division 6321  
Albuquerque, NM 87185-5800

Mr. R. Stone  
NOAA/NWS R.D. # 1, Box 105  
Sterling, VA 22170

LCDR Pat Salts, USN  
Naval Oceanography Command  
Code N512  
Stennis Space Center, MS 39529-5000

Capt. Robert Plant, USN  
Chief of Staff  
Naval Oceanography Command  
Stennis Space Center, MS 39529-5000

Mr. Robert Smith  
Center for Night Vision and E-O  
TECOM Fort Belvoir Met Team  
Fort Belvoir, VA 20660-5677

Mr. Ted Linn  
HQ AFOTEC/WE  
Kirtland AFB, NM 87117-7001

Capt. John M. Rogers, USAF  
HQ AFOTEC/WE  
Kirtland AFB, NM 87117-7001

Mr. Richard Hasbrouck  
Lawrence Livermore National Lab  
P.O. Box 808, L-154  
Livermore, CA 94550

MSgt Mike Dougherty, USAF  
6 WS/DOO  
Hurlburt Field, FL 32544-5000

## 7.0 REFERENCES

1. Knollenberg, R.G. and W.E. Neish (1969): "A New Electro-Optical Technique for Particle Size Measurements", Electro-Optical Systems Design Conference.
2. Knollenberg, R.G. (1970): "The Optical Array: An Alternative to Scattering or Extinction for Airborne Particle Size Determination", Journal of Applied Meteorology, Vol. 9, No. 1.
3. Knollenberg, R.G. (1972): "Comparative Liquid Water Content Measurements of Conventional Instruments with an Optical Array Spectrometer", Journal of Applied Meteorology, Vol. 11, 501.
4. Bentley, H.T. (1973): "Fiber Optics Particle-Sizing System", AEDC-TR-73-111.
5. Curry, M.J. (1979): "The Small-Particle Response of an Optical Array Precipitation Probe", Journal of Applied Meteorology, Vol. 18, 816.
6. Heymsfield, A.J. (1976): "Particle Size Distribution Measurement: An Evaluation of the Knollenberg Optical Array Probes", Atmospheric Technology, No. 8, 17.
7. Hovenac, E.A., E.D. Hirleman, and R.F. Ide: "Calibration and Sample Volume Characterization of PMS Optical Array Probes".
8. Jensen, D.R. (1983): "Intercomparison of Particle Measuring Systems, Inc's Particle-Size Spectrometers", Optical Engineering, Vol. 22, No. 6, 746.
9. Hess, W.N. (1974): Weather and Climate Modification, John Wiley & Sons, New York, NY.
10. Johnson, Harry W. (1991): NASA/Small Business Innovation Research (SBIR) Product Catalog, Washington, DC.
11. Banerjee, P.P. and T.C. Poon (1991): Principles of Applied Optics, Richard D. Irwin, Inc. and Aksen Associates, Inc., pp. 24-35.

## APPENDIX A

Appendix A contains various tables and drawings associated with the prototype rain rate sensor (RRS).

Table A.1 contains a listing of "off-the-shelf" parts required for the assembly of the RRS. This list of parts consist of parts that were purchased directly from various suppliers that required little or no modifications.

Table A.2 contains information on parts that were "custom-machined" for the RRS by various local machine shops. The shop drawings for each of the items listed in Table A.2 are also contained in this Appendix.

**Table A.1 "Off-The-Shelf" Parts List**

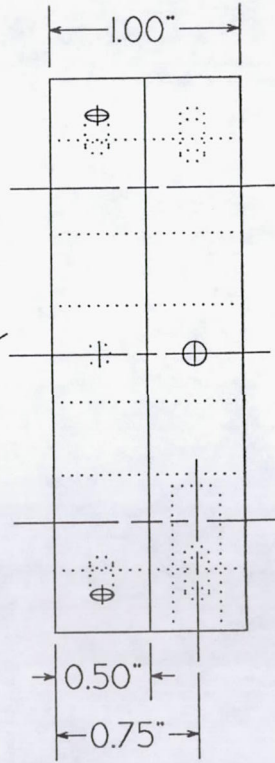
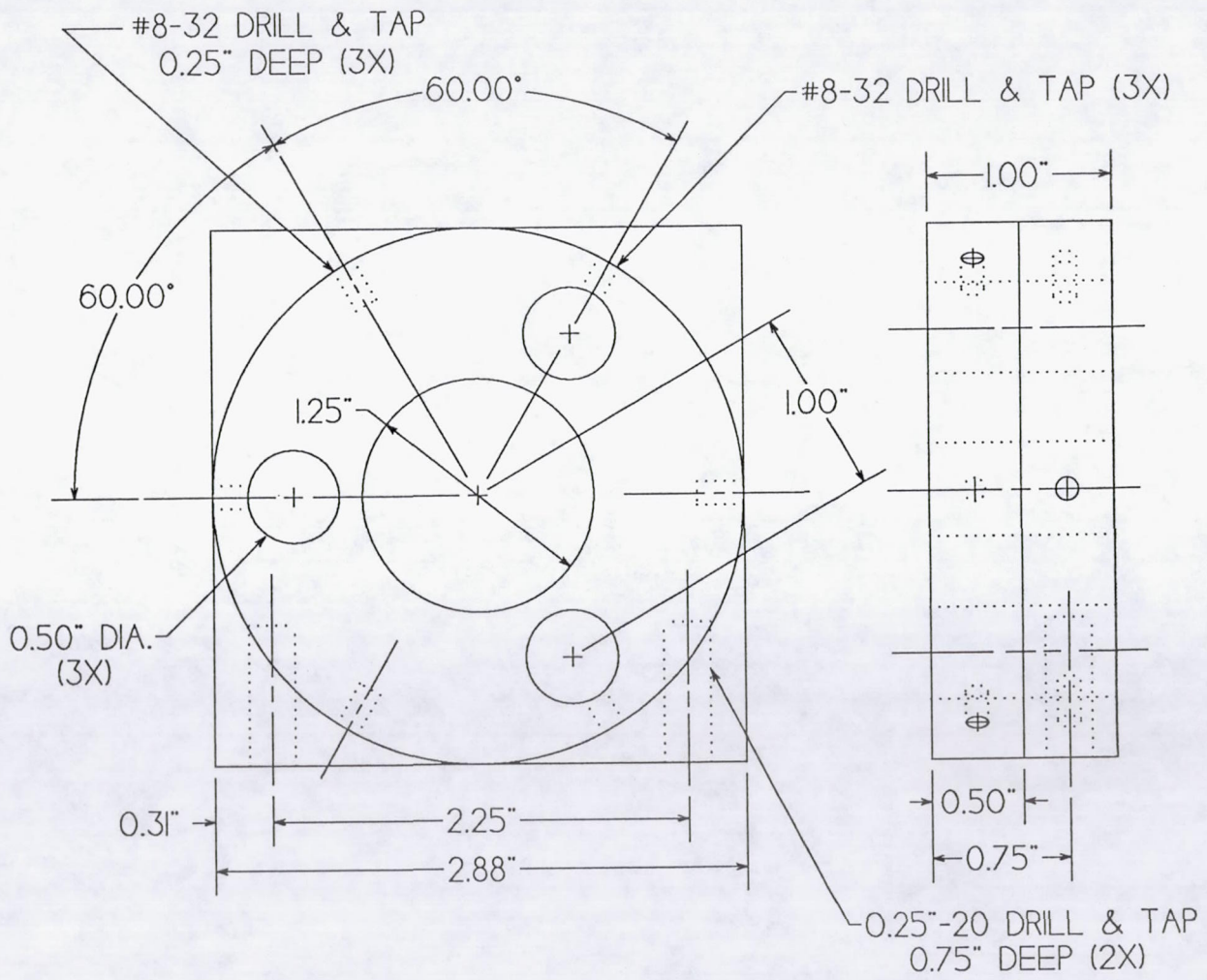
DESCRIPTION (QUANTITY)	PART NUMBER	SUPPLIER
Set-screws with recessed hex head #8-32 X 1/8" (42)	FWG-RR-S1	Hawk Hardware
Tube and Cover Screws #8-32 X 1/8" (26)	FWG-RR-S2	Hawk Hardware
Mounting bolts 1/4-20 X 1" (12)	FWG-RR-B1	Hawk Hardware
Thompson shaft 1/2" X 36" (6)	FWG-RR-004	Future Metals Inc.
Pedestal (1)	FWG-RR-007	Belle Pedestal

**Table A.2 "Custom-Machined" and Fabricated Parts List**

ITEM / DESCRIPTION (QUANTITY)	FWG PART NUMBER
Rod to Base Mounts (4)	FWG-RR-005
Mirror Base (4)	FWG-RR-016
Forward Tube (2)	FWG-RR-022
Forward Tube Cap (2)	FWG-RR-018
Aluminum Cover (1)	FWG-RR-030
Rearward Tube Window (2)	FWG-RR-028
Cylindrical Lens Mount (1)	FWG-RR-009
Window Tube (2)	FWG-RR-021
Base Plate (1)	FWG-RR-006
Fan Prism Mount (1)	FWG-RR-010
Fan Prism Assembly Mount (1)	FWG-RR-008
Mirror Holder Support (4)	FWG-RR-015
Magnifying Lens Holder (2)	FWG-RR-012
Array Holder (1)	FWG-RR-017
Mirror Mount (4)	FWG-RR-027
Rearward Tube (2)	FWG-RR-023
Fiber Array Mount (1)	FWG-RR-024
Magnifying Lens Retainer (2)	FWG-RR-013

The drawings on the following pages (pages A-4 through A-21) correspond to the parts listed in Table A.2 above.

A-4

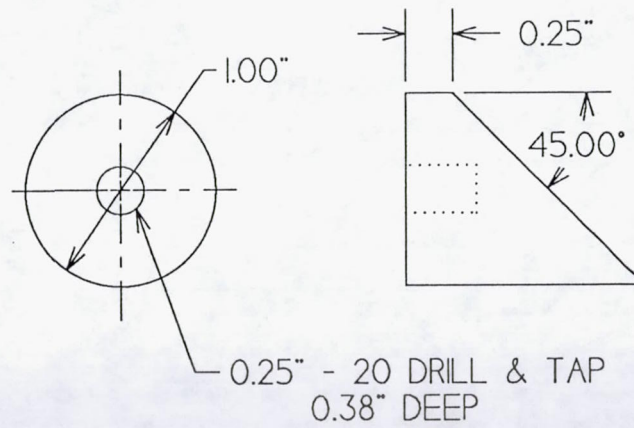


SCALE   :	DIMENSIONS IN INCHES	TITLE ROD TO BASE MOUNTS
MATERIAL ALUMINUM	TOLERANCES UNLESS NOTED	
	LINEAR +/- 0.01	PART ID FWG-RR-005
	ANGLES +/- 0.01	CADD6 FILE RR005

FWG ASSOCIATES, INC. DATE 03/13/92

QUANTITY 4

A-5



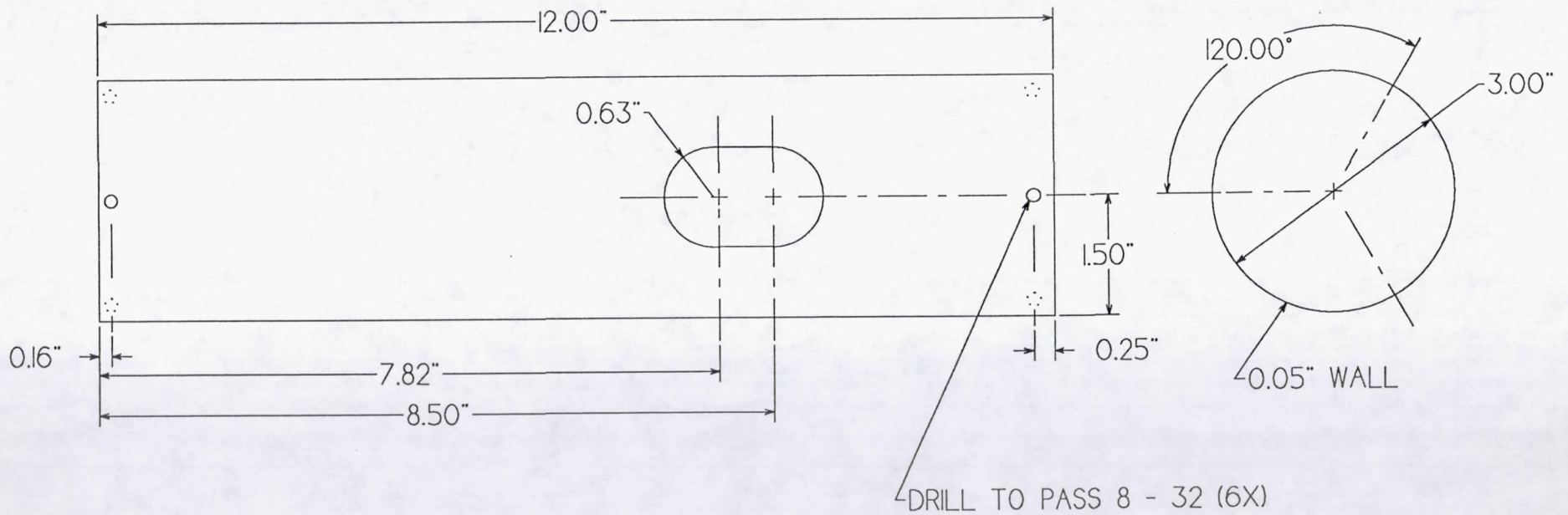
SCALE   :	DIMENSIONS IN INCHES	TITLE MIRROR BASE
MATERIAL ALUMINUM	TOLERANCES UNLESS NOTED	
	LINEAR +/- 0.01	PART D FWG-RR-016
	ANGLES +/- 0.01	CADD6 FILE RR016

FWG ASSOCIATES, INC.

DATE 03/13/92

QUANTITY 4

A-6

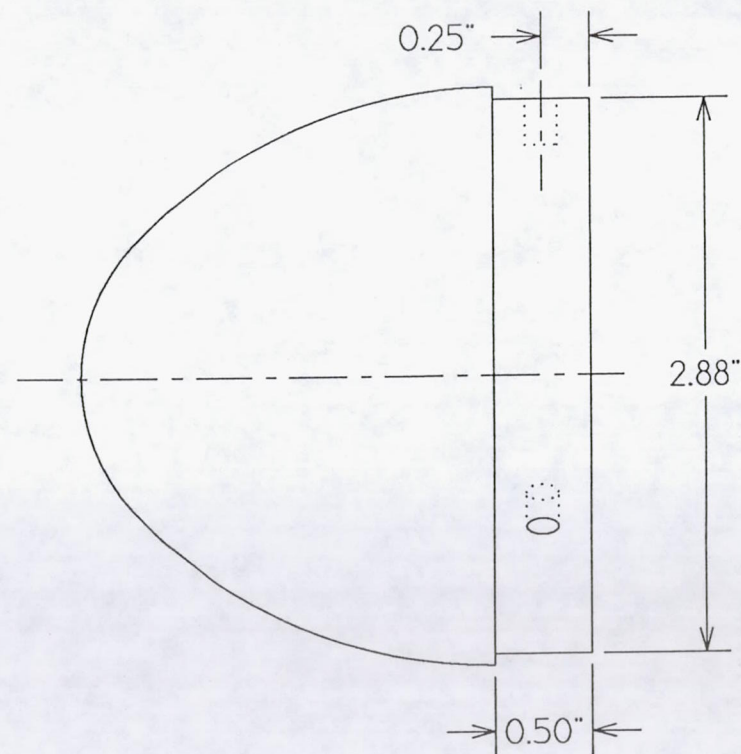
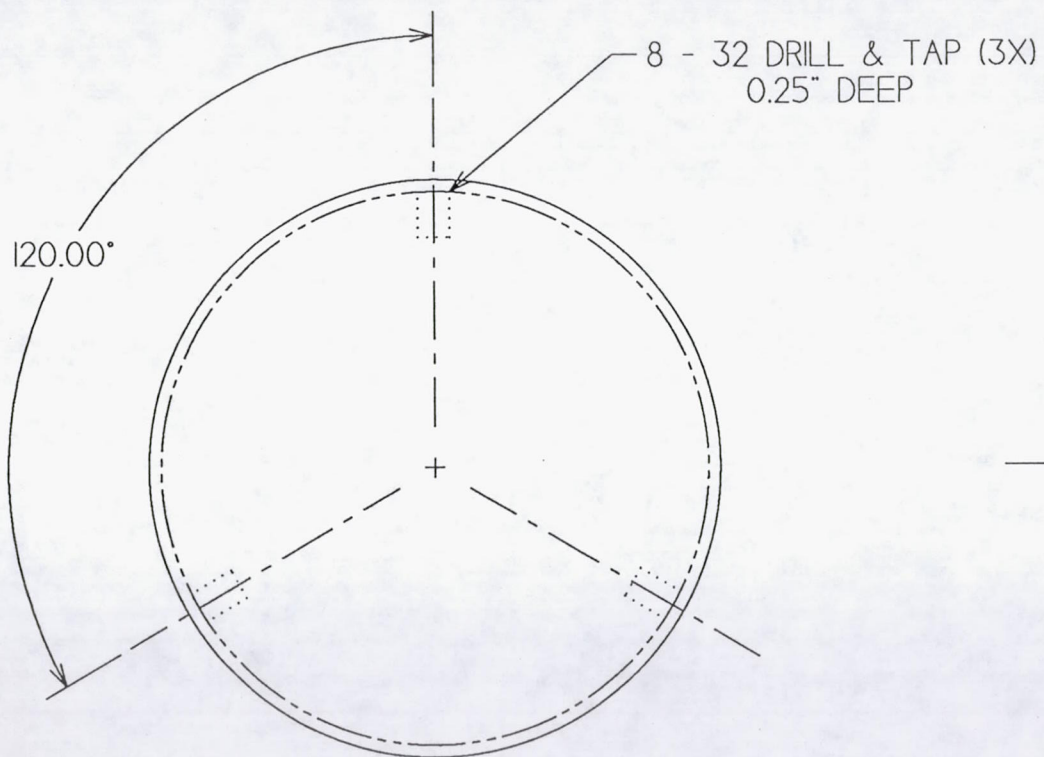


FWG ASSOCIATES, INC.

DATE 03/13/92

SCALE 1 : 2	DIMENSIONS IN INCHES	TITLE FORWARD TUBE
MATERIAL ALUMINUM	TOLERANCES UNLESS NOTED	
ANODIZED	LINEAR +/- 0.01	PART D FWG-RR-022
QUANTITY 2	ANGLES +/- 0.01	CADD6 FILE RR022

A-7



FWG ASSOCIATES, INC.

DATE 12/12/92

QUANTITY 2

SCALE 1 : 1

MATERIAL ALUMINUM

DIMENSIONS IN INCHES

TOLERANCES UNLESS NOTED

LINEAR +/- 0.01

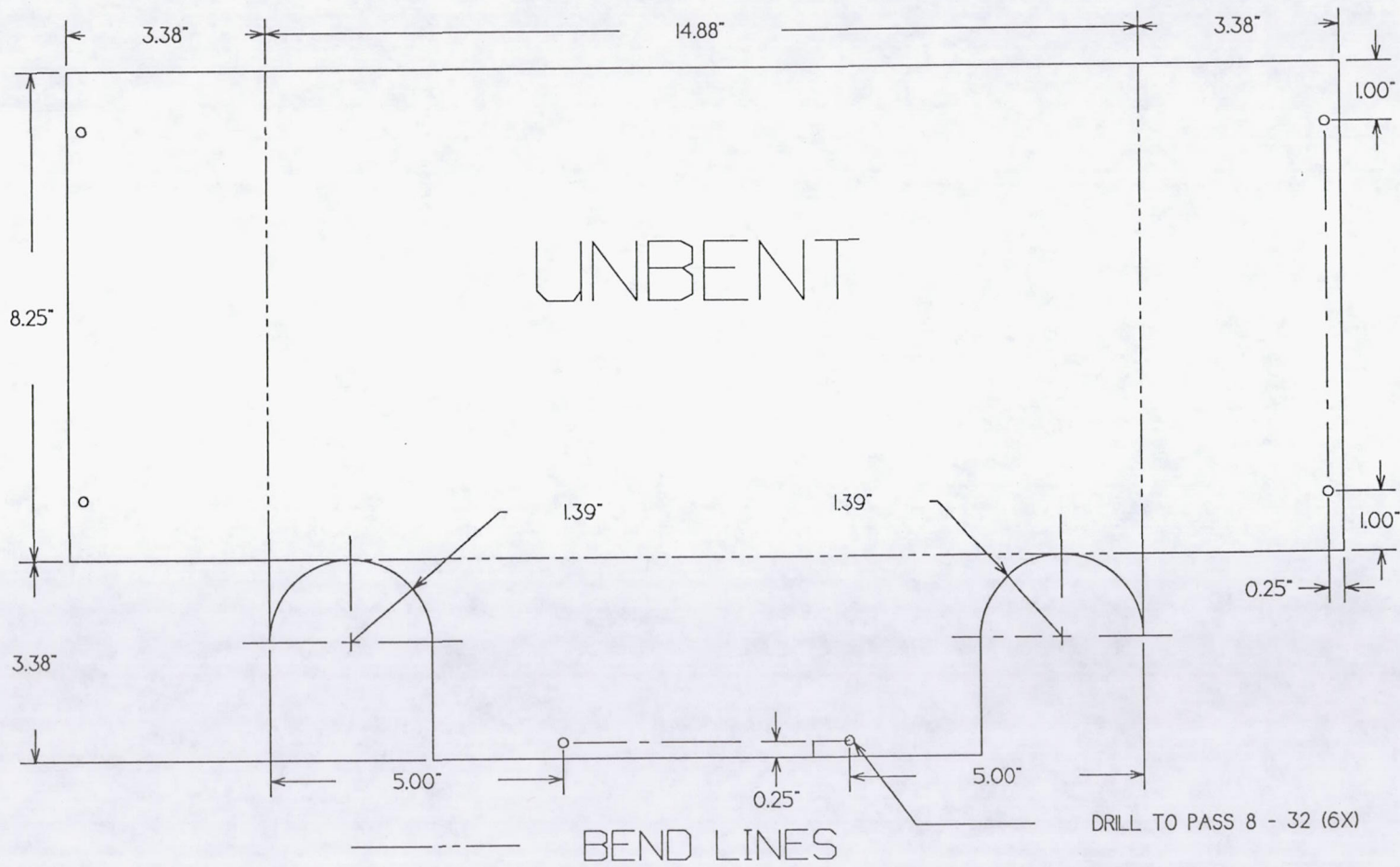
ANGLES +/- 0.01

TITLE FORWARD TUBE  
CAP

PART D FWG-RR-018

CADD6 FILE RR018

A-8

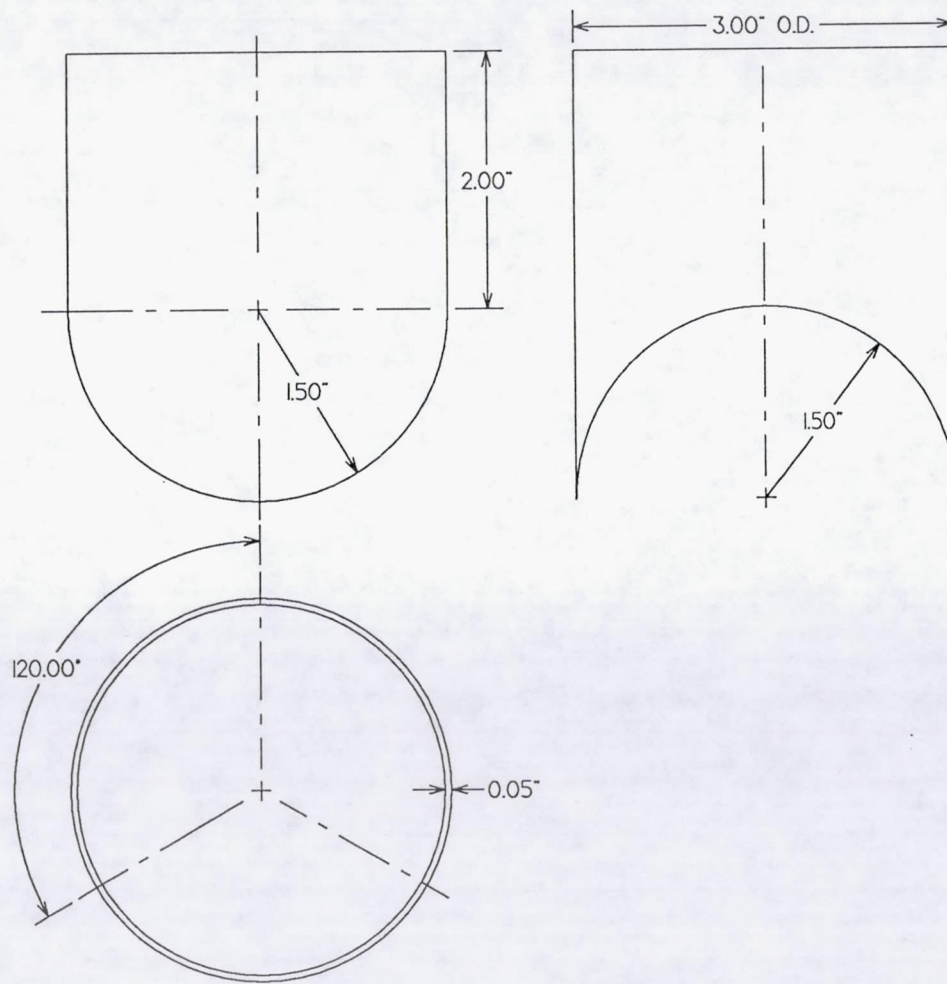


SCALE 1 : 3	DIMENSIONS IN INCHES	TITLE ALUMINUM COVER
MATERIAL ALUMINUM	TOLERANCES UNLESS NOTED	
ANODIZED	LINEAR +/- 0.01	PART ID FWG-RR-030
QUANTITY 1	ANGLES +/- 0.01	CADD6 FILE RRO30

FWG ASSOCIATES, INC.

DATE 03/13/92

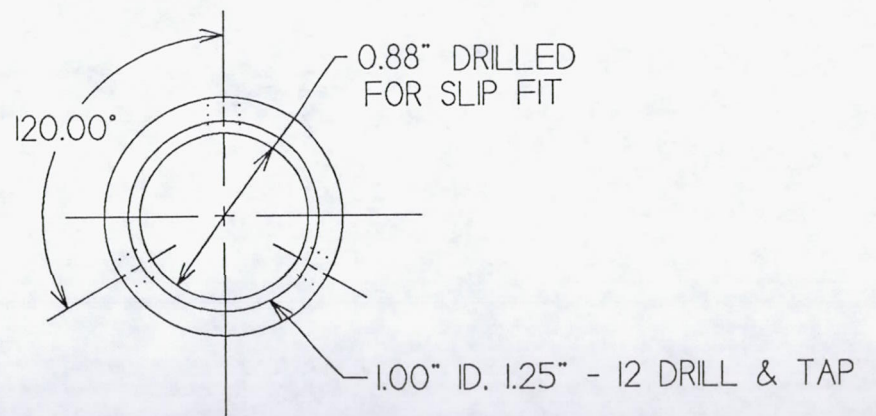
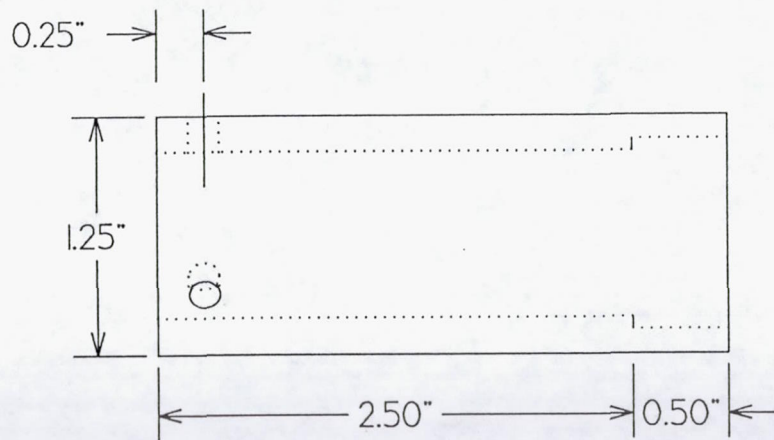
A-9



SCALE 1 : 1.5	DIMENSIONS IN INCHES	TITLE REARWARD TUBE WINDOW
MATERIAL ALUMINUM	TOLERANCES UNLESS NOTED	
ANODIZED	LINEAR +/- 0.01	PART ID FWG-RR-028
DATE 03/13/92	QUANTITY 2	CADD6 FILE RR028

FWG ASSOCIATES, INC.

A-10

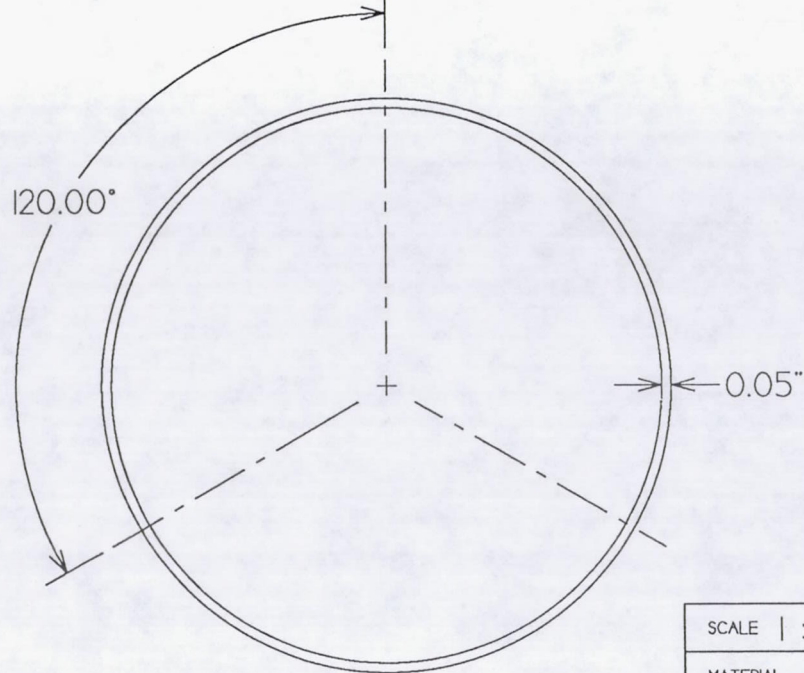
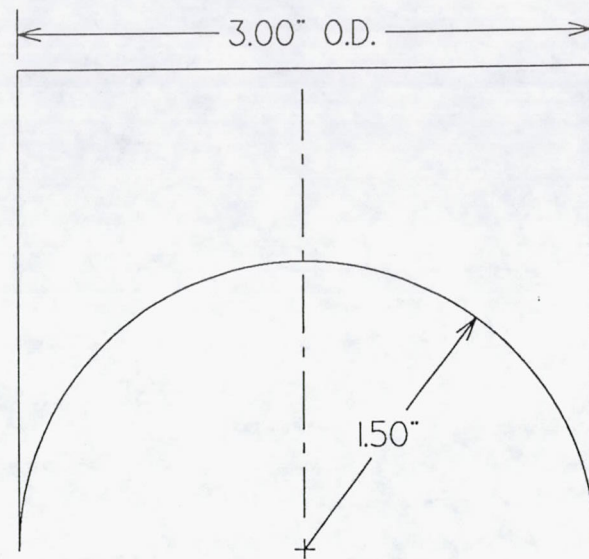
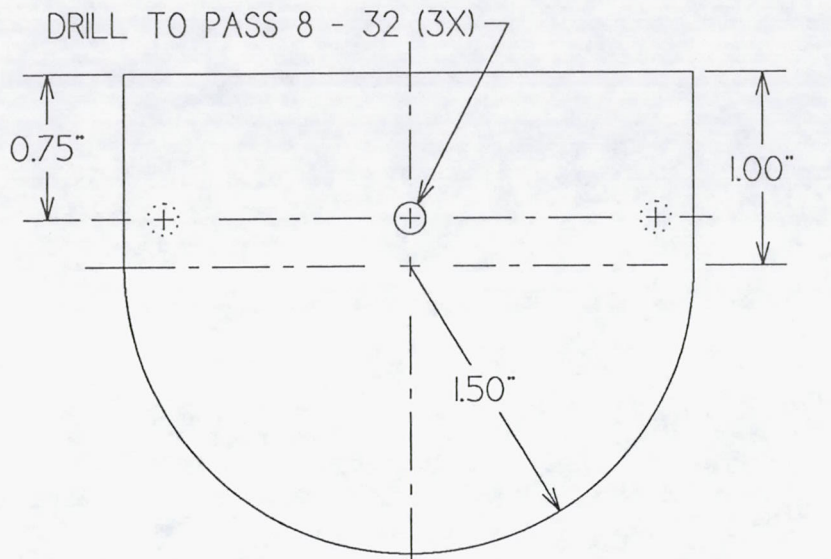


FWG ASSOCIATES, INC.

DATE 03/13/92

SCALE   :	DIMENSIONS IN INCHES	TITLE CYLINDRICAL LENS MOUNT
MATERIAL ALUMINUM	TOLERANCES UNLESS NOTED	
	LINEAR +/- 0.01	PART D FWG-RR-009
QUANTITY	ANGLES +/- 0.01	CADD6 FILE RR009

A-11

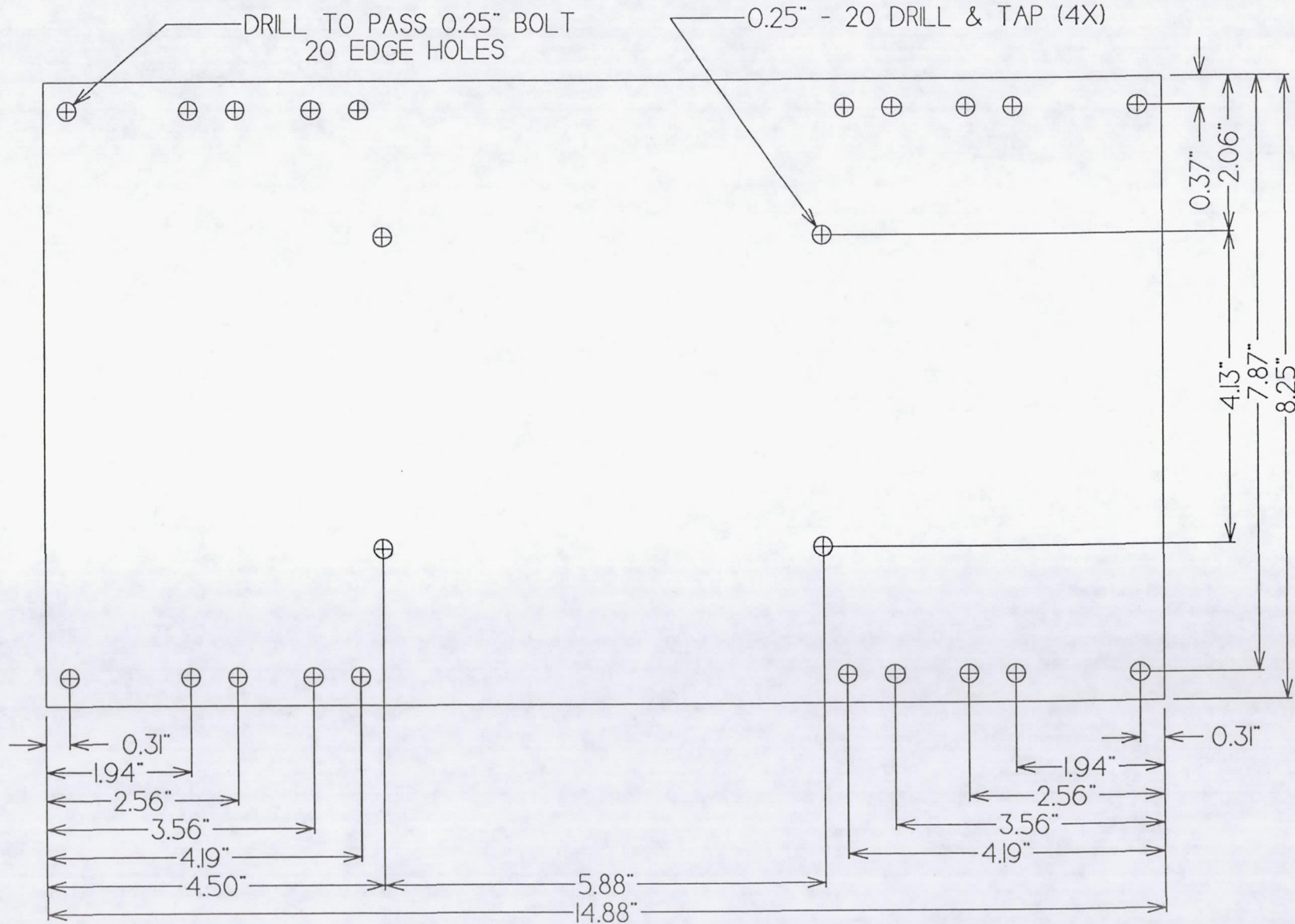


SCALE   :	DIMENSIONS IN INCHES	TITLE WINDOW TUBE
MATERIAL ALUMINUM	TOLERANCES UNLESS NOTED	
ANODIZED	LINEAR +/- 0.01	PART D FWG-RR-021
QUANTITY 2	ANGLES +/- 0.01	CADD6 FILE RR021

FWG ASSOCIATES, INC.

DATE 03/13/92

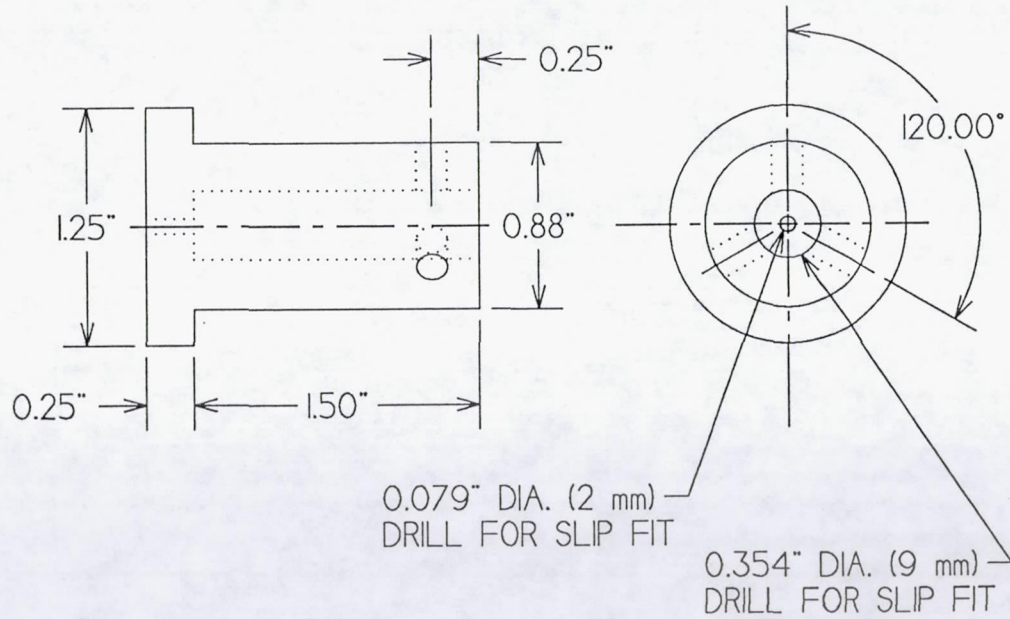
A-12



SCALE 1 : 2	DIMENSIONS IN INCHES	TITLE BASE PLATE
MATERIAL ALUMINUM	TOLERANCES UNLESS NOTED	
0.50" PLATE	LINEAR +/- 0.01	PART ID FWG-RR-006
QUANTITY 1	ANGLES +/- 0.01	CADD6 FILE RR006

FWG ASSOCIATES, INC. DATE 03/13/92

A-13



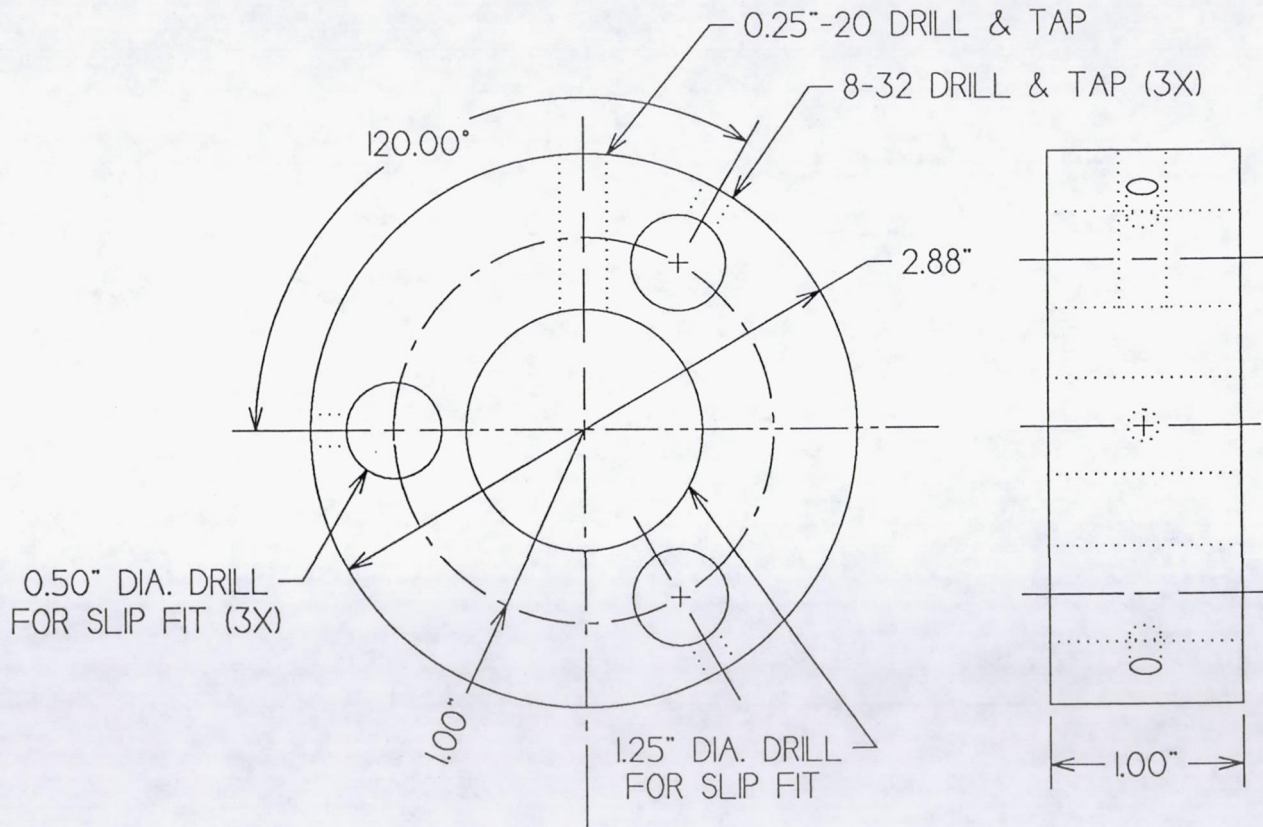
SCALE   :	DIMENSIONS IN INCHES	TITLE FAN PRISM MOUNT
MATERIAL ALUMINUM	TOLERANCES UNLESS NOTED	
	LINEAR +/- 0.01	PART ID FWG-RR-010
	ANGLES +/- 0.01	CADD6 FILE RRO10

FWG ASSOCIATES, INC.

DATE 03/13/92

QUANTITY |

A-14



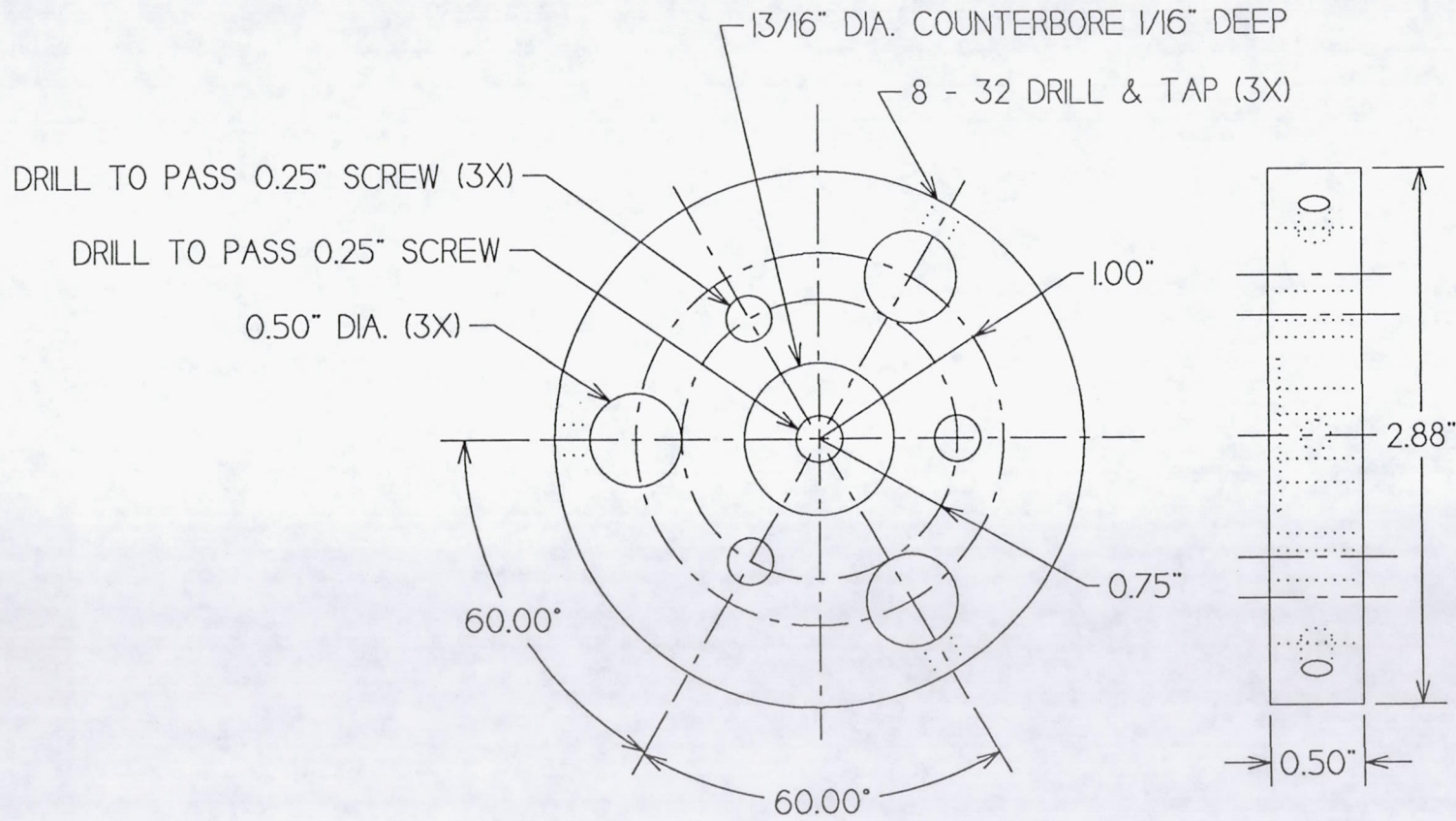
SCALE   :	DIMENSIONS IN INCHES	TITLE PRISM FAN ASSEMBLY MOUNT
MATERIAL ALUMINUM	TOLERANCES UNLESS NOTED	
	LINEAR +/- 0.01	PART D FWG-RR-008
	ANGLES +/- 0.01	CADD6 FILE RR008

FWG ASSOCIATES, INC.

DATE 03/13/92

QUANTITY |

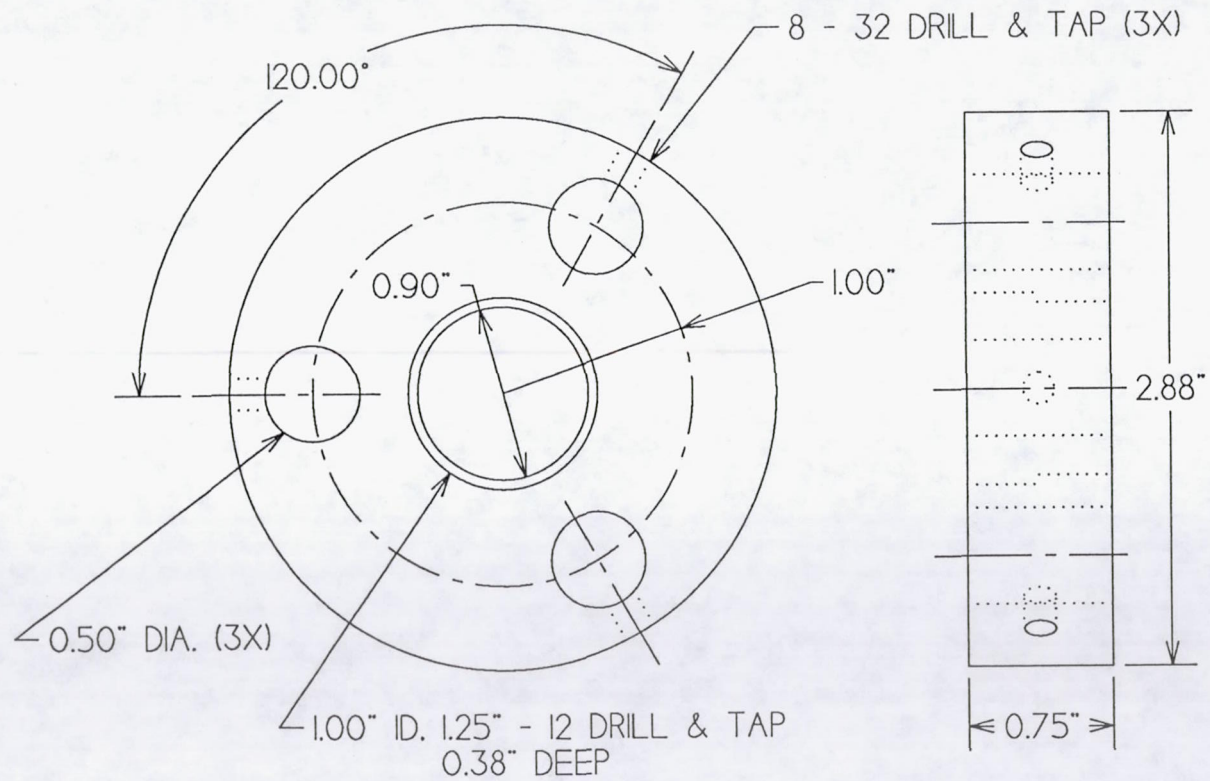
A-15



SCALE   :	DIMENSIONS IN INCHES	TITLE MIRROR HOLDER SUPPORTS
MATERIAL ALUMINUM	TOLERANCES UNLESS NOTED	
ANODIZED	LINEAR +/- 0.01	PART D FWG-RR-015
DATE 03/13/92	QUANTITY 4	CADD6 FILE RR015

FWG ASSOCIATES, INC.

A-16



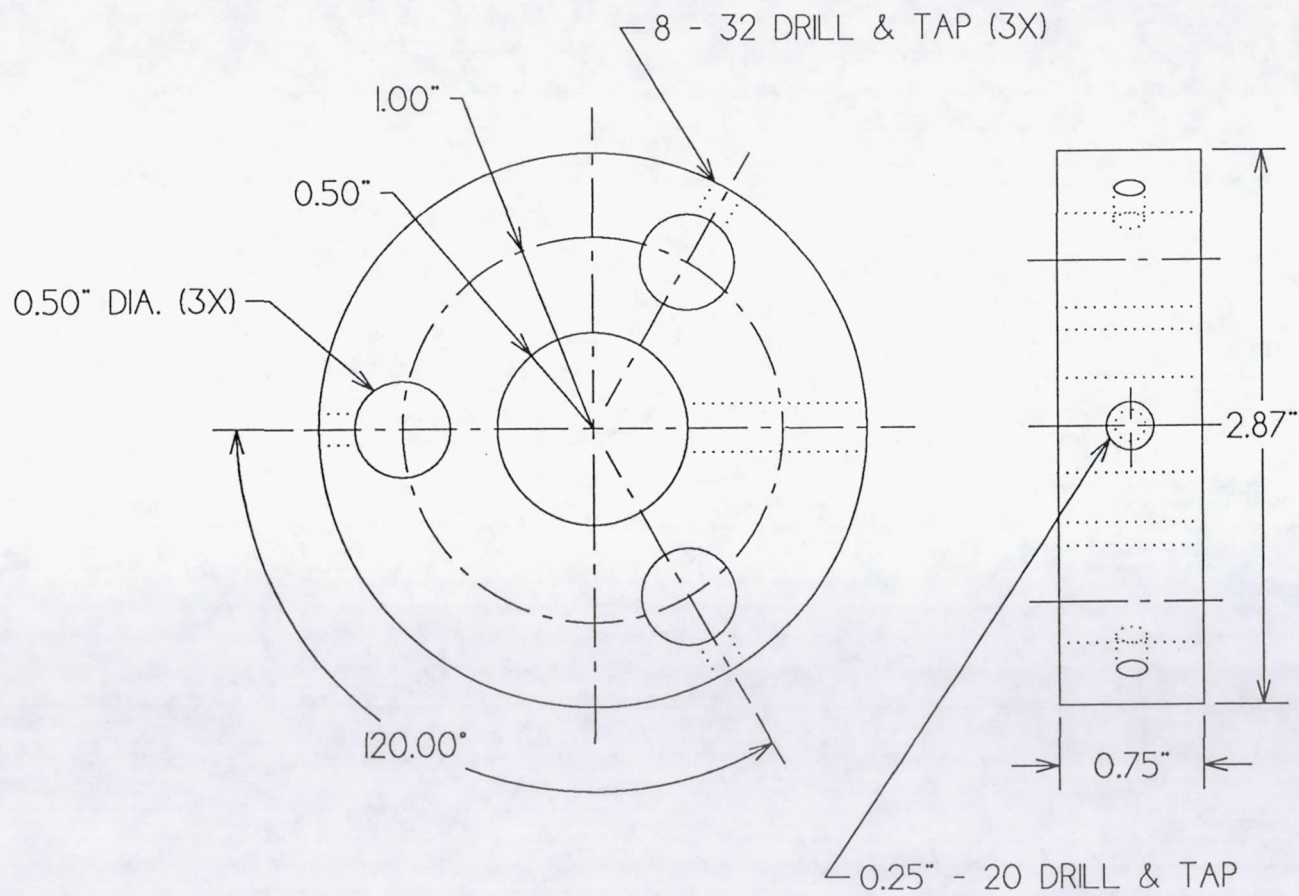
SCALE   :	DIMENSIONS IN INCHES	TITLE MAGNIFYING LENS HOLDER
MATERIAL ALUMINUM	TOLERANCES UNLESS NOTED	
	LINEAR +/- 0.01	PART D FWG-RR-012
	ANGLES +/- 0.01	CADD6 FILE RRO12

FWG ASSOCIATES, INC.

DATE 03/13/92

QUANTITY 2

A-17

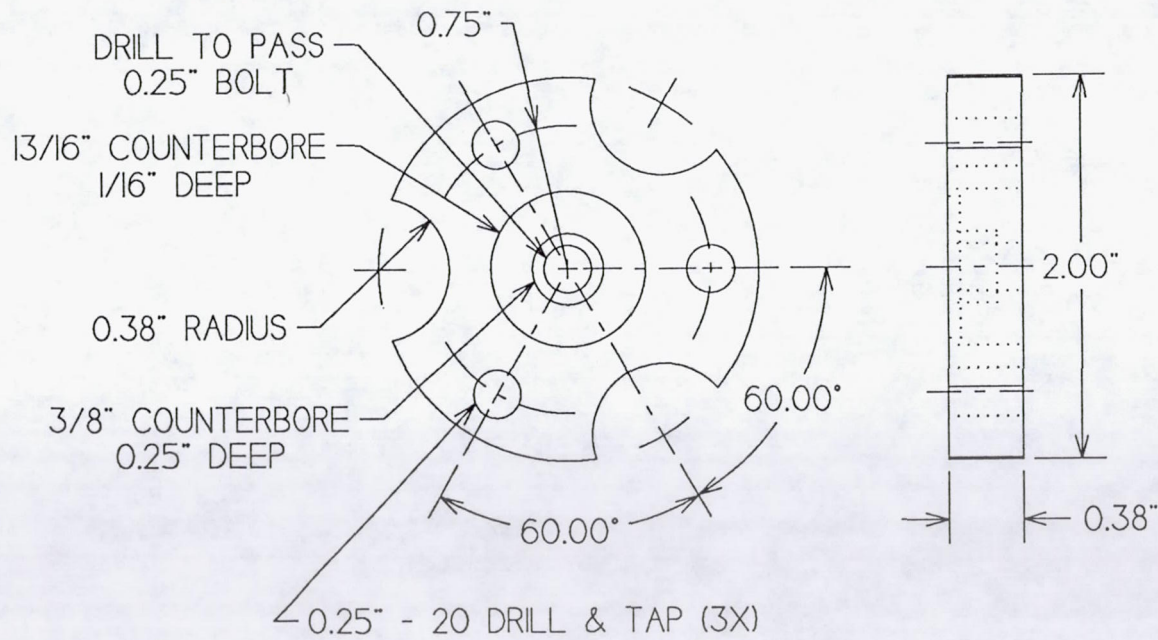


SCALE   :	DIMENSIONS IN INCHES	TITLE ARRAY HOLDER
MATERIAL ALUMINUM	TOLERANCES UNLESS NOTED	
ANODIZED	LINEAR +/- 0.01	PART ID FWG-RR-017
QUANTITY	ANGLES +/- 0.01	CADD6 FILE RRO17

FWG ASSOCIATES, INC.

DATE 03/13/92

A-18



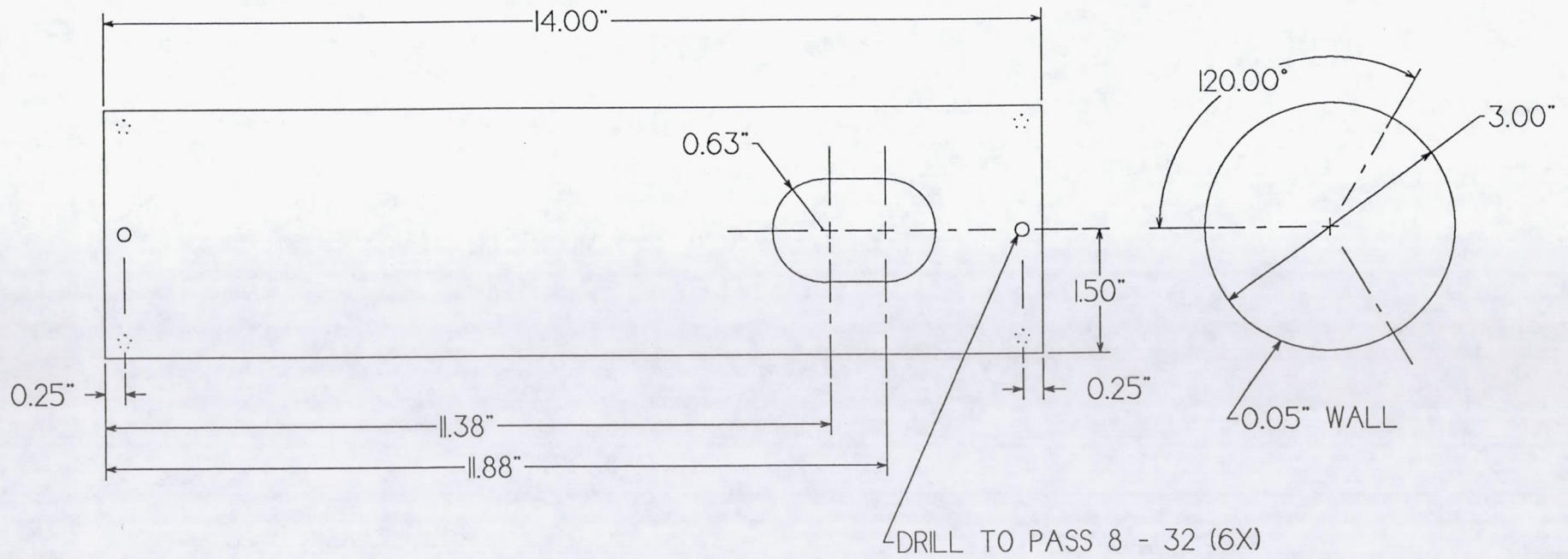
SCALE   :	DIMENSIONS IN INCHES	TITLE MIRROR MOUNT
MATERIAL ALUMINUM	TOLERANCES UNLESS NOTED	
	LINEAR +/- 0.01	PART D FWG-RR-027
	ANGLES +/- 0.01	CADD6 FILE RR027

FWG ASSOCIATES, INC.

DATE 03/13/92

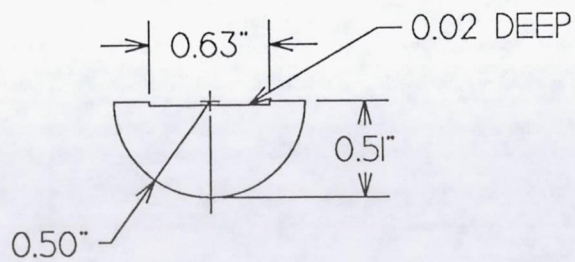
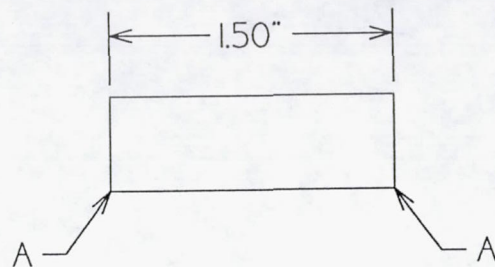
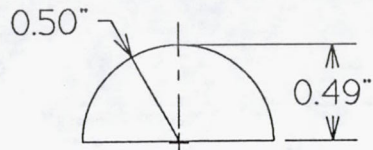
QUANTITY 4

A-19

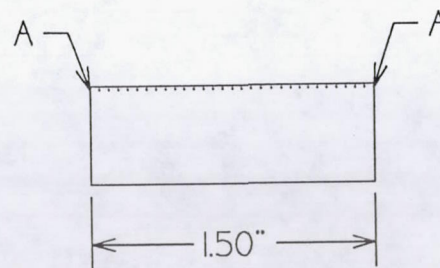


SCALE NOT TO SCALE	DIMENSIONS IN INCHES	TITLE REARWARD TUBE
MATERIAL ALUMINUM	TOLERANCES UNLESS NOTED	
ANODIZED	LINEAR +/- 0.01	PART D FWG-RR-023
FWG ASSOCIATES, INC.	DATE 03/13/92	QUANTITY 2
		ANGLES +/- 0.01
		CADD6 FILE RR023

A-20



END VIEW



SIDE VIEW

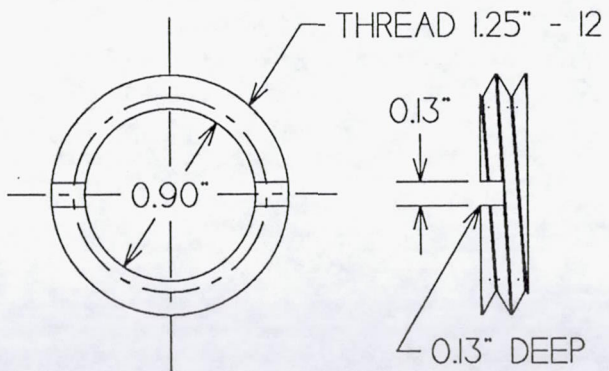
A -- SMOOTH ROUGH EDGES

FWG ASSOCIATES, INC.

DATE 03/13/92

SCALE   :	DIMENSIONS IN INCHES	TITLE FIBER ARRAY MOUNT
MATERIAL BRASS	TOLERANCES UNLESS NOTED	
1.00" DIAMETER ROD	LINEAR +/- 0.01	PART ID FWG-RR-024
QUANTITY	ANGLES +/- 0.01	CADD6 FILE RR024

A-21



SCALE   :	DIMENSIONS IN INCHES	TITLE RETAINER RING
MATERIAL ALUMINUM	TOLERANCES UNLESS NOTED	
	LINEAR +/- 0.01	PART ID FWG-RR-013
	ANGLES +/- 0.01	CADD6 FILE RRO13

FWG ASSOCIATES, INC.

DATE 03/13/92

QUANTITY 2

APPENDIX B

Appendix B contains a listing of the optical components required for the RRS.

**Table B.1 Optical Components Required for the RRS**

ITEM (QUANTITY)	PART NUMBER	SUPPLIER
Active Device SMA Receptacle (1)	905-138-5001	Radiant Communications Corp.
Single-Mode Fiber (1)	J-11-Q(SM6)-T1	Radiant Communications Corp.
0.25 Pitch GRIN Lens (1)	06LGS112	Melles Griot
30 Degree Line Generator (i.e. FAN Prism) (1)	R43473	Edmund Scientific Co.
Circular Cylinder Lens (1)	43920	Oriel Corporation
f1 Magnifying Lens (1)	KBX046	Newport Corp.
f4 Magnifying Lens (1)	KBX064	Newport Corp.
Elliptical Mirror (4)	R30,837	Edmund Scientific Co.
Fiber Optic Connector (32)	501074-1	Wesco Wholesale
Active Device Mount (32)	501184-1	Wesco Wholesale
Photodetector (32)	OSD3-5T	Centronics, Inc.
500 Micron Plastic Fiber (1440 ft)	C2542	Edmund Scientific Co.

## APPENDIX C

This Appendix contains the methods of analysis used in determining the overall system magnification and the distances between the optical components located in the sensor head portion of the RRS.

The magnification achieved with the two lens imaging system is described in the following paragraphs. The distance from the object plane to the first lens is designated as  $o$ . The letter  $f_1$  denotes the first lens and refers to the f-number of the lens. The distance between the two lenses is given by  $d$  and the letter  $f_2$  denotes the second lens and refers to its f-number. The final distance  $i$  refers to the distance from the second lens to the image plane.

This imaging system is described by the ray transfer matrix techniques of Gaussian optics. The description only considers *paraxial* rays, or rays that are close to the optical axis and assumes any angular deviation from the axis is small enough that the sine and tangent of the angles may be approximated by the angles themselves. The current analysis does not consider non-paraxial rays which can cause aberration. It was determined that aberration effects are negligible.

From Gaussian optics the optical rays can be approximated with a ray transfer matrix equation having the form

$$\begin{bmatrix} x_2 \\ v_2 \end{bmatrix} = \begin{bmatrix} A & B \\ C & D \end{bmatrix} \begin{bmatrix} x_1 \\ v_1 \end{bmatrix} \quad (\text{C.1})$$

where the ABCD matrix is the ray transfer matrix with the variable  $x$  corresponding to the rays height above the optical axis and the variable  $v$  being the product of the angle the ray makes with the optical axis and the index of refraction of the medium. The property of this matrix that is of most interest arises when  $B = 0$ . This means that our system is an imaging system with magnification  $1/A$ <sup>[11]</sup>.

Two other types of ray transfer matrices that are also of interest are the translation and refraction matrices. The translation matrix that describes the rays path over a distance  $d$  has the form

$$\begin{bmatrix} 1 & d/n \\ 0 & 1 \end{bmatrix} \quad (\text{C.2})$$

where  $n$  is the refractive index of the medium. The thin lens refraction matrix is also of interest to us and is given by,

$$\begin{bmatrix} 1 & 0 \\ -1/f_1 & 1 \end{bmatrix} \quad (\text{C.3})$$

where  $f$  corresponds to the  $f$ -number of the lens.

These two matrices now allow us to derive the two lens combine ray transfer matrix equation as

$$\begin{bmatrix} x_i \\ v_i \end{bmatrix} = \begin{bmatrix} 1 & 0 \\ -1/f_2 & 1 \end{bmatrix} \begin{bmatrix} 1 & d \\ 0 & 1 \end{bmatrix} \begin{bmatrix} 1 & 0 \\ -1/f_1 & 1 \end{bmatrix} \begin{bmatrix} x_o \\ v_o \end{bmatrix} \quad (\text{C.4})$$

Equation (C.4) yields the combined two lens matrix which is used to describe the overall two lens imaging system utilized by the RRS, Figure 2.6. The equation for this system is

$$\begin{bmatrix} x_i \\ y_i \end{bmatrix} = \begin{bmatrix} 1 & i \\ 0 & 1 \end{bmatrix} \begin{bmatrix} 1-d/f_1 & d \\ d-f_1-f_2/f_1f_2 & 1-d/s \end{bmatrix} \begin{bmatrix} 1 & o \\ 0 & 1 \end{bmatrix} \quad (\text{C.5})$$

where  $i$  and  $o$  are the image and object distances, respectively.

Multiplication of the three matrices in Equation (C.5) yields the overall ray transfer matrix for the RRS imaging system. This matrix is given by

$$\begin{bmatrix} \frac{d(i-s)+f(s-i)-is}{fs} & -\frac{d(i-s)(f-o)+f(i(o-s)-os)+ios}{fs} \\ \frac{d-s-f}{fs} & -\frac{d(f-o)+f(o-s)+os}{fs} \end{bmatrix} \quad (\text{C.6})$$

Currently the system is configured with  $f_1 = 4$ ,  $f_2 = 1$ , and  $d = 48$  inches. Substituting these values into the matrix, Equation (C.6) simplifies to

$$\begin{bmatrix} \frac{d(i-1)-5i+4}{4} & 11d(i-1)-59i+48 \\ \frac{d-5}{4} & 11d-59 \end{bmatrix} \quad (\text{C.7})$$

Recall from above that for an imaging system with  $B = 0$ , requires that

$$11d(i-1) - 59i + 48 = 0 \quad (\text{C.8})$$

Also recall that our system magnification  $M$  is given by  $1/A$ , thus

$$d(i-1) - 5i + 4 = 4/M \quad (C.9)$$

A desirable system magnification for measuring tropical rainfall was determined as approximately 1.5. Thus, Equation (C.9) becomes

$$d(i-1) - 5i + 4 = 2.66 \quad (C.10)$$

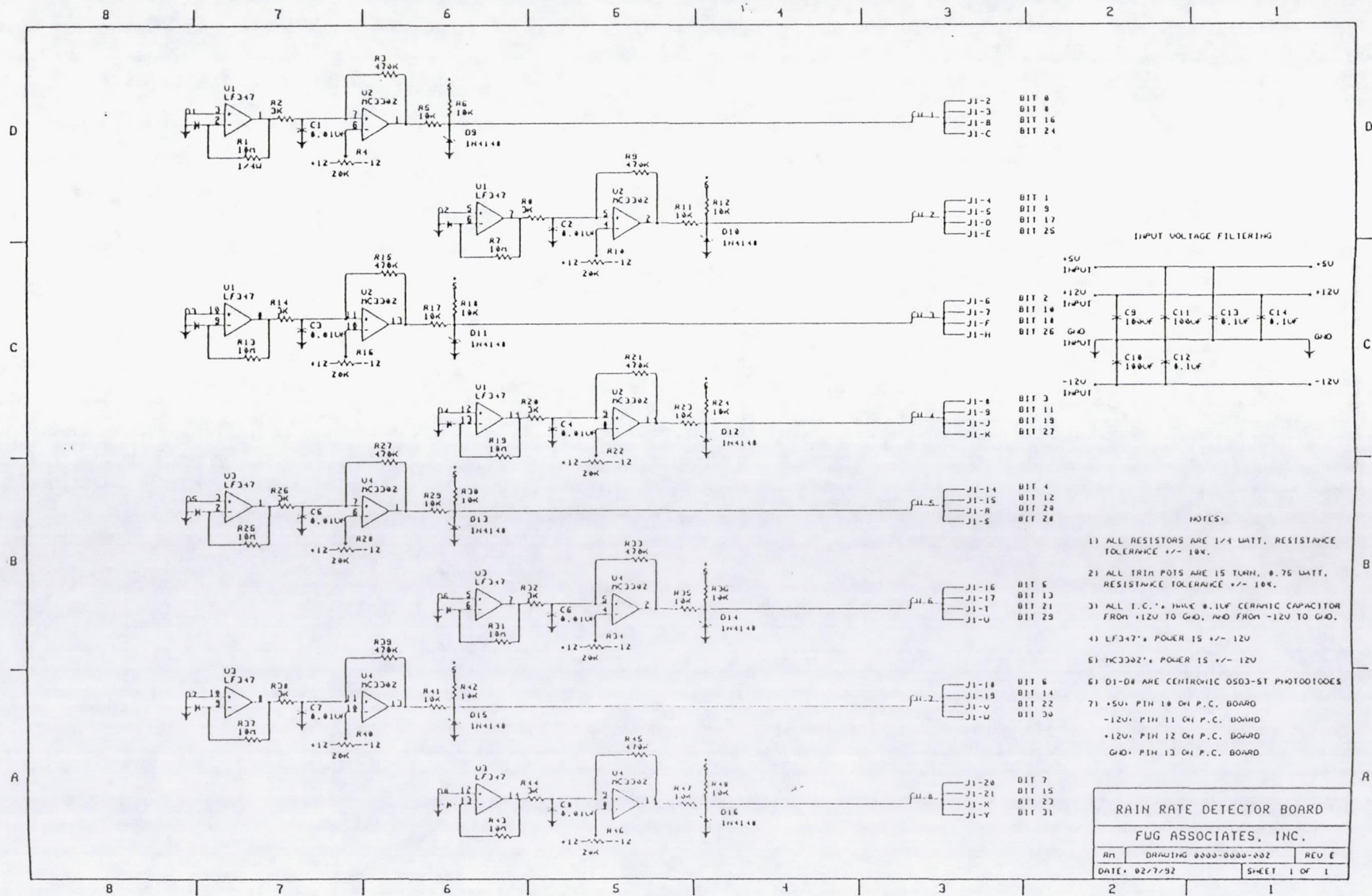
Solving Equations (C.8) and (C.10) simultaneously gives the distance between the two lenses and the distance from the second lens to the image plane as  $d = 5.5$  and  $i = 8.3$ , respectively.

The value of the magnification of the sensor can be determined from this analysis when different magnifications are required.

## APPENDIX D

Appendix D contains the wiring schematics for the various electronic components developed for the RRS. Included in this Appendix are wiring schematics for the RRS's detector and processor boards, as well as the schematic for its cardcage backplane.

D-2







## APPENDIX E

Appendix E is comprised of the User's Operations Manual which includes detailed instructions on the assembly and calibration procedures required for use with the RRS.

# **RAIN RATE AND DROPLET SIZE DISTRIBUTION INSTRUMENT**

## **OPERATIONS MANUAL**

**Model Number: FWG Model RP101A**  
**Serial Number: F92W03G0001A**

**RAIN RATE AND DROPLET SIZE  
DISTRIBUTION INSTRUMENT**

**OPERATIONS MANUAL**

**Table of Contents**

		<u>Page</u>
I.	INTRODUCTION	3
II.	SYSTEM REQUIREMENTS	3
	A. Optical System Requirements	3
	B. Required Calibration Equipment	5
	C. Host Computer/Microprocessor Compatibility	6
III.	OPTICAL IMAGING SYSTEM SETUP AND ALIGNMENT	6
	A. Single-Mode Fiber Coupling	6
	B. Assembling the Optical Head and Components	11
	C. Optical Beam Alignment	11
IV.	SOFTWARE INSTALLATION	13
V.	SYSTEM CALIBRATION	15
	A. Overview	15
	B. Definitions	15
	C. Calibration Procedures	15
VI.	SYSTEM TESTING AND TROUBLESHOOTING	19
	A. System Testing Procedures	19
	B. Troubleshooting	21
VII.	RECORDING AND ANALYZING RAINFALL DATA	23

## I. INTRODUCTION

This manual fully describes the equipment and procedures required to operate the rain rate sensor model number RP101A. The RP101A consist of two major components. These two components are depicted in Figure E.1. The two components are pictured from left to right and are referred to as the Sensing Head and the Rain Rate and Droplet Size Analyzer (RRDSA).

The RRDSA contains the signal detecting, rain droplet processing, and interfacing electronics. The Sensing Head portion of the instrument consists of a rail/lens system housed inside aluminum tubes and covers. Figure E.2 depicts the Sensing Head with its aluminum covers and tubes removed. As can be seen in Figure E.2, the Sensing Head consists of a three rail system that easily lends itself to "in-the-field" configuration and component replacement. This means that the RP101A can be configured to measure particles of various sizes. However, in this manual, the RP101A is limited to applications where the measurement of rainfall is involved.

## II. SYSTEM REQUIREMENTS

### A. Optical System Requirements

The RP101A was designed to be operated with a Helium-Neon laser light source. However, other light sources may work just as well in some applications. For example, preliminary testing was done using a configuration of three Infrared (IR) LEDs focused with a concave spherical mirror. The IR light was sufficient to trigger the detectors but, due to it's invisibility to the naked eye, a means of transport to the optical head was never designed.

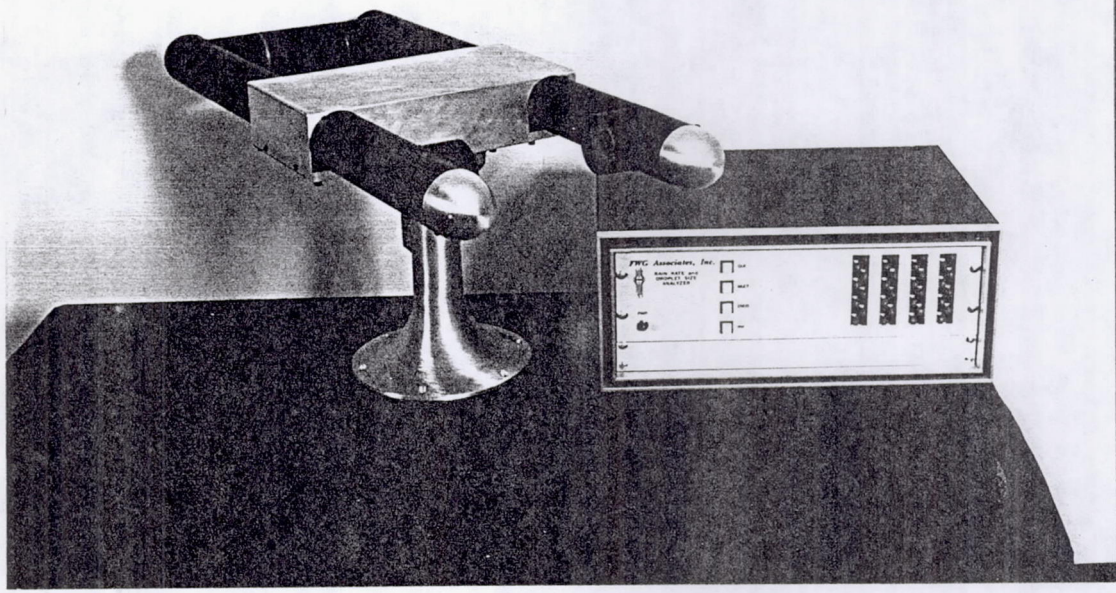


Figure E.1 Rain rate sensor FWG Model RP101A.

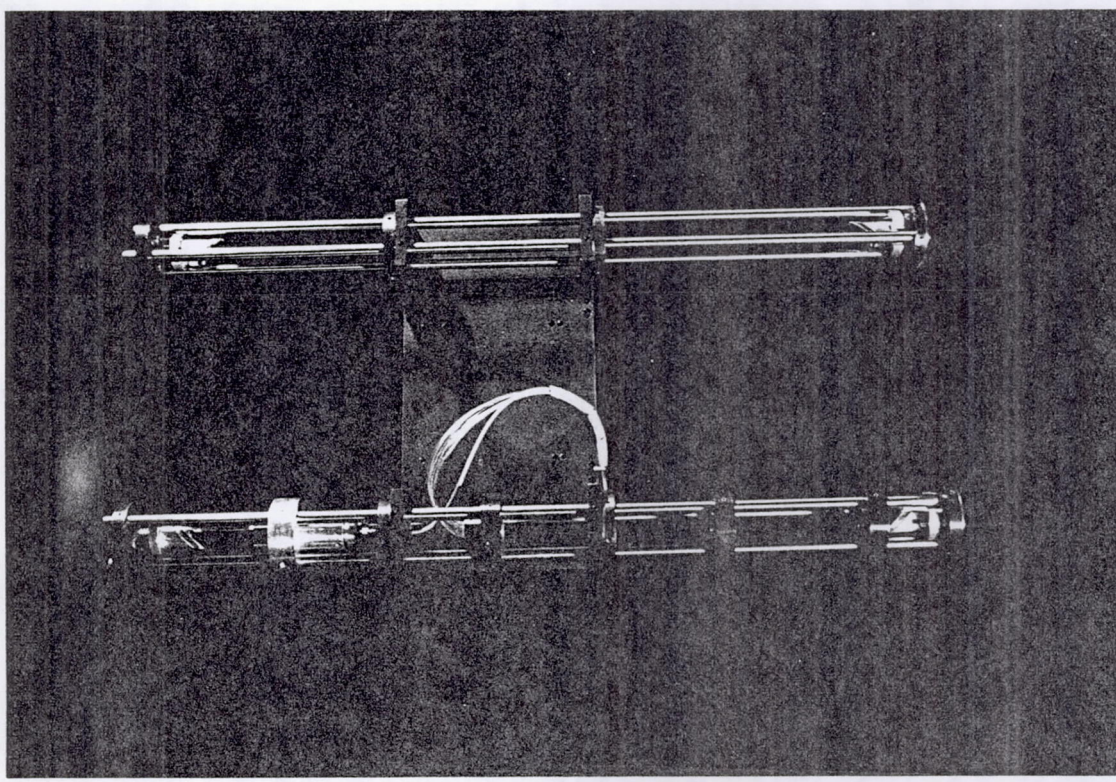


Figure E.2 Rail/lens system.

The He-Ne laser source is transported to the optical sensing head over a single-mode optical fiber. Single-mode fibers are wavelength specific and the RP101A is equipped with a single-mode fiber designed to pass light with a wavelength at or near 632.8 nanometers. When mounting the laser or other light source, vibration and movement of any kind must be minimized. The detector circuits are incredibly sensitive and even the slightest movement can trigger the channels. The light source should be mounted on an optical table or vibration isolated breadboard with some type of precision adjustable mounting device. A Newport 811 Laser Mount works very well. The Newport 811 Laser Mount is a stable kinematic mount that allows for drift-free pointing of the laser head. It features hardened and polished ball and v-groove kinematic pivots which assures repeatable angular orientation, as well as thermal stability. This type mount is highly recommended for use with the RP101A.

B. Required Calibration Equipment

Calibration of the system is critical to proper performance. The system consists of 32 independent fiber optic channels, each of which requires independent calibration. This procedure will require the following:

- 1---Dual channel oscilloscope
- 1---Edge card extender
- 1---Small flathead screwdriver

The object of the calibration is to adjust the sensing threshold voltage for each channel with maximum power incident upon the photodetector boards (no fibers blocked). There are two options to this calibration procedure. **Option #1** allows viewing of the system on the computer screen (this requires the card cage electronics to be interfaced to the

system computer, via a 44 wire ribbon cable). **Option #2** requires the computer to be disconnected from the card cage electronics (this procedure is preferred for initial system setup). The light source must always be connected to the system. Both options are described completely in Section IV of this manual.

### C. Host Computer/Microprocessor Compatibility

An IBM compatible personal computer is required to act as the host processor for the RP101A. Even though the RP101A system will run and work properly on a 286 based AT system, it needs a slightly higher platform to perform rain rate sampling in real time. This limits the system requirements to a 386 or 486 based system. It is recommended that the RP101A be interfaced to at least a 386 based system configured with a math coprocessor and a clock speed of greater than or equal to 20 MHz. In order to log the rain droplet data, the computer should be configured with a hard disk drive with an average access time not greater than 23 milliseconds. Naturally, the bigger the hard drive the more data it can store, but a 40 megabyte capacity drive can hold several hours of rain data.

## III. OPTICAL IMAGING SYSTEM SETUP AND ALIGNMENT

### A. Single-Mode Fiber Coupling

As mentioned in the section on System Requirements, the RP101A has been configured for use with a 10 milliwatt He-Ne laser light source. This section describes, in detail, the procedure for coupling the laser signal into the single-mode fiber. A single-mode fiber for the He-Ne laser light propagating at a wavelength of 632.8 nanometers has a mode-pass diameter of approximately 4.6 microns. Good coupling efficiency requires precise positioning of the fiber to center the core in the focused laser beam. This requires

submicron positioning resolution. Maximizing the coupling efficiency is accomplished by matching the incident field distribution to that of the fiber mode. Through research, and with the help of application engineers, the Newport F-91-C1 single-mode Precision Fiber Coupler was selected. The F-91-C1 has removable chucks that accommodate connectorized fibers such as the one included with the RP101A. The fiber chuck selected was the Newport FPH-CA3 chuck for Amphenol 905/906 SMA connectors. This chuck-coupler combination is compatible with the single-mode fiber obtained from Radiant Communications Corporation. An optical power meter is also recommended for initial setup and troubleshooting.

The single-mode fiber coupler also requires a microscope objective lens to focus the laser beam to a point. The idea is to focus this small point onto the surface of the single-mode fiber. In order to achieve this efficiently the microscope objective must be matched to the laser and the fiber by the following formula:

$$f = D \left( \frac{\pi \omega}{4\lambda} \right) \quad (\text{E.1})$$

where  $f$  is the focal length of the objective lens,  $D$  is the approximate laser beam diameter at the coupler,  $\omega$  is the mode field diameter, and  $\lambda$  is the wavelength of the light. Newport's M-60X microscope objective was selected for the coupling and has a numerical aperture of 0.85, a focal length of 2.9 mm, and a working distance of 0.3 mm.

Like the laser and its mount, the fiber coupler must be mounted on some type of vibration isolated table or breadboard. Figure E.3 illustrates the fiber coupling arrangement utilized by FWG during testing of the RP101A.

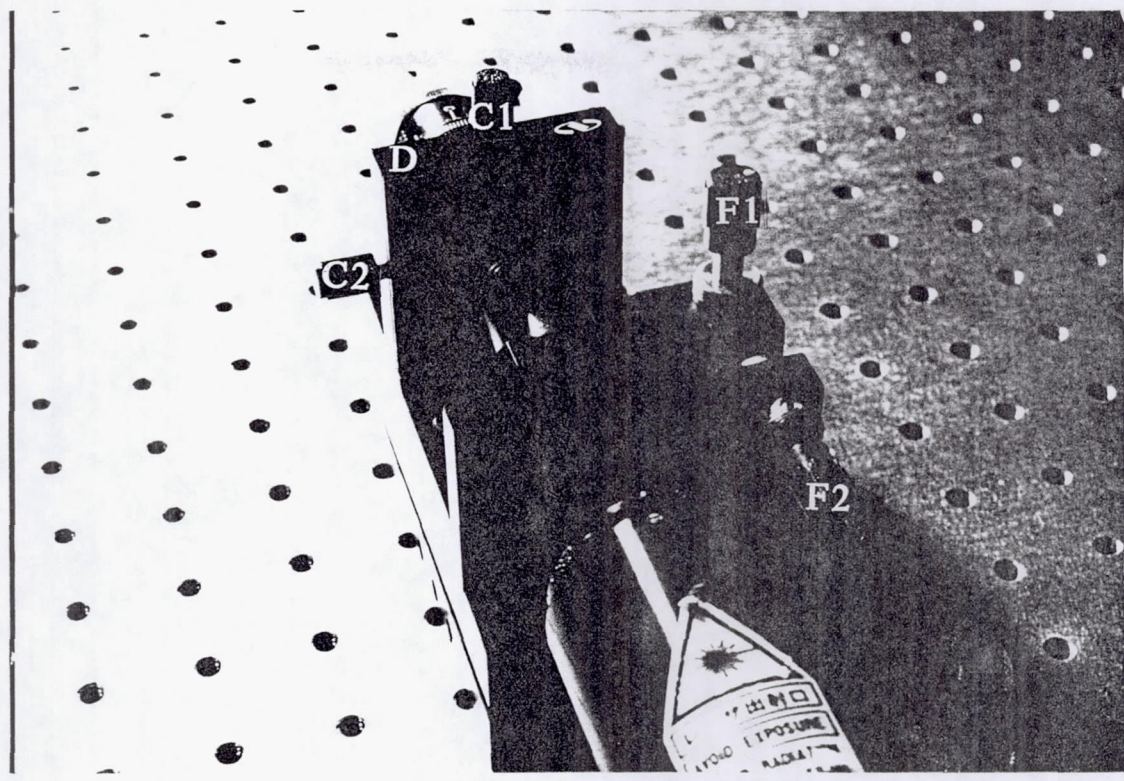


Figure E.3 (a) Laser-coupler arrangement (First View).

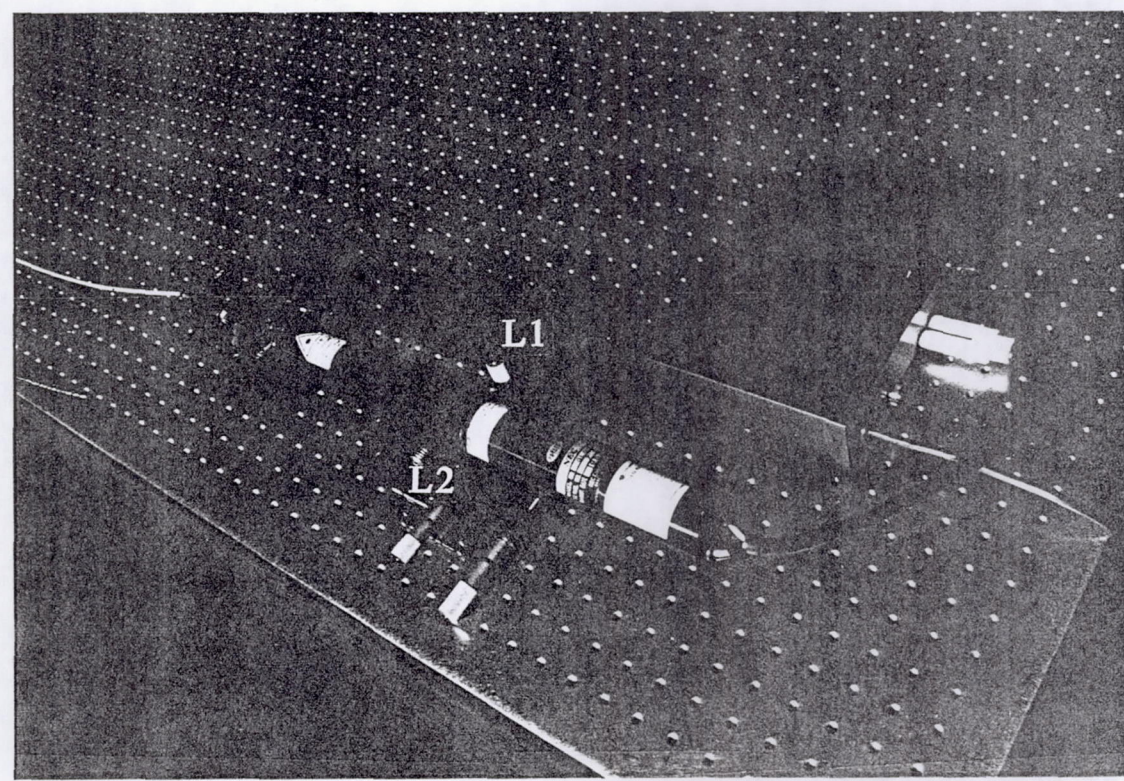


Figure E.3 (b) Laser-coupler arrangement (Second View).

When setting up the coupling arrangement, the first step (Step 1) is to position the laser mount on the vibration isolated table or breadboard and secure it with bolts or clamps. The next step (Step 2) is to insert the laser into the laser mount and secure it with the nylon tipped screw taking precautions not to overtighten the screw and damage the laser head. Once the laser is secured to the vibration isolated surface, the single-mode coupler can be installed.

Once the laser has been mounted and secured, the coupler can be mounted on the vibration isolated surface. When mounting the coupler be sure that the laser beam enters the center of the microscope objective. The coupler needs to be positioned correctly in the vertical, as well as the horizontal directions. The distance between the laser and the coupler is not of primary concern but, shorter distances minimize the effects of vibration. When the coupler is secured directly in front of the laser beam the single-mode fiber can be fastened to the fiber chuck. The chuck can then be inserted into the coupler. The single-mode fiber is bundled together with the 32 fiber array bundle but is unattached at each end and is easily recognizable because of its bright orange PVC jacket. The end of the fiber needs to be within the working distance of the microscope objective which is around 0.3 mm. The distance from the fiber end to the microscope objective is adjusted by turning the large screw, adjustment D, as depicted in Figure E.3(a). An approximation to this 0.3 mm working distance can be made first and the distance fine tuned at a later point. With the coupler and laser in place, and one end of the fiber connected to the coupler, preliminary adjustments can be made.

After turning on the laser power, wait for the laser to power up. Coarse positioning adjustments are made by looking at the unconnected covered end of the

single-mode fiber and slowly turning screw adjustments C1 and C2 as seen in Figure E.3(a). The object of making these coarse adjustments visually is to get enough signal coming through the fiber to register on the optical power meter. This can be accomplished by carefully viewing the red end cap on the end of the fiber. Do not remove the RED FIBER CAP! Due to the diverging optical rays coming from the end of the fiber, it is not likely to produce enough power to harm one's eyes as long as the fiber cap is in place. Once the signal is detected on the optical power meter, the coarse adjustments can be slowly turned to maximize the signal reaching the power meter. The larger screw adjustments F1 and F2 (see Figure E.3(a)) are used to finely adjust the position of the fiber relative to the microscope objective. These two adjustments are made to maximize the optical power signal coming through the fiber. Once these fine adjustments are made, use the larger adjustment screw D to adjust the distance between the fiber end and the microscope objective. When this adjustment is made, the F1 and F2 adjustments may need to be made once more. This process may require as many as three or four iterations before maximum coupling efficiency is achieved.

Once the coupler adjustments are completed, it may be necessary to modify the adjustments on the laser mount. This can be accomplished by turning the screw type adjustments on the laser mount, L1 and L2 (see Figure E.3(b)). The adjustment of the laser mount positioners can also be made concurrently with the adjustments on the fiber coupler. This may provide for a more efficient alignment technique, but usually is only a matter of personal preference. The adjustment procedure may require several iterations to achieve the maximum coupling efficiency and should be "tweaked" during operation of the RP101A if the signal begins to drift.

## B. Assembling the Optical Head and Components

Once the optical signal propagating through the single-mode fiber has been maximized the unconnected end of the fiber is ready to be connected to the optical head portion of the instrument. Assemble the rail/lens system as it is depicted in Figure E.2 of this manual. If the rail/lens system is already assembled, remove the cover and the four aluminum tubes and place them aside. Connect the free end of the single-mode fiber to the modified SMA receptacle fastened to the fan prism holder as illustrated in Figure E.4.

Insert the 2 mm GRIN lens into the 2.0001 mm hole just ahead of the fiber end. The GRIN lens must touch the end of the fiber for maximum efficiency. The fan prism holder must now be inserted into the cylindrical lens holder (see Figure E.4). Make sure that the cylindrical lens is also inserted into its holder and the holder is secured to the rail system with the three set screws. Adjust the fan prism holder relative to the cylindrical lens holder such that the laser beam emanating from the cylindrical lens is approximately three-quarters of an inch in width. When this adjustment is made properly, the laser beam will be collimated and its width will remain constant from the cylindrical lens, throughout the entire path of the instrument to the array head.

## C. Optical Beam Alignment

Before attempting to adjust the four turning mirrors, be sure to place the imaging lenses in their lens holders and secure the lens holders to the rails. The f1 lens is the fat lens and should be placed in the lens holder that is closest to the array head. The f4 lens is the thinner of the two and is to be placed in the holder closest to the last turning mirror, or mirror number four. Position the f1 lens approximately 8.3 inches from the array head and then position the f4 lens approximately 5.5 inches from the f1 lens. These

E-13

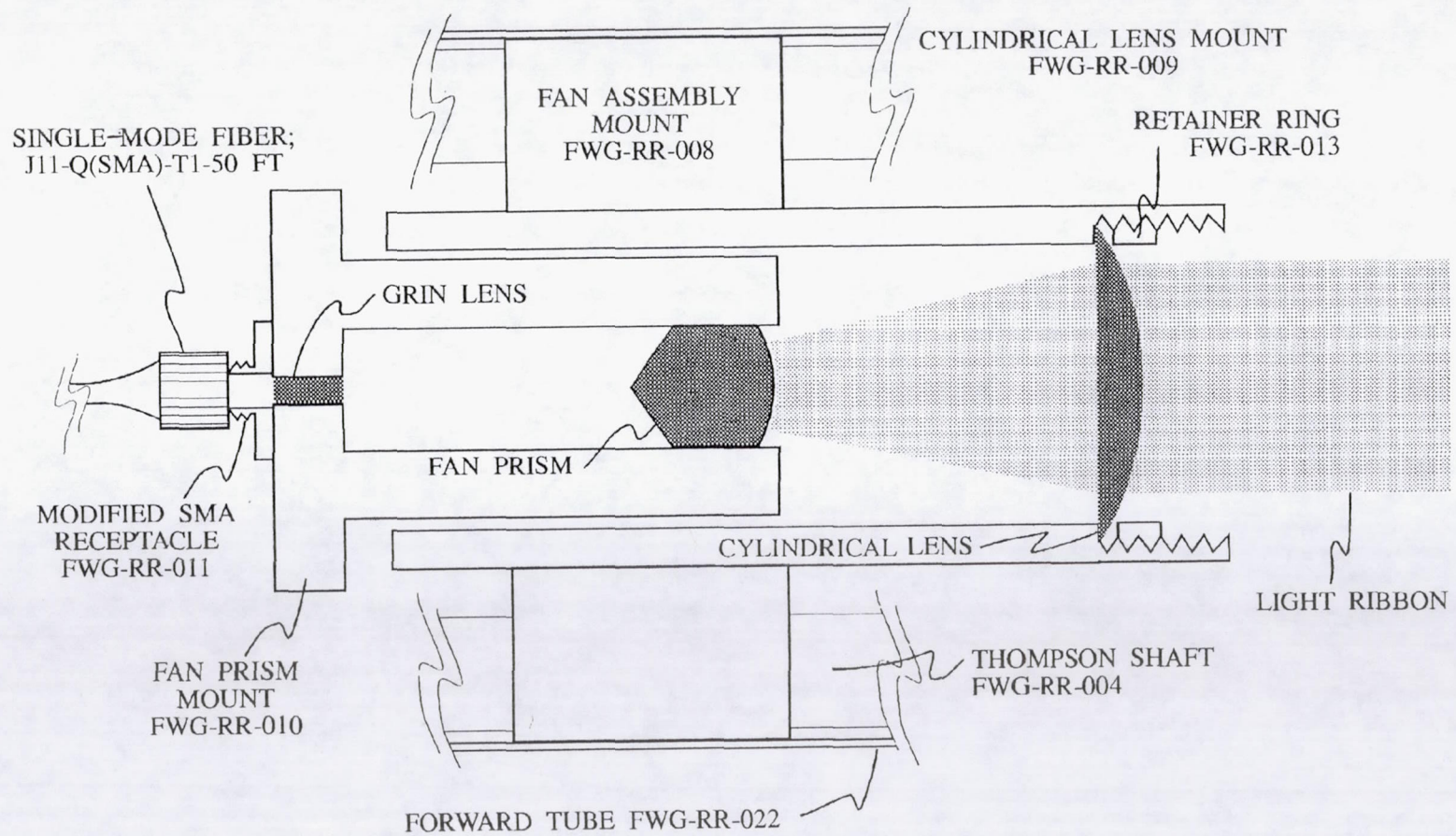


Figure E.4 Beam transforming components (Internal View).

distances correspond to the optimal magnification factor of 1.5. Adjustments can now be made on the four turning mirrors, if necessary.

The three screws that hold the mirror and its base to the rail mounts may also be used to make adjustments. The screw that holds the mirror to its base can also be used to adjust the mirrors. When adjusting the mirrors, be sure to start with mirror 1 first, then proceed to mirrors 2, 3, and 4, in that order. This will ensure alignment of the beam as it propagates through the instrument. Figure E.5 illustrates how the laser beam should appear when it is incident on the fiber array. All fiber ends should be illuminated with a beam of uniform intensity. The lens holders for the f1 and f4 lenses can be repositioned slightly, if necessary, to better focus the beam onto the array head.

Once the laser beam is aligned and focused onto the fiber array, the four mirrors must be locked into place by tightening the three lock nuts on each mirror and the three set screws that secure them to the rails. When all four mirrors are secured, tighten the set screws on the lens holders. Now the tubes can be installed or replaced, but leave the silver aluminum cover off for now.

#### IV. SOFTWARE INSTALLATION

The software delivered with the RP101A consists of two testing and calibration programs, one data acquisition program, and the data processing/analysis software. These programs are all on the accompanying floppy diskette and should be copied onto the hard drive of the host computer into a subdirectory by themselves. This can be accomplished by inserting the floppy diskette into the computer's floppy drive and entering the following commands from the DOS prompt.

```
MD <dir name>
```

```
COPY A:\*.*
```

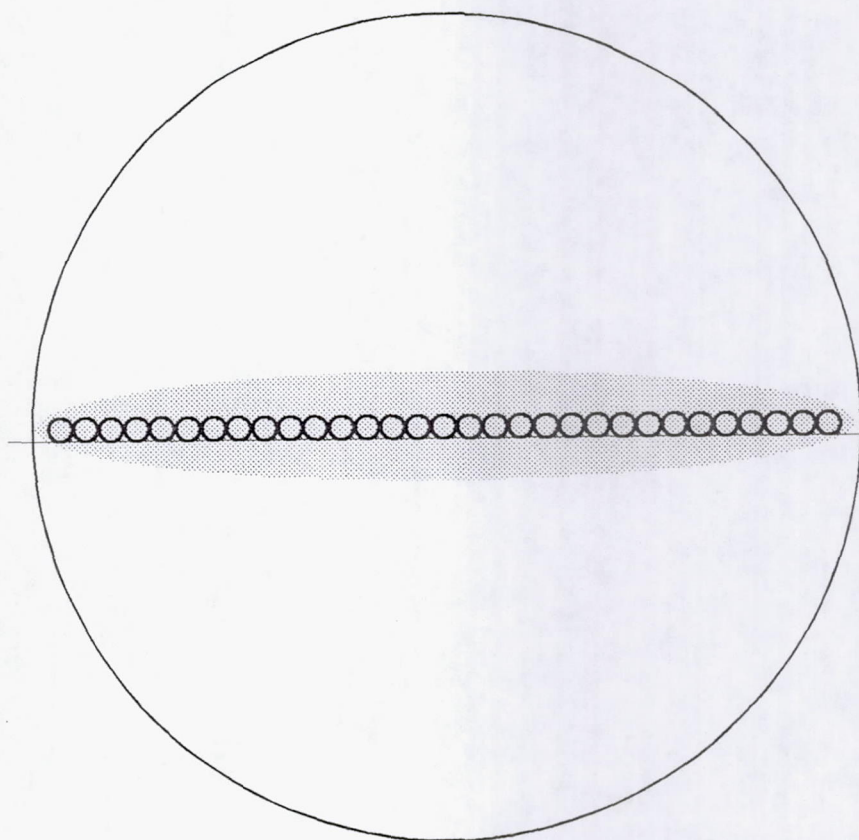


Figure E.5 32 Fiber array head.

Once the RP101A system files are copied into the directory the system is ready to be calibrated.

## V. SYSTEM CALIBRATION

### A. Overview

The system has a total of four light detector boards having 8 channels each, for a total of 32 system channels. The boards are numbered 1 through 4, counting from right to left. Individual channels on each detector board are numbered 1 through 8, counting from top to bottom. Detector board #1 will correspond to channels 1 through 8, detector board #2 will correspond to channels 9 through 16, detector board #3 will correspond to channels 17 through 24, and detector board #4 will correspond to channels 25 through 32.

### B. Definitions

SYSTEM POWER - refers to all power at each system (i.e. computer, light source, card cage electronics, etc.). This includes any and all components connected to the system.

### C. Calibration Procedures

#### OPTION #1 ONLY -

Confirm that the system computer is connected to the card cage system electronics via the 44-pin ribbon cable inserted into slot 4 in the card cage.

Turn the SYSTEM POWER ON. After the computer boots up, switch to the subdirectory in which the RP101A system files were installed and enter the following command:

**VIEWALL <RETURN>**

The computer monitor will now display all data slices in REAL TIME.

**THE ABOVE COMMANDS WILL HAVE TO RE-ENTERED EACH TIME THE SYSTEM POWER IS TURNED OFF AND BACK ON.**

**OPTION #2 ONLY -**

This option procedure is recommended for initial system setup. Confirm that the card cage electronics is NOT interfaced to the system computer. (THE 44 WIRE RIBBON CABLE IS DISCONNECTED FROM THE SYSTEM COMPUTER.)

Proceed to Step #1.

**OPTIONS #1 AND #2 HAVE THE SAME PROCEDURE STARTING AT STEP #1. GREAT CARE MUST BE TAKEN TO ENSURE THAT THE FIBER OPTIC STRANDS ARE NOT TWISTED, BENT, OR CRIMPED IN ANY WAY.**

**STEP #1**

Turn SYSTEM POWER OFF. Carefully remove detector board #1 from its card cage slot.

**STEP #2**

Insert the edge card extender into the detector board #1 slot and insert the detector board into the edge card extender.

**STEP #3**

Setup the oscilloscope for dual trace sweep in AUTO mode; set both channels to 1 volt per division. The ground reference for both channels should be set to the same level (i.e. both traces set on the bottom line of the display - on top of each other).

**STEP #4      **REFER TO TABLE E.1****

Ground both scope probes to the detector board ground. Connect one scope probe to U2 (MC3302 quad voltage comparator) pin 6, and the other probe to U2 pin 7 (this corresponds to channel 1).

TABLE E.1. FOR USE IN STEP #4

CHANNEL	CONNECT SCOPE PROBES	ADJUST TRIM-POT
1	U2 PINS 6 & 7	#1
2	U2 PINS 4 & 5	#2
3	U2 PINS 10 & 11	#3
4	U2 PINS 8 & 9	#4
5	U4 PINS 6 & 7	#5
6	U4 PINS 4 & 5	#6
7	U4 PINS 10 & 11	#7
8	U4 PINS 8 & 9	#8

STEP #5

Turn SYSTEM POWER ON:

- 1) Turn on the computer (IF USING OPTION #1)
- 2) Turn on the power to the card cage electronics
- 3) Turn on the laser's power source.

### STEP #6

The oscilloscope will display two traces which are termed: 1) threshold sensing voltage and, 2) detector voltage. The detector voltage will vary by the amount of light that is present at the detector. Setting the threshold sensing voltage to the proper level is the object of this calibration procedure. There are 8 trim-pots (variable resistors) numbered 1 through 8 on each detector board. Adjust trim-pot #1 to set the threshold sensing voltage, on channel 1, to 51.5 percent of the detector voltage. This 51.5 percent corresponds to the optimum 48.5 percent threshold value. After setting this voltage to the proper value, turn the SYSTEM POWER OFF.

### STEP #7

Steps #4, #5 and #6 must be repeated for the remaining channels. Table E.1 is separated into individual channels. Across from each channel is a list of which pins the oscilloscope probes must be connected to for that individual channel (U2 and U4 are MC3302 quad voltage comparators). The channel also corresponds to the trim-pot that must be adjusted to set the threshold sensing voltage.

### STEP #8

Turn ALL SYSTEM POWER OFF. **CAREFULLY** remove the detector board from the edge card extender. Carefully remove the edge card extender from the card cage. Carefully replace the detector board back into the card cage. **EXTREME CARE MUST BE TAKEN TO PREVENT DAMAGE TO THE OPTICAL FIBERS.**

### STEP #9

Repeat Steps #1 through #8 for each of the remaining detector boards (detector boards #2, #3, and #4).

## VI. SYSTEM TESTING AND TROUBLESHOOTING

### A. System Testing Procedures

The computer programs **VIEWALL.EXE** and **VIEWER.EXE** are included for testing purposes. As explained in the Calibration Section, **VIEWALL** displays every slice of data in real time. If the optical imaging system has been properly aligned and the electronic system has been properly calibrated, then every line displayed by **VIEWALL** should read

0 fibers blocked, er1 = 0, er2 = 0

This indicates that all systems are functioning properly and the system is ready for testing. If this is not what **VIEWALL**'s screen output looks like, see the section on troubleshooting below.

If **VIEWALL**'s screen output conforms to the line displayed above, preliminary tests can be performed. The first test recommended is to check the system's particle sizing ability. This can be accomplished by placing objects with known or measurable sizes, such as drill bits, in the probe volume and watching the number of fibers blocked displayed by **VIEWALL** on the computer's display screen. For example, a drill bit with a diameter of 1,000 microns, when placed vertically in the probe volume, should cast a shadow across an area of width 1,000 x 1.5 or 1,500 microns. This means that the drill should block no more than three fibers anywhere across the array. Keep in mind that due to the digital nature of this process, sometimes only two fibers will be blocked. This test can be carried out with any size object that is comparable to the size of raindrops (i.e. between 300 microns and 6 mm in diameter). If the number of fibers blocked does not correspond to what is expected, then recheck the distances between the two imaging lenses.

Once it has been determined that the RP101A's object sizing capability is functioning properly, the next step is to check the operation of the two error signals. The first error signal is denoted as er1 on VIEWALL's display screen. er1 corresponds to the multiple particle error that occurs when two or more particles are in the probe volume at the same time. This can be checked by placing two objects in the probe volume that are approximately 1-2 mm apart. When a bright spot appears between two dark spots on the array, er1 should be set to 1. If er1 does not work properly, the threshold level settings may require modification.

The second error signal is referred to as er2 and corresponds to the end-reject fiber signals. In order to check out these error channels an object must shadow either of the two end fibers. This can be accomplished by observing the illuminated fiber array (with the silver colored aluminum cover removed) when the object is placed in the probe volume and noting when either of the end fibers is blocked. When either of the end channels is shadowed, the er2 signal should be set to 1. If er2 is not working properly it is necessary to double check the threshold levels on the two end fibers.

The program entitled VIEWER.EXE can also be used for preliminary testing purposes. VIEWER performs the same function as LOGGER.EXE, but instead of logging the data on the hard drive, it displays the data on the computer's screen. When running VIEWER, objects can be sized as they are passed through the probe volume. VIEWER displays the number of fibers blocked by the object, the number of samples acquired for that particular object, the time in seconds, and the number of samples in which each of the error signals were present. VIEWER can be executed during setup to determine if the RP101A is actually measuring raindrops. The program LOGGER.EXE works the same

as VIEWER.EXE except that all output is directed to the hard drive. Its output will be described in more detail in a later section.

## B. Troubleshooting

This section describes some of the problems that are most likely to occur during setup and calibration of the RP101A and gives an approach to solving them.

\* Problem:

No light signal or very weak light signal.

\* Solution Approach:

1. Make sure laser is connected to its power supply and that its power supply is connected to 120 VAC.
2. Check the single-mode fiber connections.
3. Check and/or reset the adjustments on the laser mount and the single-mode fiber coupler.
4. Repair or replace the fiber.

\* Problem:

Not enough voltage at the detectors to trigger the comparator.

\* Solution Approach:

1. See weak light signal approach above.
2. Check or realign the optical components in the sensing head.

\* Problem:

VIEWALL shows fibers blocked when nothing is in the probe volume.

\* Solution Approach:

1. Check for an optical path obstruction within the optical head assembly.
2. Check for dirty lenses or mirrors.
3. Recheck the system calibration and threshold levels.
4. Determine which channels are not working and replace the detector board(s).

\* Problem:

Computer does not seem to communicate with the RP101A.

\* Solution Approach:

1. Make sure the I/O card is installed in the computer properly.
2. Make sure the 50-pin ribbon cable is connected to the computer.
3. Make sure the 50-pin ribbon cable is connected to the electronic processor.
4. Make sure all components are connected to 120 VAC power outlets.

\* Problem:

LOGGER.EXE does not save any data file(s).

\* Solution Approach:

1. Make sure the computer's hard disk is not full.
2. Make sure the computer has a math coprocessor installed.

\* Problem:

Error bits are not working properly.

\* Solution Approach:

1. Set/check the threshold adjustments.
2. Repair/replace detector board(s).
3. Repair/replace processor board.

\* Problem:

RP101A does not detect objects.

\* Solution Approach:

1. Set/check threshold adjustments.
2. Particles are too small.
3. Repair/replace processor board.

## VII. RECORDING AND ANALYZING RAINFALL DATA

Once the RP101A is completely setup and calibrated and passes all of the preliminary tests, it is ready to record rain amount and droplet data. `LOGGER.EXE` is the program used to record the data. `LOGGER` saves rain droplet data in a file named `RAIN.DAT`. Each time `LOGGER` is executed, it logs data for 1,000 rain drops. `LOGGER` was written in such a way to lend itself to batch processing rather easily. For example, a batch file used to log 5,000 rain droplets should have the form:

```
LOGGER
COPY RAIN.DAT RAIN.D01
LOGGER
COPY RAIN.DAT RAIN.D02
LOGGER
COPY RAIN.DAT RAIN.D03
LOGGER
COPY RAIN.DAT RAIN.D04
LOGGER
COPY RAIN.DAT RAIN.D05
```

The five data files named RAIN.D01 through RAIN.D05 would contain the droplet data for each of the 5,000 sampled droplets. LOGGER records the number of fibers blocked, the number of data samples acquired for each drop, the time in seconds, and the number of samples in which each error signal was set.

This rain droplet data will now be ready for analysis.

## APPENDIX F

This Appendix contains the Microsoft QUICK BASIC program for analyzing the rain rate.

```

10 DEFDBL A-Z

20 DIM
   NDM(32),VOLM(32),CFN(32),CFV(32),CFO(32),CFU(32),OVER(32),UNDER(32)

30 DIM NDR(32),VOLR(32),DROPTS(32),DROPS(32),SIZE(32),ASS(50),BSS(50)

40 PRINT CHR$(12)

50 REM ***** SET RUN PARAMETERS
   *****

60 PI=ATN(1)*4:PICON=4*PI/3:RF=250:MAGIF=1.5:NRAND%=0

70 REM ***** READ CORRECTION FACTORS
   *****

80 HAN$=RIGHT$(STR$(ITOL%),1)

90 HWC$="G:\BASIC\CORR1.PRN"

100 OPEN "I",1,HWC$

110 FOR I%=0 TO 31

120 INPUT #1, CFN(I%),CFV(I%),CFO(I%),CFU(I%)

130 NEXT I%

140 CLOSE #1

150 REM ***** INITIATE DATA ANALYSIS DO LOOP
   *****

160 FOR ITOL%=1 TO 4

170 FOR I%=1 TO 32

180 OVER(I%)=0:UNDER(I%)=0:NDM(I%)=0:NDR(I%)=0:VOLR(I%)=0:VOLM(I%)=0

190 NEXT I%

```

```

200  REM  *****  READ  MEASURED  DATA
*****

210  RATER=0:NRAND%=0:TIMEE=0:NDE1%=0:NDE2%=0

220  IF ITOL%>9 THEN HAN$=RIGHT$(STR$(ITOL%),2):GOTO 240

230  HAN$="0"+RIGHT$(STR$(ITOL%),1)

240  HWM$="G:\BASIC\RAIN32192\RAIN.D"+HAN$

250  HWD$="G:\BASIC\RAIN32192\DSTP"+HAN$+".PRN"

260  HRM$="G:\BASIC\RAIN32192\RPROB"+HAN$+".PRN"

270  PRINT HWM$;HRM$

280  OPEN "I",2,HWM$

290  INPUT#2,DUM1,DUM2,TIME0,DUM3,DUM4

300  IF EOF(2) THEN TIME=TIMEE/60:PRINT "TIME=";TIME:GOTO 390

310  INPUT#2,NF%,DUM1,TIME1,ERR2%,ERR1%

320  IF ERR1%>0 THEN NDE1%=NDE1%+1: GOTO 360

330  IF ERR2%>0 THEN NDE2%=NDE2%+1:TIME0=TIME1:GOTO 380

340  NRAND%=NRAND%+1

350  NDM(NF%)=NDM(NF%)+1

360  TIMEE=TIMEE+(TIME1-TIME0)

370  TIME0=TIME1

380  GOTO 300

390  CLOSE #2

400  REM  *****  APPLY  CORRECTION  FACTORS
*****

```

```

410 FOR I%=0 TO 32
420 OVER(I%)=CFO(I%)*NDM(I%)
430 UNDER(I%)=CFU(I%)*NDM(I%)
440 NEXT I%
450 FOR I%=1 TO 32
460 NDM(I%)=NDM(I%)-OVER(I%)-UNDER(I%)
470 IF I%=32 THEN 490
480 NDM(I%+1)=NDM(I%+1)+OVER(I%)
490 IF I%=0 THEN 510
500 NDM(I%-1)=NDM(I%-1)+UNDER(I%)
510 NEXT I%
520 FOR I%=1 TO 31
530 NDR(I%)=NDM(I%)*CFN(I%)
540 VOLM(I%)=(NDR(I%)*(PICON*(I%*RF)^3)*1E-09)/(MAGIF^3)
550 VOLR(I%)=VOLM(I%)*CFV(I%)
560 RATER=RATER+VOLR(I%)
570 NEXT I%
580 REM ***** PRINT DISTRIBUTION TO FILE
*****
590 OPEN "O",1,HWDS$
600 PRINT#1, ITOL%
610 FOR I%=1 TO 32

```

```

620 PRINT USING " ##### ";I%;
630 PRINT USING " #####.## ";NDR(I%);
640 PRINT USING " #####.## ";VOLR(I%)
650 PRINT#1, I%,
660 PRINT#1, NDR(I%),
670 PRINT#1, VOLR(I%)
680 NEXT I%
690 PRINT USING "\ \ #####.### "; "WATER=";RATER/(16*140);"mm"
700 PRINT USING "\ \ #####.###
"; "RATE=";RATER/(16*140*(TIME/60));"mm/hr"
710 PRINT USING "\ \ ##### "; "TWO DROP ERROR=";NDE2%
720 PRINT USING "\ \ ##### "; "END OF FIBER ERROR=";NDE1%
730 PRINT USING "\ \ ##### "; "TOTAL NUMBER OF
DROPS=";NRAND%
740 PRINT#1, RATER/(16*140)
750 PRINT#1, RATER/(16*140*TIME/60)
760 PRINT#1, NDE2%
770 PRINT#1, NDE1%
780 PRINT#1, NRAND%
790 NEXT ITOL%
800 END

```



# Report Documentation Page

1. Report No.		2. Government Accession No.		3. Recipient's Catalog No.	
4. Title and Subtitle Phase II - Rain Rate Instrument for Deployment at Sea				5. Report Date March 30, 1992	
7. Author(s) Jimmy W. Steele, Computer Scientist				6. Performing Organization Code FWG Associates, Inc.	
				8. Performing Organization Report No.	
9. Performing Organization Name and Address FWG Associates, Inc. 217 Lakewood Drive Tullahoma, TN 37388				10. Work Unit No.	
12. Sponsoring Agency Name and Address NASA Washington, DC 20546-0001 National Aeronautics and Space Administration George C. Marshall Space Flight Center Marshall Space Flight Center, AL 35812				11. Contract or Grant No. NAS8-38481	
				13. Type of Report and Period Covered Final 04/10/90 - 03/10/92	
15. Supplementary Notes				14. Sponsoring Agency Code	
				16. Abstract <p>This report describes, in detail, the SBIR Phase II contracting effort provided for by NASA Contract Number NAS8-38481 in which a prototype Rain Rate Sensor was developed. FWG Model RP101A is a fully functional rain rate and droplet size analyzing instrument. The RP101A consists of a fiber optic probe containing a 32 fiber array connected to an electronic signal processor. When interfaced to an IBM compatible personal computer and configured with appropriate software, the RP101A is capable of measuring rain rates and particles ranging in size from around 300 microns up to 6 or 7 millimeters in diameter. FWG Associates, Inc. intends to develop a production model from the prototype and continue the effort under NASA's SBIR Phase III program.</p>	
17. Key Words (Suggested by Author(s)) Rain Rate Measurement Tropical Rainfall Measuring Mission (TRMM) Rain Droplet Size Distribution Sma-1 Business Innovation Research (SBIR) Distrometer, Fiber Optic Probe			18. Distribution Statement  Unclassified - Unlimited		
19. Security Classif. (of this report) Unclassified		20. Security Classif. (of this page) Unclassified		21. No. of pages 127	22. Price



## FWG ASSOCIATES, INC.

CORPORATE HEADQUARTERS • 217 LAKEWOOD DRIVE TULLAHOMA, TN 37388 • TELEPHONE (615) 455-1982 FAX (615) 455-1805

HUNTSVILLE OPERATION • P.O. BOX 12056 HUNTSVILLE, AL 35815-2056 • TELEPHONE (205) 880-2553 FAX (205) 880-2554